USGS
science for a changing world

Sources, Dispersal, and Fate of Fine Sediment Supplied to Coastal California

Scientific Investigations Report 2007–5254

U.S. Department of the Interior
U.S. Geological Survey

COVER

Turbid sediment plumes along the California coast near Gaviota following storms of February 1998. Picture by Mark Defeo and used by permission.

Sources, Dispersal, and Fate of Fine Sediment Supplied to Coastal California

By Katherine L. Farnsworth and Jonathan A. Warrick

Scientific Investigations Report 2007–5254

U.S. Department of the Interior
U.S. Geological Survey

U.S. Department of the Interior
DIRK KEMPTHORNE, Secretary

U.S. Geological Survey
Mark D. Myers, Director

U.S. Geological Survey, Reston, Virginia: 2007

For product and ordering information:
World Wide Web: http://www.usgs.gov/pubprod
Telephone: 1-888-ASK-USGS

For more information on the USGS--the Federal source for science about the Earth, its natural and living resources, natural hazards, and the environment:
World Wide Web: http://www.usgs.gov
Telephone: 1-888-ASK-USGS

Suggested citation:
Farnsworth, K.L., Warrick, J.A., 2007, Sources, Dispersal, and Fate of Fine Sediment Supplied to Coastal California: U.S. Geological Survey Scientific Investigations Report 2007–5254, 77 p.

Contents

Figures

Tables

Sources, Dispersal, and Fate of Fine Sediment Supplied to Coastal California

By Katherine L. Farnsworth and Jonathan A. Warrick

Executive Summary

We have investigated the sources, dispersal, and fate of fine sediment supplied to California coastal waters in a partnership between the U.S. Geological Survey (USGS) and the California Sediment Management Workgroup (CSMW). The purpose of this study was to document the rates and characteristics of these processes so that the State can better manage its coastal resources, including sediment. In this study, we made the following observations:

- Rivers dominate the supply of fine sediment to the California coastal waters, with an average annual flux of 34 megatonnes (Mt).
- Cliff and bluff erosion in central and southern California is a source of fine sediment, with a delivery rate of approximately 10 percent of river loads. In the southern most part of the State, however, where river-sediment loads are low, cliff and bluff erosion represent approximately 40 percent of the total fine-sediment flux.
- Temporal variation in the sources of fine sediment is high. River floods and bluff erosion are episodic and dominated by winter storms, which supply most sediment flux to the coast. The magnitude of winter storms is generally related to the El Niño-Southern Oscillation (ENSO) and Pacific Decadal Oscillation (PDO) climate cycles.
- The three rivers that dominate fine-sediment flux to the California coast are the Eel, Salinas, and Santa Clara Rivers. Because the sediment delivery from these and all other California coastal watersheds is episodic, individual rivers discharge most of their annual loads over the course of only a few days per year.
- Spatial variation in river-sediment discharge is high and generally related to such watershed characteristics as geology, precipitation, and drainage area. For example, the Transverse Range of southern California represents only 9 percent of the watershed-drainage area but 18 percent of the fine-sediment flux, a function of the young sedimentary bedrock and active tectonics of this region. The urban rivers of southern California were observed to discharge sediment at rates consistent with those of the surrounding Transverse Range rivers, which share the same geologic setting.
- Direct observations of fine-sediment dispersal have been limited to the river-mouth settings of the Eel and Santa Clara Rivers, where sediment has been observed to settle quickly from buoyant plumes and be transported along the seabed during periods of storm waves.
- After heavy loading of fine sediment onto the continental shelf during river floods, there is increasing evidence that fluid-mud gravity flows occur within a layer 10 to 50 cm above the seabed and efficiently transport fine sediment offshore.
- All along the California coast, the timing of river discharge and coastal winds and waves from storm events are strongly coherent; however, of large wave events with the potential for resuspending and transporting fine sediment occur during periods without significant rainfall and therefore no significant river discharge.
- Although fine sediment dominates the midshelf mud belts offshore of California river mouths, these mud belts are not the dominant sink of fine sediment, much of which is deposited across the entire continental shelf, including the inner shelf, and offshelf into deeper water depths.
- Accumulation rates of fine sediment, which can exceed several millimeters per year, are generally highest near river sources of sediment and along the inner shelf and midshelf.
- Sediment-accumulation rates, as summarized from both long-term and recent investigations of continental-shelf geochronology, are generally consistent across California except in southern California, where recently the sediment-accumulation rate has been tenfold greater than the long-term rate, possibly as a result of increased river discharge, wastewater outfall inputs, or other anthropogenic sources.

Thus, fine sediment is a natural and dynamic element of the California coastal system because of large, natural sediment sources and dynamic transport processes.

Introduction

The California Sediment Management Workgroup (CSMW) was established in 1999 to formulate regional approaches to protecting, enhancing, and restoring California's coastal beaches and watersheds. The CSMW is a State and Federal partnership created to integrate ongoing work on multiple scales by many government agencies. The present study was funded through an agreement between the U.S. Geological Survey (USGS) and the CSMW to increase knowledge of the flux and fate of fine sediment delivered to the coastal ocean. The coastal delivery, dispersal, and fate of terrestrially derived fine sediment is important to characterize because (1) turbidity and sedimentation may affect marine biota, (2) the pathways and residence times of fine sediment in coastal waters are poorly understood, and (3) natural processes of sediment dispersal may be used as a model for the fate of human-introduced sediment in the coastal ocean.

Typically, four stages of sediment dispersal are evident on the continental shelf (Wright and Nittrouer, 1995): (1) initial supply, (2) initial deposition, (3) resuspension and transport, and (4) final deposition and long-term net accumulation. Much fine sediment is delivered to California coastal waters from such natural sources as rivers and bluffs; however, little is known about the amounts and timing of fine-sediment discharge, largely because of the attention focused on quantifying the delivery and transport of coarser (that is, sand size) material (for example, Inman and Jenkins, 1999; Warrick and Milliman, 2003; Willis and Griggs, 2003), particularly in relation to the stability of shorelines. Furthermore, little work has been conducted to evaluate the dispersal and fate of sediment along the entire California coastal margin.

The goal of this study is to fill these informational gaps through new calculations and a synthesis of existing data and results. We have used a sediment-budget technique throughout, with an emphasis on calculating the rates of sediment transport and flux of various portions of the sediment budget. Sediment budgets for coastal California have commonly been calculated on a littoral-cell basis, focusing on the coarser material that remains close to shore (for example, Willis and Griggs, 2003). However, the fine sediment delivered to the coastal ocean is not constrained to these littoral cells because it is more easily kept in suspension and transported long distances in buoyant freshwater plumes or far offshore along the seabed. Therefore, coastal fine-sediment budgets require a regional basis for proper analysis.

The following report is organized by the three main elements of fine-sediment for California coastal waters: sources, dispersal, and fate. After a brief discussion of fine-sediment properties, we discuss these three main elements in separate sections. In a final section we present our results with respect to a fine-sediment budget and identify future research needs.

What Is Fine Sediment?

Fine sediment is commonly defined by a particle-size threshold which, though somewhat arbitrary, approximately differentiates between particles that undergo suspended-load transport and those that undergo mixed bedload and suspended-sediment transport (McCave and Syvitski, 1991). Although various classification schemes exist, particle-size thresholds in all these schemes agree within a factor of 2. Here we use the Wentworth classification scheme because of its general acceptance across the geosciences (Boggs, 1987; McCave and Syvitski, 1991; Komar, 1998). In this scheme, fine sediment includes all particles with grain sizes smaller than 0.0625 mm in diameter, whereas sand ranges in grain size from 0.0625 to 2 mm (see app. A).

Fine sediment includes both silt and clay. Although the distinction between silt and clay is defined by a particle-size threshold of 0.002 mm, the silt- and clay-size particles typically have diverse physiochemical properties (Hillel, 1982). Thus, clay-size particles are generally dominated by clay minerals, which are the weathering products of primary, or source-rock, minerals. Characteristics of clay minerals include their ability to exchange cations on the particle surface because of a negative charge, and their ability to absorb water. These properties are strongly influenced by the specific clay mineralogy and, thus, the source rock, weathering environment, and extent of weathering (Hillel, 1982). In contrast, silt-size particles are typically dominated by fragments of the source rocks without mineral alteration. Silt-size particles, however, have a much greater surface area per unit mass than sand and may be coated with clay-size particles, resulting in similar characteristics to clay (Hillel, 1982). For the purposes of this study, silt- and clay-size particles have generally not been divided into separate size classes, owing to a lack of information regarding these distinctions in the data available.

Fine sediment has several other characteristics relevant to its transport and fate in the California coastal ocean. First, as discussed in further detail below, fine sediment commonly flocculates in seawater, a process that both increases the bulk particle size and enhances rates of vertical settling (Hill and others, 2000; Curran and others, 2002). Once deposited on the seabed, fine sediment may be ingested by benthic fauna and excreted as fecal pellets, packaging these small particles into larger, sand-size aggregates and altering their transport properties (Wheatcroft and Butman, 1997; Drake and others, 2002). Fine-sediment particles may also have materials adhering to their surfaces, allowing for dating by using radiometric tracers, or providing a means for nutrient and pollutant transport. These qualities can aid in the evaluation of sediment-transport pathways and sediment-accumulation rates, as discussed below, and may also lead to effects that are beneficial to the greater ecosystem of the California Current. For example, fine sediment on the continental shelf, originally derived from rivers, provides the dominant source of nutrient iron to phytoplankton in the California Current, which, in turn, provides

the dominant source of primary production to this system (Johnson and others, 1999; Bruland and others, 2001; Buck and others, 2007). Finally, fine sediment is highly efficient at scattering light in suspension, causing turbidity and attenuating sunlight within seawater (Kirk, 1996). This may disrupt feeding or other life-history functions or marine biota (Anchor Environmental CA L.P., 2003), although this characteristic also allows for efficient measurement of suspended-sediment concentration with optical sensors. Together, these characteristics make fine sediment a dynamic and important constituent of the California coastal ocean.

Sources of Fine Sediment

Fluvial Sources

We calculated sediment input from rivers by using USGS stream-discharge records, which allow for a determination of the total suspended-sediment discharge from California coastal watersheds, as well as of the fine-sediment fraction. This study used multidecadal records from 25 coastal rivers (fig. 1; table 1). Because of this, we used extrapolation techniques to estimate the fine-sediment flux from unmonitored areas or those with insufficient sediment data. Although some rivers (e.g., Santa Maria River) have extensive discharge records, they were not evaluated due to insufficient suspended-sediment concentration or grain-size information. An estimation of the inherent errors in calculating river-sediment load is discussed in detail below. We note that none of the rivers that drain into San Francisco Bay (including the Sacramento and San Joaquin Rivers and numerous smaller streams) have been considered in these estimates. Fine-sediment contributions from San Francisco Bay to the ocean are not accurately known, and no rigorous monitoring program has been conducted to measure fluxes through the Golden Gate. San Francisco Bay acts to modify the amount and timing of the sediment discharge from the Sacramento and San Joaquin Rivers and other streams draining into the bay. As an estuary, the bay allows transport of water and sediment both into and out through the Golden Gate during times of flood and ebb tides, respectively. Schoelhamer and others (2005) estimated an annual average net export of approximately 4 Mt of fine sediment out of the bay to the coastal ocean as a result of material delivered from rivers and streams, as well as eroded from the bay floor. Although this estimate is the best available at present, we note that it was calculated on the basis of accretion and erosion rates throughout the expanse of the estuary, not from direct measurements of suspended-sediment concentrations in the water passing through the Golden Gate.

Table 1. U.S. Geological Survey gaging stations used in this study, listed from north to south.

[USGS, U.S. Geological Survey]

Watershed (fig. 1)	USGS gaging station	Length of record (yr)	Drainage area (km^2)
Smith River	11532500	73	1,590
Supply Creek	11530020	6	40
Trinity River	11530000	77	7,390
Klamath River	11523000	77	21,950
Redwood Creek	11482500	53	720
Mad River	11481000	57	1,260
Eel River	11477000	92	8,060
Russian River	11467000	65	3,470
Pine Creek	11460170	3	20
Pescadero Creek	11162500	53	120
San Lorenzo River	11160500	68	270
Salinas River	11152500	75	10,760
Carmel River	11143250	42	640
San Jose Creek	11120510	25	20
Ventura River	11118500	75	490
Santa Clara River	11114000	57	4,130
Calleguas Creek	11106550	23	640
Santa Ana River	11078000	80	4,400
San Juan Creek	11046550	16	300
San Mateo River	11046370	22	340
Santa Margarita River	11046000	74	1,920
San Luis Rey River	11042000	68	1,440
San Dieguito River	11030500	6	880
San Diego River	11022500	67	980
Tijuana River	11013500	46	4,390

Rating Curves

The USGS operates numerous gaging stations throughout California that measure river stage (height above a referenced datum), which is then converted to river discharge by using a stage-discharge rating curve, constructed from coincident measurements of both stage and discharge at a given station. Data are then reported as average daily flow rates and published in annual water-year (Oct. 1–Sept. 30) summaries, as well as online (URL *http://waterdata.usgs.gov/nwis/*). Operation and maintenance of the stream gages are standardized, as described by Rantz (1982). Although many U.S. rivers have been monitored for water discharge for a century or more, sediment-discharge data are relatively few and limited in scope. Also, many river-discharge stations have been removed and the coverage of small rivers reduced in recent years (Rantz, 1982).

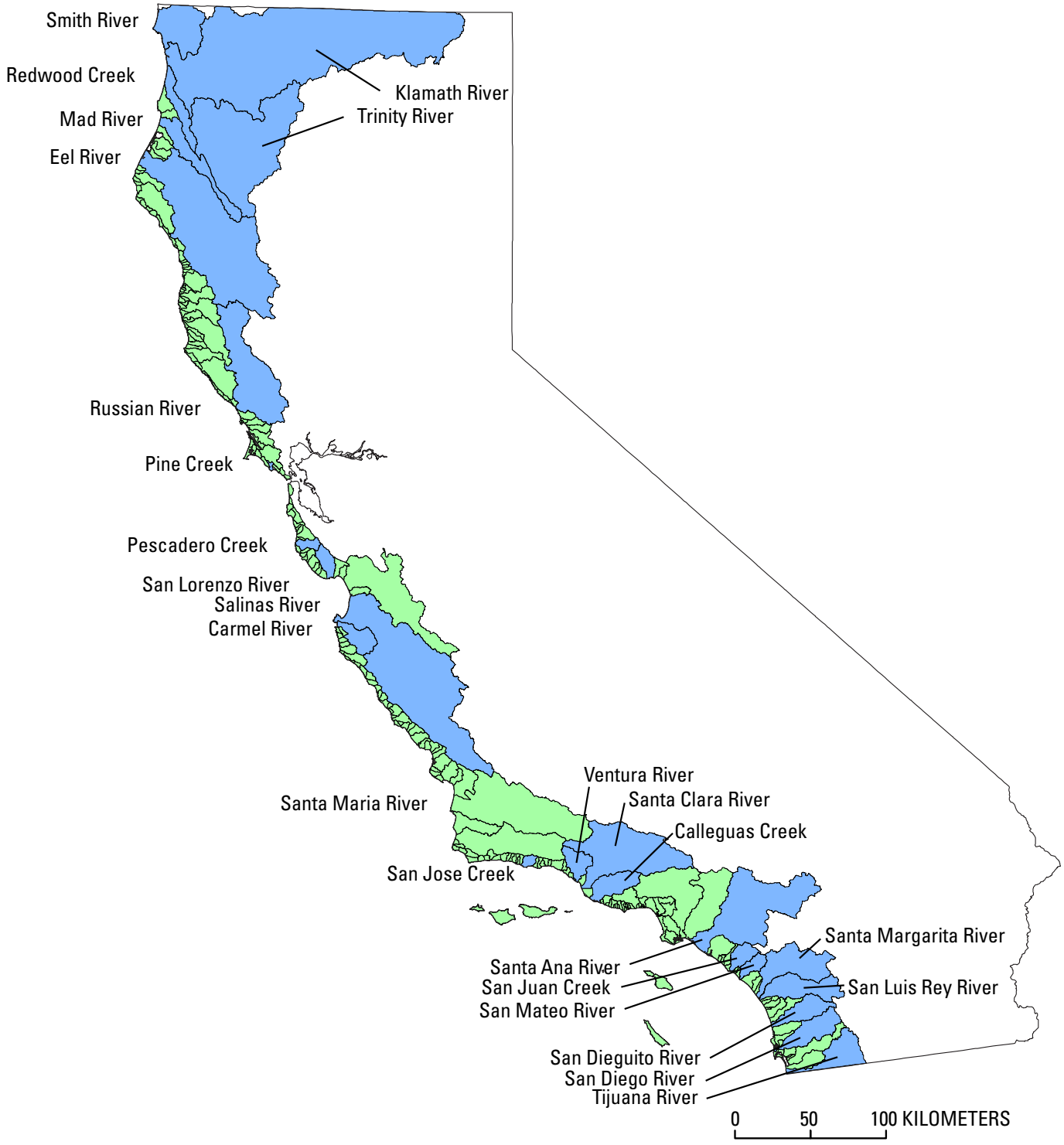

Figure 1. Outline map of California coast, showing locations of watersheds used in this study. Sediment loads from monitored watersheds (blue areas), for which both suspended-sediment-concentration and discharge data are available, were used to calculate watershed and regional rating curves; sediment loads from watersheds with insufficient data (green areas) were calculated from regional rating curves.

Suspended-sediment data are collected as flow-weighted, depth-integrated samples across a stream section and compiled into a single value (Guy and Norman, 1970). In contrast to water discharge, which is continuously or nearly continuously measured from stage-discharge recorders, suspended-sediment concentration is typically measured manually at fixed time intervals or during flood events. In the absence of these continuous sediment-discharge data, empirical relations, such as rating curves, have been used to estimate river-sediment loads; these curves describe the average relation between water-discharge rate and suspended-sediment concentration at a given station.

Numerous methods are available for quantifying sediment-discharge relations (Campbell and Bauder, 1940; Walling, 1977; Ferguson, 1987; Asselman, 2000). The sediment-discharge rating curves calculated for this study were constructed by a localized regression ("loess") curve-fitting technique, originally proposed by Cleveland (1979), that allows for a locally weighted polynomial regression to be calculated around each data point. As shown by Hicks and others (2000) and Warrick and others (2004a), this approach works well for small, steep rivers, such as those in California. At each point, a low-degree polynomial is fitted to a surrounding data subset (the subset window) by using a weighted-least-squares method, giving more weight to points near the center of the data subset and less weight to those on the subset margins. Further details of this method are provided in appendix B. Loess rating curves were calculated for each California coastal watershed on the basis of average-daily-discharge (Q) and suspended-sediment concentration (C) data from the USGS database (URL *http://co.water.usgs.gov/sediment/stationanchor.cfm*). Residuals were analyzed for assurance of nonsystematic distributions in the estimation. Examples of loess rating curves and residual analyses for the Santa Clara River (fig. 1) are plotted in figure 2, and all the calculated loess rating curves and residual analyses are plotted in appendix B. A summary of error calculations from these data is included below.

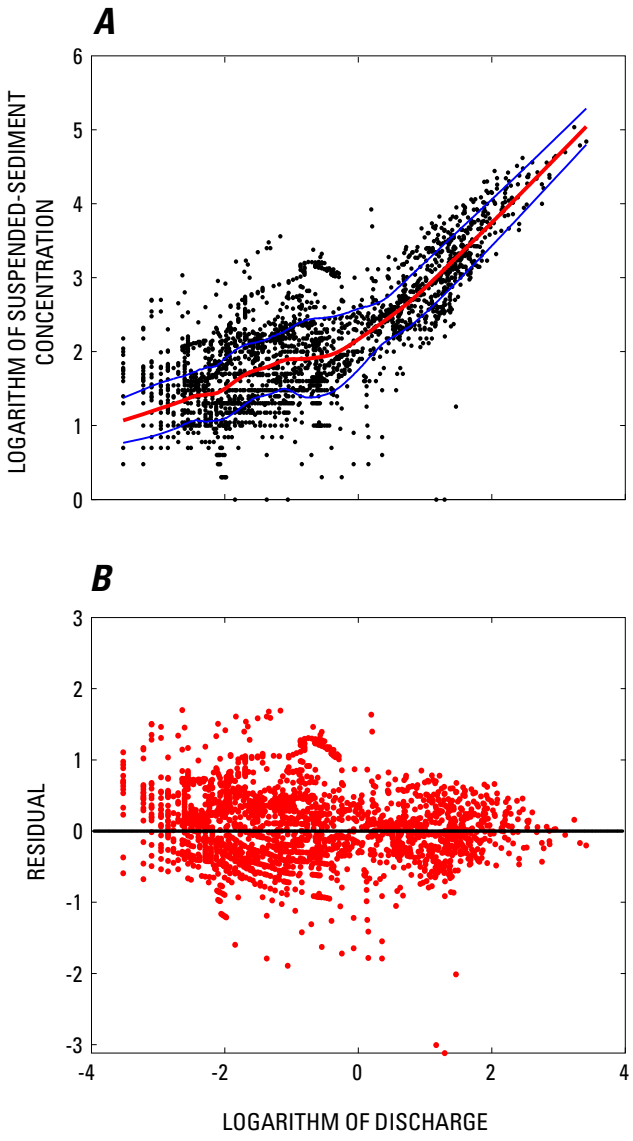

Figure 2. Suspended-sediment concentration versus discharge for the Santa Clara River (fig. 1). *A*, Loess rating curve (red), with ±2σ deviations (purple) shown for reference. *B*, Residuals of data points in figure 2*A*. Data from U.S. Geological Survey gaging station 11114000 (see fig. 23*C* for location). See appendix B for rest of calculated loess rating curves.

Fine-Sediment Fraction

The amount and grain size of sediment transported by a river depend on the velocity and total discharge rate and the supply of sediment available to the river. In most rivers, suspended sediment makes up most (commonly >80 percent) of the total sediment load (Walling and Webb, 1981; Hadley and others, 1985). As river discharge increases, suspended-sediment concentration also commonly increases, and the grain-size distribution may also change (fig. 3). This distribution may become either coarser or finer with increasing discharge, depending on watershed and channel characteristics (Walling and Moorehead, 1989).

To account for the changing grain-size characteristics of rivers, we calculated the fine-sediment fraction of the total suspended-sediment load over a wide range of discharges for each river. Data were obtained from the USGS National Water Information System (NWIS)'s Water Quality section (URL *http://waterdata.usgs.gov/nwis/*). The temporal variation in grain-size distribution was quite large, especially for southern arid rivers. To account for this variation and to be able to apply grain-size distributions across a wide discharge range, a loess rating curve was used to relate the fine-sediment fraction of the suspended-sediment load to discharge. An example of a grain-size/discharge relation is plotted in figure 4, and all the fine-sediment-fraction/discharge curves are plotted in appendix C.

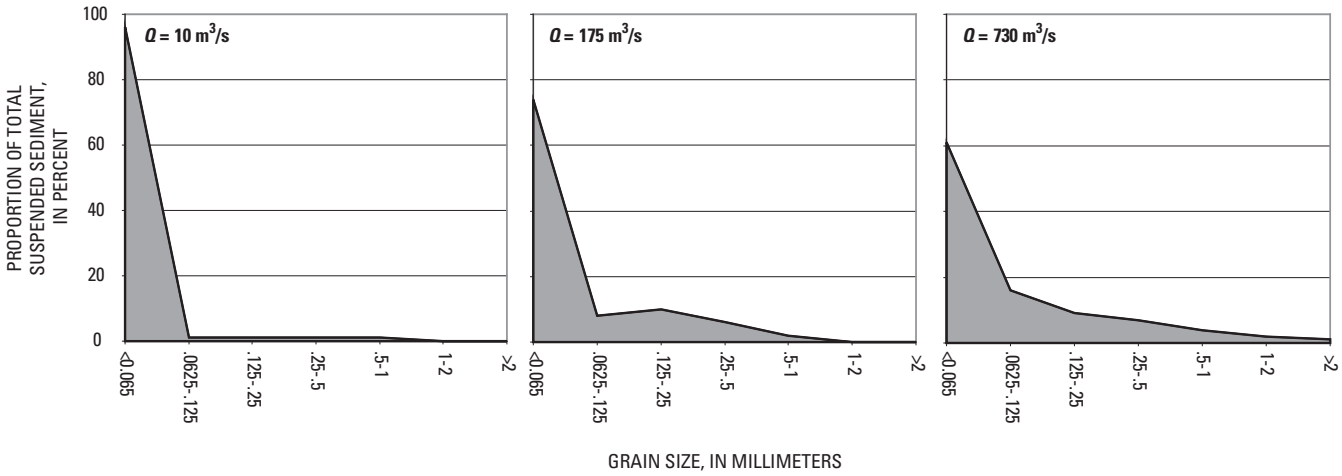

Figure 3. Grain-size distribution at three different discharges (Q) for the Santa Clara River (fig. 1), showing how suspended sediment varies with discharge. Data from U.S. Geological Survey gaging station 11114000 (see fig. 23C for location).

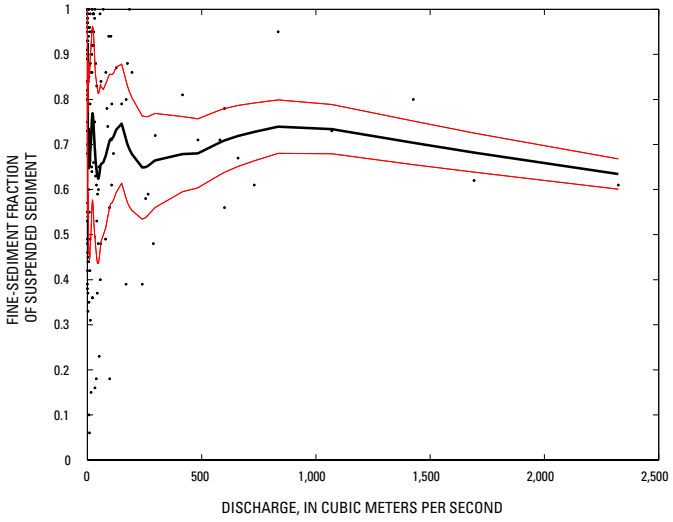

Figure 4. Fine-sediment fraction of suspended sediment versus discharge (Q) for the Santa Clara River (fig. 1), showing how suspended sediment varies with discharge, as shown in figure 3. Data from U.S. Geological Survey gaging station 11114000 (see fig. 23C for location).

Error Calculations

Errors are inherent in all the calculations to determine the sediment delivery from rivers to the coastal ocean; the estimated accuracy of rating curves ranges from 30 to 50 percent (Komar, 1996; Willis and Griggs, 2003). For this study, we considered five types of errors to estimate the total error in calculating annual sediment delivery, as summarized below. Once determined, the sum of the squares of all errors was calculated to provide an envelope of confidence around annual estimates (Taylor, 1997).

Original Measurement and Reporting

Error in the original measurements stems from depth-integrated sampling methods based on the discharges estimated from stage-discharge rating curves. Yu (2000) stated that the average relative error of these curves is approximately 8 percent, but some error is also present in the depth-integrated sampling method. Accordingly, we estimated a total measurement error of 10 percent (Guy and Norman, 1970; Wass and Leeks, 1999) for both of these errors together.

Sediment-Discharge Rating Curve

Error associated with the sediment-discharge rating curves was calculated at the same time as the loess rating curve for each river. Because the loess rating curve is calculated by using weighted local regression, the error for each estimate was calculated by using the standard error of estimate. This error was then associated with that portion of the loess rating curve and applied to estimates calculated from the sediment-discharge rating curve.

Extrapolation of Loess Rating Curve

Sediment-discharge rating curves were calculated by using the range of discharges represented by the sampling. However, it was common for there to be days when the discharge was higher or lower than values contained in the loess rating curve. Therefore, the loess rating curve was extrapolated by using the mean of the last five maximum/minimum values sampled. We estimate that an error of 10 percent was associated with this extrapolation, mostly from the extrapolation to higher values.

Fine-Sediment-Fraction/Discharge Relation

The error associated with accounting for the fine-sediment fraction was calculated in the same manner as for the sediment-discharge rating curve. The standard estimated error was calculated for the loess rating curve; this error was then applied to each of the estimates of daily sediment discharge.

Extrapolation of Fine-Sediment-Fraction/Discharge Relation

The fine-sediment-fraction/discharge relation was similar to the sediment-discharge rating curve in that discharges were larger or smaller than those used in calculating their relation. Therefore, we used the same extrapolation method in this relation as in the sediment-discharge rating curve. An error of 10 percent was applied to measurements extrapolated to higher or lower values.

Calculation of Sediment Load

Daily sediment loads were calculated for each of the rivers in this study. Daily fine-sediment fluxes were calculated by using daily discharges, sediment-discharge rating curves, and fine-sediment-fraction/discharge relations. Daily sediment loads were then summed within each water year (Oct.–Sept.) to determine total annual sediment loads (fig. 5). Errors in these estimates were also calculated, allowing for determination of both a lower and an upper bound to annual sediment loads (table 3). Once these values were determined, fine-sediment yields were calculated and extrapolated to unmonitored watersheds, as discussed below.

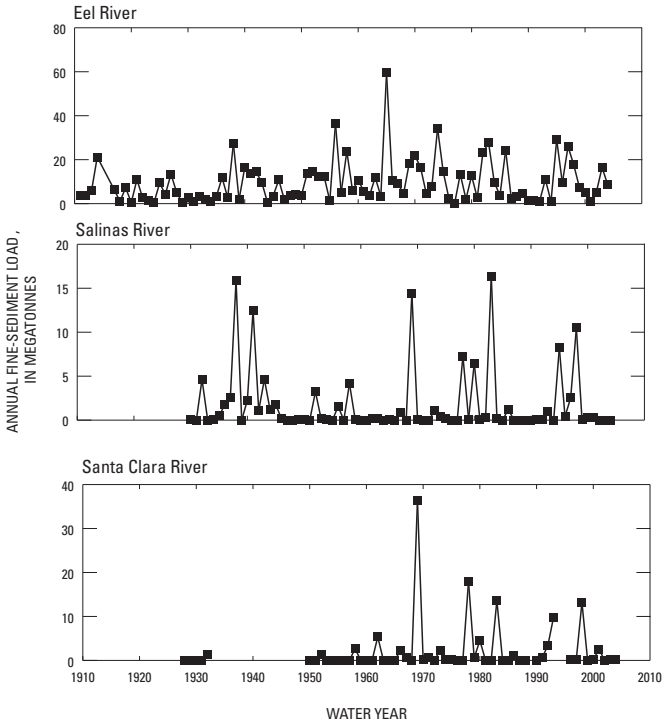

Figure 5. Annual time series of fine-sediment flux from three largest river-sediment sources to the California coast (fig. 1). Annual discharge from each of these rivers varies widely, regardless of sediment load.

Extrapolation to Unmonitored Watersheds

The region draining directly into the California coastal ocean (excluding San Francisco Bay and its tributaries) encompasses an area of slightly less than 100,000 km^2, of which monitored watersheds account for 79 percent and unmonitored watersheds the remaining 21 percent (fig. 1). To extrapolate estimated sediment loads from monitored to unmonitored watersheds, we used sediment yield, defined as the average annual sediment load per unit area of watershed, equivalent to an average erosion rate (in millimeters per year).

For this study, we calculated sediment yields for monitored watersheds only on the basis of uncontrolled-watershed area (that is, the area downstream from any dams), assuming that negligible sediment passes through the dams, an assumption consistent with the coarse-sediment results of Willis and Griggs (2003). Although fine sediment would be more likely to pass through reservoirs than would sand-size sediment, owing to slower settling velocities, most structures built on the coastal watersheds in this study area are large enough to eliminate fine-sediment discharge. We then calculated regional sediment loads by extrapolating estimated sediment yields from monitored to neighboring unmonitored watersheds. Five regions of similar sediment yield were defined on the basis of similar geology and land use (Inman and others, 1998): (1) North Coastal Range rivers (49 percent of total land area; north of San Francisco Bay); (2) South Coastal Range rivers (22 percent of total land area; south of San Francisco Bay and north of the Santa Ynez River); (3) Transverse Range rivers (9 percent of total land area; from the Santa Ynez River to Malibu Creek); (4) Urban rivers (5 percent of total land area; south of Malibu Creek through Los Angeles to the Santa Ana River); and (5) Peninsular Range rivers (15 percent of total land area; from the Santa Ana River to the Tijuana River).

Measured sediment yields from each watershed were then used to estimate a mean regional sediment yield. One important issue to be taken into account when using an extrapolation of sediment yield from monitored to unmonitored watersheds is the well-described inverse relation between sediment yield and watershed area (fig. 6; Milliman and Syvitski, 1992). This issue is relevant because most unmonitored watersheds are the smallest along the California coast. To account for this condition, only the small monitored watersheds in each region were used to estimate regional sediment yields. A mean sediment yield was calculated for each region, along with estimates of upper and lower bounds (fig. 7*A*). These regional mean sediment yields were then applied to unmonitored watersheds to estimate the regional fine-sediment fluxes (fig. 7*B*).

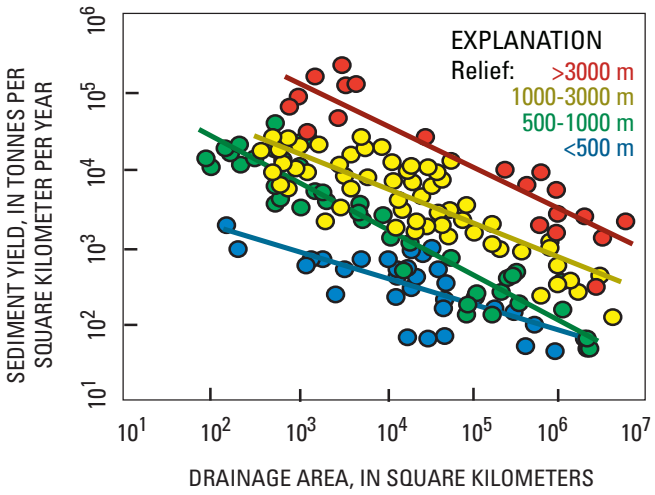

Figure 6. Sediment yield of global rivers, showing how yield increases as watershed area decreases. Curves are fitted for various watershed reliefs. After Milliman and Syvitski (1992).

River-Sediment Discharge

Overall, we calculate that an average of 34 Mt (range, 15–60 Mt) of fine sediment is discharged by rivers to California coastal waters each year, excluding sediment from San Francisco Bay (fig. 8; table 2), on the basis of available discharge data for monitored watersheds (table 3), together with extrapolation to neighboring unmonitored watersheds (table2). Note that these values vary both spatially and temporally. The Eel River dominates the fine-sediment flux from all of coastal California with approximately 9 Mt/yr, or more than 25

A

Step 1: Regional sediment yields for small monitored watersheds are determined

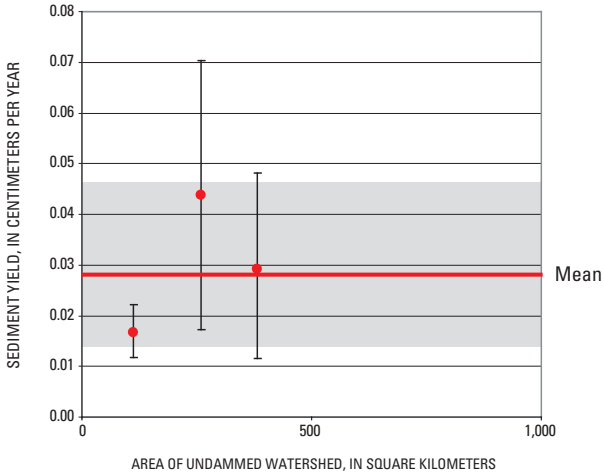

B

Step 2: Regional means are then applied to unmonitored watersheds

Santa Cruz coastal creeks (watershed area, 200 km^2)

	Sediment yield (cm/yr)	Volume (m^3/yr)	Mass (t/yr)
High	0.047	94,000	150,400
Mean	0.030	60,000	96,000
Low	0.015	30,000	48,000

Figure 7. Steps involved in extrapolation of regional average sediment yields (*A*) to unmonitored watersheds (*B*), using mean yield from South Coast region rivers (fig. 1) as an example. Uncertainty envelope in figure 7*A* is indicated by high and low estimates (gray areas).

Table 2. Regional mean annual fine-grained sediment loads from California coastal watersheds.

[All values in tonnes]

Region/cell	Monitored rivers	Unmonitored rivers	Total supply
North Coast region:			
Input (t)	13,667,000	5,320,000	18,987,000
Proportion (percent)	72	28	
South Coast region:			
Input (t)	2,146,000	3,502,000	5,648,000
Proportion (percent)	38	62	
Transverse Ranges:			
Input (t)	2,989,000	3,217,000	6,206,000
Proportion (percent)	48	52	
Urban rivers:			
Input (t)	140,000	2,221,000	2,361,000
Proportion (percent)	6	94	
Peninsular Ranges:			
Input (t)	288,000	116,000	404,000
Proportion (percent)	71	29	

Table 3. Mean annual sediment loads for California coastal rivers.

[USGS, U.S. Geological Survey. Lower and upper bounds of fine-sediment load are based on error estimates]

Watershed (fig. 1)	USGS gaging station	Length of record (yr)	Drainage area (km^2)	Lower bound (t)	Mean annual fine-sediment load (t)	Upper bound (t)	Total suspended-sediment load (t)
Smith River	11532500	73	1,590	135,800	206,700	277,700	389,500
Supply Creek	11530020	6	40	1,200	4,100	7,000	9,700
Trinity River	11530000	77	7,390	444,000	1,779,400	3,114,900	3,186,400
Klamath River	11523000	77	21,950	741,100	1,211,800	1,682,400	1,761,700
Redwood Creek	11482500	53	720	309,500	623,700	961,600	816,100
Mad River	11481000	57	1,260	767,700	1,328,900	1,890,200	1,921,600
Eel River	11477000	92	8,060	4,915,800	9,485,600	14,055,300	11,798,600
Russian River	11467000	65	3,470	466,500	804,300	1,142,200	897,000
Pine Creek	11460170	3	20	3,500	5,400	11,000	6,400
Pescadero Creek	11162500	53	120	21,300	30,100	40,100	42,900
San Lorenzo River	11160500	68	270	72,000	183,300	294,600	284,700
Salinas River	11152500	75	10,760	851,000	1,752,500	2,654,100	2,211,200
Carmel River	11143250	42	640	71,300	179,800	296,700	393,900
San Jose Creek	11120510	25	20	– –	10,600	23,800	14,400
Ventura River	11118500	75	490	– –	197,000	401,500	274,400
Santa Clara River	11114000	57	4,130	283,100	2,152,200	4,021,200	3,092,100
Calleguas Creek	11106550	23	640	435,500	628,700	822,000	883,900
Santa Ana River	11078000	80	4,400	– –	140,500	305,600	237,000
San Juan Creek	11046550	16	300	13,000	70,400	127,700	98,100
San Mateo River	11046370	22	340	700	2,100	3,700	2,700
Santa Margarita River	11046000	74	1,920	27,600	66,500	109,000	79,800
San Luis Rey River	11042000	68	1,440	– –	20,800	58,000	46,000
San Dieguito River	11030500	6	880	1,100	1,900	2,700	2,000
San Diego River	11022500	67	980	11,300	16,000	21,500	16,500
Tijuana River	11013500	46	4,390	– –	110,100	322,900	148,300

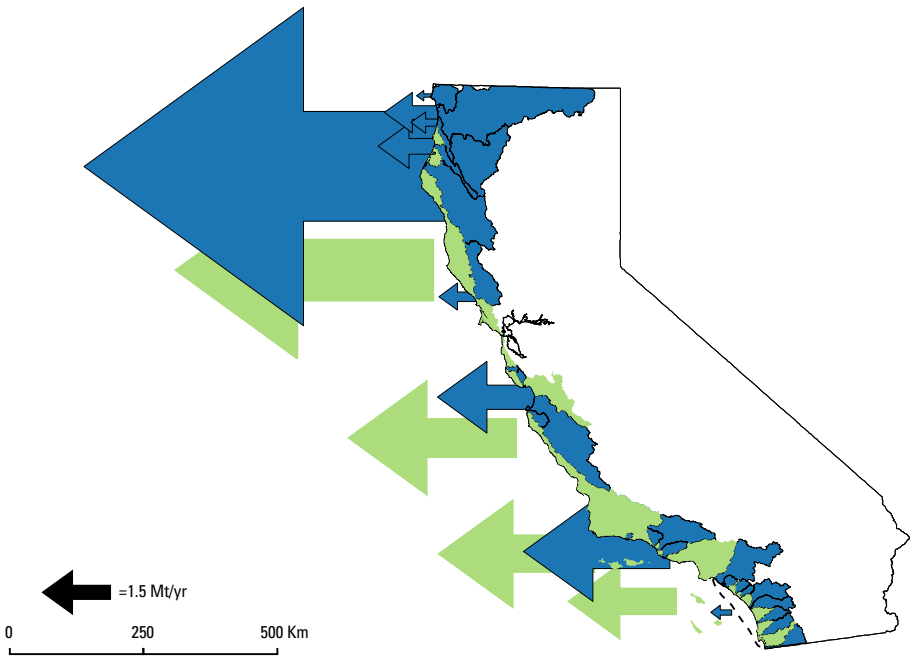

Figure 8. Average annual fine-sediment flux from California coastal rivers (blue areas, monitored watersheds; green areas, unmonitored watersheds; see fig. 1 for locations), excluding input from San Francisco Bay, which is estimated at 4 Mt/yr. Size of arrows is proportional to total fine-sediment flux; black reference arrow corresponds to a value of 1.5 Mt/yr. See tables 2 and 3 for details.

percent of the average total sediment flux from all of coastal California (fig. 8). North Coastal Range rivers dominate this fine-sediment flux, with greater than 50 percent originating from these watersheds, a rate approximately equivalent to this region's proportion of the total coastal drainage area (fig. 9). The second-largest regional fine-sediment load is from the Transverse Range, with the Santa Clara River dominating the region (figs. 8, 9), which produces a disproportional amount of sediment (18 percent of load from only 9 percent of area), owing to its geology, land use, and tectonics (see Scott and Williams, 1978; Inman and Jenkins, 1999). The third-largest regional fine-sediment load is from South Coastal Range rivers, with the Salinas River dominating the region (fig. 9). Regional sediment discharge from Peninsular Range rivers is comparatively small with respect to the rest of the State, at an average rate of 0.4 Mt/yr (figs. 8, 9).

Urban rivers have sediment yields that are the second highest of the five regions and slightly less than Transverse Range rivers (fig. 9). An equivalent annual sediment yield should be expected for these regions, however, owing to their similar geologic settings (Scott and Williams, 1978; Inman and Jenkins, 1999). Thus, our results suggest a possibly slight decrease in annual sediment yield due to urbanization or other watershed differences. Urbanization in southern California has been shown to change the dominant areas of erosion within a watershed (Trimble, 1997). Another effect of urbanization may include increased stormwater runoff, which can decrease suspended-sediment concentrations (Warrick and Rubin, 2007).

Sediment delivery from these coastal watersheds is extremely episodic. We see sharply rising and falling hydrographs during and after storms, mainly owing to the rapid routing of stormwater through the watersheds (fig. 10), resulting in episodic delivery of suspended sediment to the coastal ocean, and the delivery of much of the annual sediment load from these rivers within only a few days. For example, most rivers in southern California deliver 90 percent of the long-term fine-sediment load during less than 1 percent of the year (that is, in less than 4 days per year on average; fig. 11). Significant sediment discharge from central and northern California rivers, though still episodic, occurs over slightly longer periods (fig. 11).

The number and magnitude of storm events during the year drives the transport and delivery of sediment from these rivers. The interannual variation in this "storminess" is driven by large-scale climatic forcings, which, in turn, can cause orders-of-magnitude variations in year-to-year fine-sediment fluxes (fig. 5). The El Niño/Southern Oscillation (ENSO) plays a key role in river flooding within southern California (Andrews and others, 2004). Recently, the

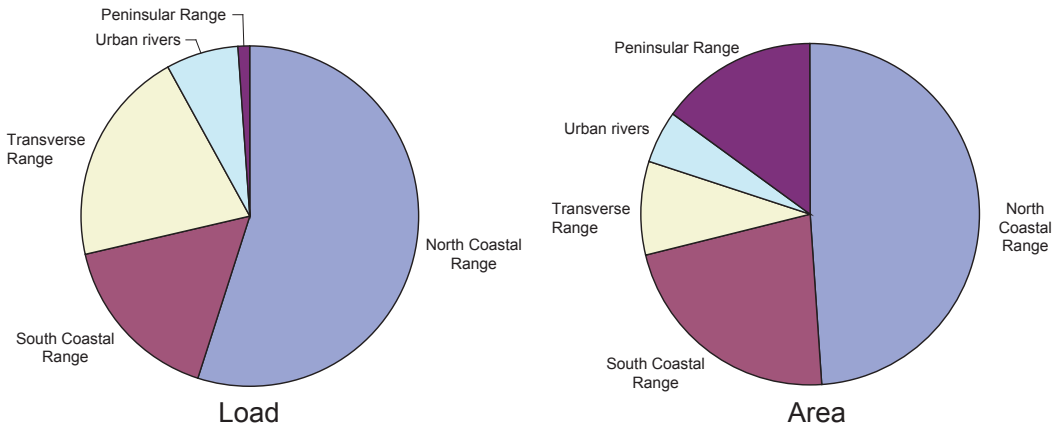

Region	Total fine-sediment load (Mt)	Percentage of total load	Percentage of total area	Load/area ratio
North Coastal Range	19	57	49	1.16
South Coastal Range	5.7	17	22	0.77
Transverse Range	6.2	18	9	2.00
Urban rivers	2.4	7	5	1.40
Peninsular Range	0.4	1	15	0.07

Figure 9. Regional distribution of annual fine-sediment flux from California coastal rivers (fig. 1). Transverse Range rivers (Santa Barbara region) discharge a disproportionate amount of sediment from local watersheds, mostly owing to regional geology, whereas Peninsular Range rivers discharge much less sediment than would be predicted on the basis of watershed area alone.

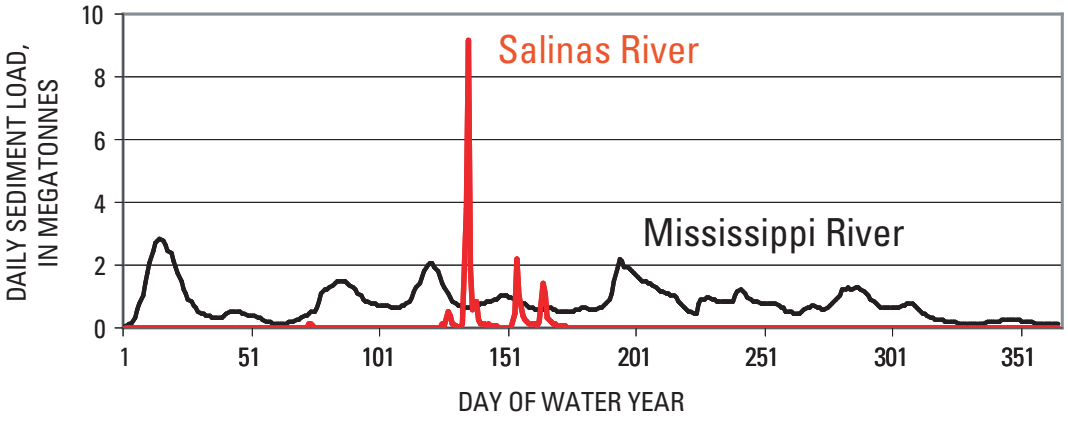

Figure 10. Annual hydrographs for the Salinas River (fig. 1) in 1938, which has a drainage area of about 11,000 km^2, and the Mississippi River in 1960, which has a drainage area of about 3.3 million km^2. Smaller rivers, especially those draining steep watersheds, have very steep rising and falling limbs on hydrographs, as shown by major flood event over the course of a few days on the Salinas River, whereas the Mississippi River has a much more protracted flood events, owing to its large drainage area. Water year is defined as October 1 through September 30.

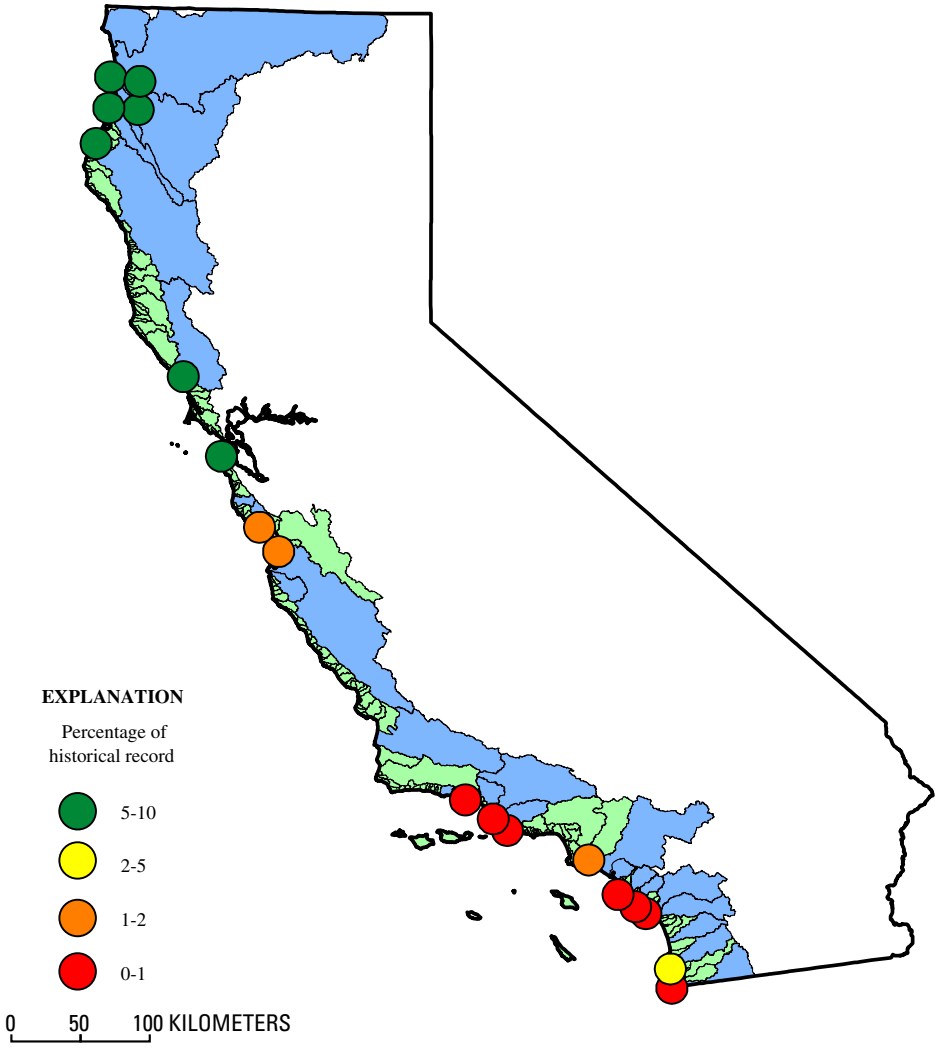

Figure 11. Outline map of California, showing percentages of historical record needed to account for 90 percent of total sediment load from coastal rivers. All the watersheds mentioned in this study are event driven, but sediment load from southern California rivers is extremely episodic because of the semi-arid environment.

influence of the Pacific Decadal Oscillation (PDO), an ENSO-like atmospheric/oceanic phenomenon in the North Pacific Ocean, has also been observed to be important to California river discharge (Mantua and others, 2002). These two large-scale climatic phenomena, ENSO and PDO, are significantly correlated with annual discharge from California coastal rivers (fig. 12). When the warm phases of these phenomena occur, discharge from the rivers of southern and central California increases. The opposite is true in the Pacific Northwest, where the cool phases of ENSO and PDO result in greater river discharge (Mantua and Hare, 2002). Northern California appears to lie within the transition zone between the warm-phase region in the south and the cool-phase region in the north and thus shows an almost-equal importance of both the warm and cool phases (fig. 12).

Cliff and Bluff Sources

Many factors influence the delivery of fine sediment from coastal cliffs and bluffs, including, but not limited to, sea-level rise, degree of consolidation of the material, hardness of the material, wave climate in the area, protective barriers (natural or anthropogenic), tidal range, and ground-water flow. Approximately 72 percent of the California coastline consists of cliffs and bluffs (Patsch and Griggs, 2007), some of which are fronted by beaches and others not. Long-term rates of seacliff erosion are difficult to constrain, owing to wide spatial variation and the episodicity of seacliff failure (Komar, 1996). This variation, together with the size of the study area (fig. 1), adds to the complexity of estimation for this sediment source.

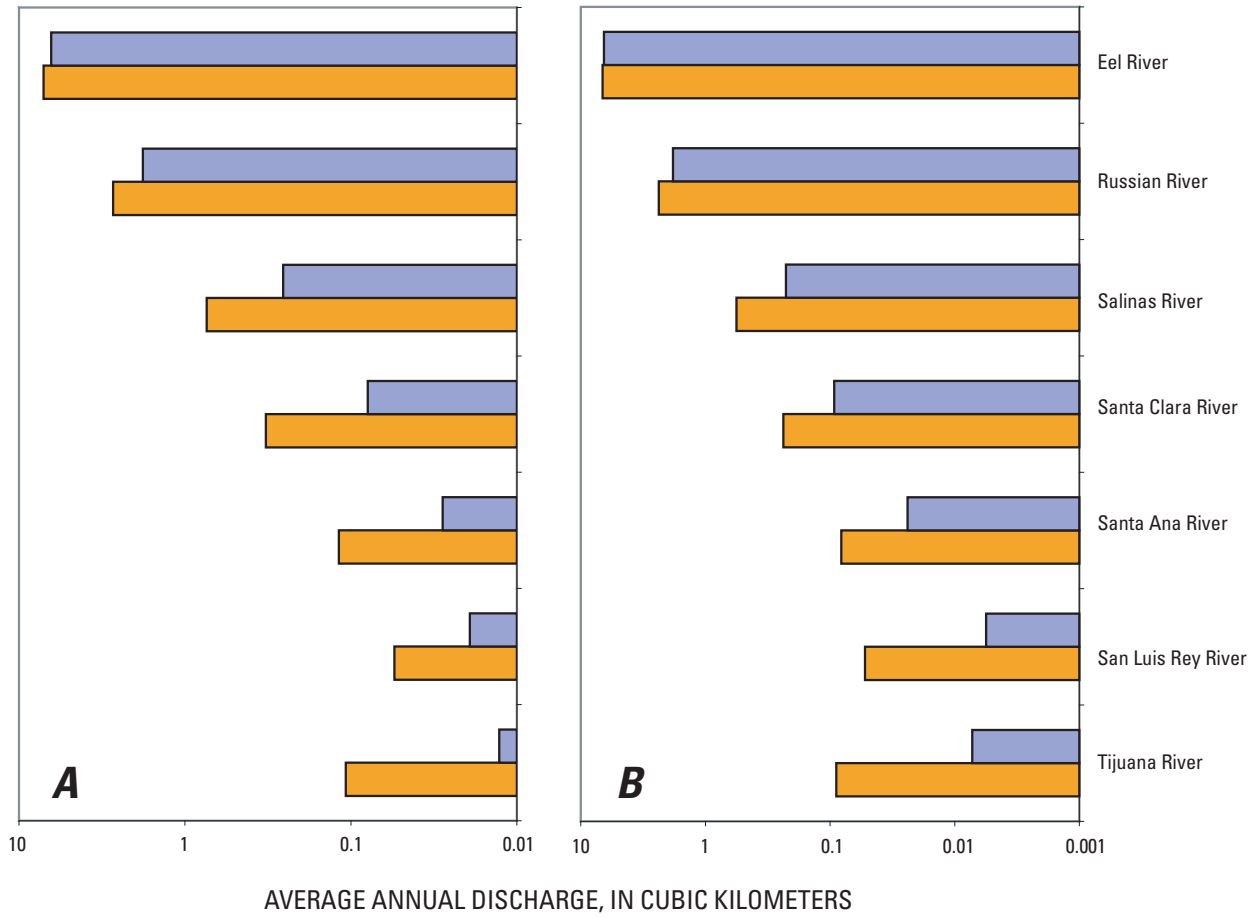

Figure 12. Logarithmic bar charts showing influence of El Niño-Southern Oscillation (ENSO) (*A*) and Pacific Decadal Oscillation (PDO) (*B*) on discharge from several California rivers (see fig. 1 for locations). Warm phases of ENSO and PDO shown with orange bars, and cool phases shown with blue bars. Discharge from rivers in southern California is strongly influenced by warm phases of both ENSO and PDO, whereas that from rivers in northern California is equally influenced by both warm and cool phases.

Fine-sediment inputs from cliff and bluff erosion for this study were calculated on the basis of the work of Patsch and Griggs (2007), whose estimates of the volumetric erosion rate (V_{IC}) were calculated by using the equation

$$V_{IC} = \text{cliff length} \times \text{cliff height} \times \text{cliff-erosion rate} \times \text{grain-size fraction}.$$

Patsch and Griggs calculated the contribution of sand-size material from cliff erosion, using estimated percentages of sand in the cliff and bluff material. Here we were interested in the fine-sediment fraction, and so we used an estimated percentage of fine sediment in the material instead, defined to be 100 percent minus the percentage of sand, assuming a negligible amount of grain sizes larger than sand (for example, gravel and cobbles).

Cliffs along the California coastline are commonly made up of multiple rock types. For example, bedrock is commonly capped with an alluvial deposit, whereby the equation becomes

$$\begin{aligned} V_{IC} &= (\text{length} \times \text{erosion rate} \times \text{rock1} \times \%\text{mud1}) + \\ &\quad (\text{length} \times \text{erosion rate} \times \text{rock2} \times \%\text{mud2}) \\ &= \text{length} \times \text{erosion rate} \times [(\text{rock1} \times \%\text{mud1}) + \\ &\quad (\text{rock2} \times \%\text{mud2})], \end{aligned}$$

where rock1 and rock2 are the vertical heights of bedrock and alluvial deposits, respectively, and %mud1 and %mud2 are the percentages of these two rock types that are fine grained. The erosion rates used here were based on the locally determined long-term cliff-retreat rates calculated by Patsch and Griggs (2007). We note, however, that cliff retreat commonly occurs episodically and not always annually.

Using this framework, we calculated the annual contribution of fine sediment from cliffs and bluffs only for the region south of San Francisco Bay. Data coverage on grain size, erosion rate, and the heights of cliffs and bluffs in northern California is unavailable, and so we excluded this region from our analysis. Annual southern California cliff and bluff sediment-supply rates range from approximately 0 to 400,000 m^3/yr (see app. D). Using a dry bulk density of 1,600 kg/m^3 (Griggs and Hein, 1980) these sediment-supply rates are equivalent to a sediment load of approximately 0 to 660,00 Mt/yr, for a total sediment load of 1.3 Mt/yr (fig. 13). The largest input is from the Urban rivers region (Los Angeles area), owing to high erosion rates (~0.3 m/yr) and high mud content in the bedrock (fig. 13). Lower sediment-supply rates (120,000–190,000 m^3/yr) are observed in the South Coastal Range, Transverse Range (Santa Barbara), and Peninsular Range (San Diego) regions (fig. 13). Negligible fine sediment is supplied from the relatively pure eolian sand dunes of southern Monterey Bay (part of the South Coastal Range), which are rapidly eroding (0.5–1.5 m/yr; Thorton and others, 2006), but have little fine sediment.

Cliff and bluff sediment inputs account for anywhere from 0 to 36 percent of the regional fine-sediment supply, suggesting that bluffs are generally a secondary contributor of fine sediment to the California coastal ocean (fig. 14; table 4), except for the Peninsular Range (San Diego region), which contributes 36 percent of the total fine-sediment flux of from cliff and bluff erosion. The Big Sur coastline (part of the South Coastal Range) may also contribute significant amounts of fine sediment from cliffs; however, even-fewer data are available from this region for estimating sediment load.

These results are based on regional rather than local characteristics of the cliffs and bluffs. If more precise values of the sediment load from cliffs and bluffs are desired for the coast, systematic analyses of the grain size of the material making up the cliffs and bluffs are needed. In addition, localized determination of the ease of erosion (hardness, degree of consolidation, presence or absence of internal weaknesses) and local processes (wave energy, storm frequency, protective barriers, ground-water flow, and so on) would improve our understanding of cliff-retreat rates (Benumof and Griggs, 1999; Young and Ashford, 2006) and sediment delivery to the coastal ocean.

Summary

Much fine sediment is delivered to the California coastal ocean from both rivers and coastal cliff and bluff erosion. Rivers dominate this sediment delivery with inputs ranging from 70 to 95 percent of regional fine-sediment budgets (fig. 14). The largest sediment inputs are from the Eel, Salinas, and Santa Clara Rivers (fig. 1), which together discharge an average of approximately 13 Mt/yr (fig. 8; table 3), dominating their respective physiographic regions and accounting for 30 to 50 percent of regional fine-sediment-budget inputs.

The fine-sediment inputs presented here need to be considered within the context of the episodicity of sediment delivery to the California coastal ocean. All California coastal rivers discharge episodically, with large proportions of their annual sediment loads delivered over the course of only a few winter days (fig. 11), and with wet winters dominating long-term sediment loading (fig. 10). Coastal cliff and bluff erosion is also episodic, mostly occurring during infrequent storm events (Storlazzi and Griggs, 2000). Owing to the small watershed areas and proximity to the coast, these storm events may occur simultaneously, resulting in the delivery of large amounts of material concurrently from both river sources and coastal cliff and bluff erosion. Acquisition of additional data on grain sizes and cliff-erosion rates, along with additional suspended-sediment monitoring during storm events, will allow a more accurate estimate of the sources of sediment delivered to the California coastal ocean.

Table 4. Annual fine-sediment contribution from cliff/bluff erosion in central and southern California in comparison with fluvial sources.

Region/cell	Rivers	Cliffs/bluffs	Total supply
South Coast/Santa Cruz:			
Input (t)	2,188,000	195,000	2,383,000
Proportion (percent)	92	8	
Southern Monterey Bay:			
Input (t)	1,753,000	– –	1,753,000
Proportion (percent)	100	– –	
Transverse Range:			
Input (t)	5,335,000	307,000	5,642,000
Proportion (percent)	95	5	
Urban Rivers:			
Input (t)	2,809,000	658,000	3,467,000
Proportion (percent)	6	94	
Peninsular Range:			
Input (t)	404,000	224,000	628,000
Proportion (percent)	64	36	

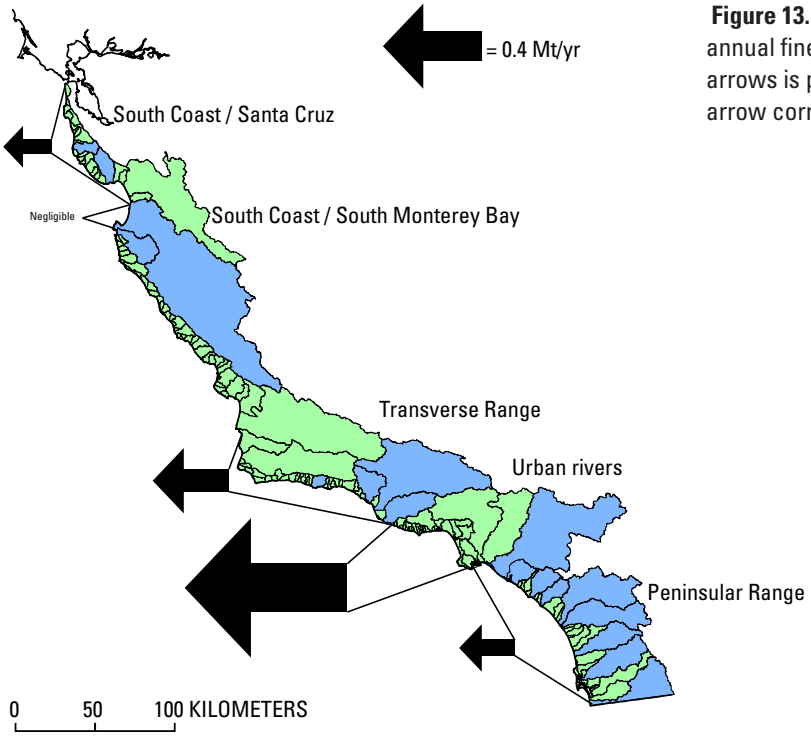

Figure 13. Outline map of southern California coast, showing annual fine-sediment flux due to cliff and bluff erosion. Size of arrows is proportional to total fine-sediment flux; black reference arrow corresponds to a value of 0.4 Mt/yr. See table 4 for details.

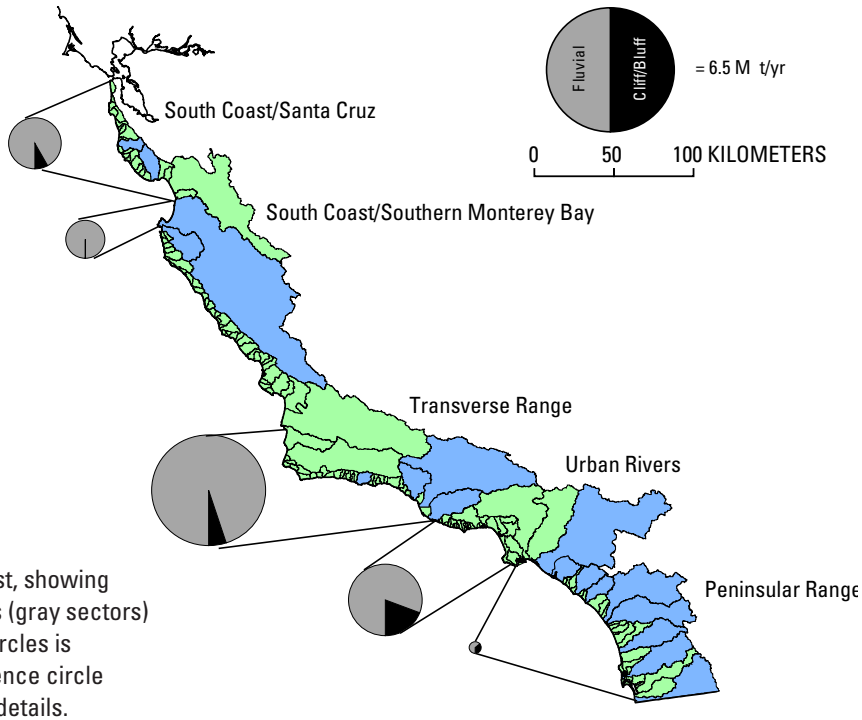

Figure 14. Outline map of southern California coast, showing proportions of fine-sediment flux from river sources (gray sectors) and cliff and bluff erosion (black sectors). Size of circles is proportional to total fine-sediment flux; black reference circle corresponds to a value of 6.5 Mt/yr. See table 4 for details.

Dispersal of Fine Sediment

Introduction

After sediment is introduced into coastal waters, it undergoes intervals of deposition, resuspension, and transport until it is ultimately deposited where it will no longer be disturbed (Wright and Nittrouer, 1995). At this point, the sediment becomes part of the geologic record (Drake, 1999). During this transit from source to sink, the pathways of dispersal are dominantly controlled by sediment-input rates, the physical-oceanographic regime, and the geometries of the margin.

In the previous section, we discussed fine-sediment supply to the California coast, and in this section we discuss sediment-dispersal processes before final deposition. First, we review the current understanding of coastal dispersal of fine sediment, with emphasis on research conducted offshore of the California coast. Most of this work has focused on the dispersal of river sediment because rivers are the dominant sediment source along this coastal margin and cliff and bluff failure events are difficult to observe. We then provide data and analysis to examine the potential for fine-sediment transport after river-discharge events along the California coast. A key element of these analyses is whether river sediment is delivered to the coast under unique oceanographic conditions that could affect the transport and dispersal of this material. If so, the transport of river-flood sediment may not be applicable to other fine-sediment-transport events. Alternatively, if river-discharge events are not unique oceanographically, then studies of the transport and dispersal of flood-derived sediment may be applicable to other fine-sediment sources.

Previous Investigations

As material is introduced into the coastal ocean from rivers, it is exposed to the saline waters of the ocean. Because freshwater is less dense than seawater, river water will typically enter the ocean as a buoyant plume (Wright and Nittrouer, 1995; Geyer and others, 2000). These buoyant plumes, which are commonly quite turbid, owing to fine sediment in suspension, have been observed to extend tens of kilometers from the California shoreline (fig. 15). However, mass balances of the sediment in these plumes suggest that, though turbid, the buoyant plumes offshore of the California coast rapidly lose sediment within kilometers of the river mouths (Geyer and others, 2000; Mertes and Warrick, 2001; Warrick and others, 2004b).

The rapidity of sediment loss from buoyant plumes is partly related to enhancement of settling rates due to flocculation of fine sediment (Geyer and others, 2004). The resulting flocs have low densities because of their large amounts of void space, and are considerably larger than the individual grain sizes within the floc (fig. 16). The resulting floc diameters are large enough to counteract the lower densities, resulting in

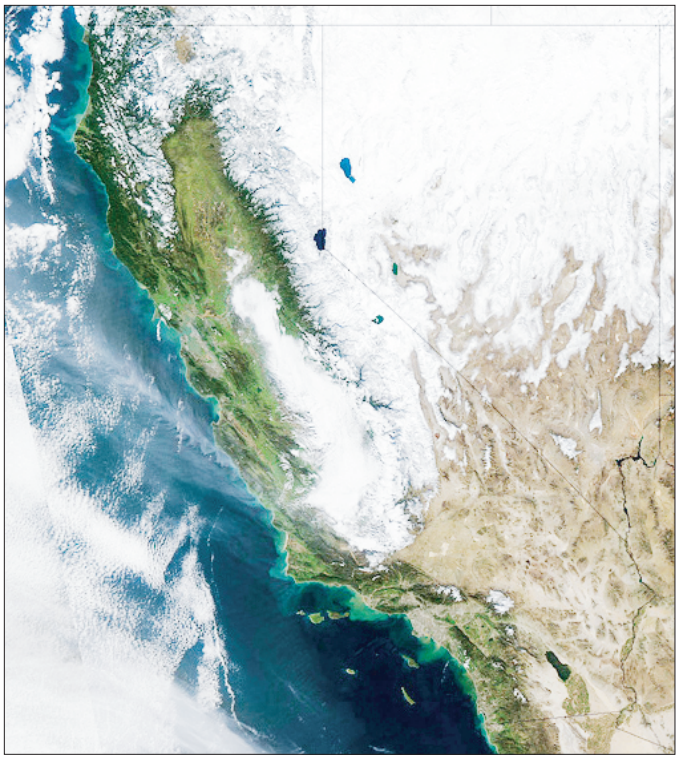

Figure 15. California coast, showing turbid plumes offshore after a winter storm event. National Aeronautics and Space Administration MODIS Aqua satellite image, taken January 12, 2005.

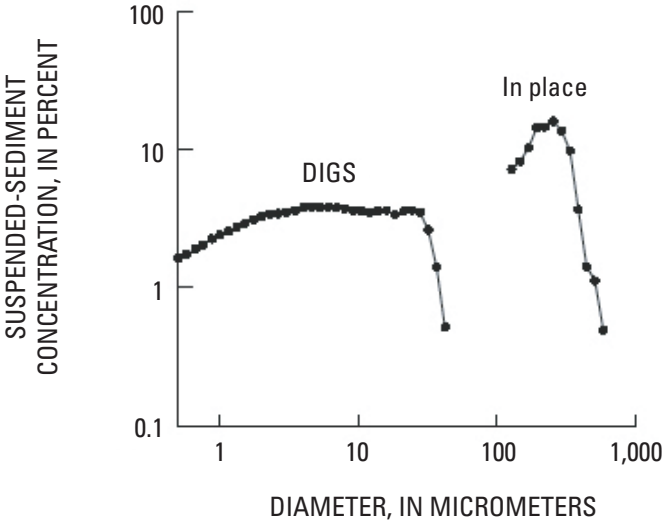

Figure 16. Logarithmic plot of suspended-sediment concentration versus inplace and disaggregated inorganic grain size (DIGS) of sediment particles captured in the Eel River plume (fig. 1) during a flood event (from Geyer and others, 2004). Difference between inplace and DIGS data reflects effect of flocculation on particle size. Inplace flocs are broken apart during laboratory grain-size analysis.

higher settling velocities (~1 mm/s) than those of individual particles (Hill and others, 2000). Laboratory investigations suggest that fine sediment in exceptional concentrations (>1 g/L) may result in even higher rates of settling (~10 mm/s) due to convective instabilities (McCool and Parsons, 2004). Furthermore, a freshwater-sediment mixture with suspended-sediment concentrations higher than 40 g/L will be negatively buoyant in California coastal waters (Mulder and Syvitski, 1995; Warrick and Milliman, 2003). Although California coastal rivers in flood stage commonly produce suspended-sediment concentrations higher than these reported thresholds (Warrick and Milliman, 2003), no field evidence exists to directly indicate the presence of negatively buoyant plumes. Once sediment settles from the buoyant plume, it will continue to settle through the water column toward the seabed, where it may be deposited or transported in suspension.

Thus, much of the fine sediment discharged to the California coast from rivers settles near the river mouths. A well-studied example is the Eel River shelf (fig. 1), where fine sediment is delivered to the ocean in a buoyant plume that hugs the shoreline as it is transported northward (Geyer and others, 2000; Pullen and Allen, 2000) resulting in considerable initial deposition of fine sediment shoreward of the 40-m isobath north of the river mouth (fig. 17). Much of this sediment is eventually transported offshore, however, to the midshelf mud belt that lies between the 60- and 90-m isobaths (fig. 17). This flux of sediment occurs by both resuspension and advection and by fluid-mud gravity flows along the seabed (Ogston and others, 2000; Traykovski and others, 2000), which result from overloading of suspended sediment in the bottom boundary layer and plunge offshore because of the combined effects of negative buoyancy and suspension by bottom-wave orbital velocities (Traykovski and others, 2000; Scully and others, 2002; Harris and others, 2005; Wright and Friedrichs, 2006). Thus, fine-sediment transport on the Eel River shelf is greatly enhanced after river supply of sediment (fig. 18; Ogston and others, 2000), and sediment introduced to this margin may be moved over successive storm events as nearshore deposits of fine sediment are resuspended and transported offshore (fig. 19; Fan and others, 2004).

Fine-sediment dispersal has been studied in only a few other California river-margin settings. Sediment dispersal from the Santa Clara River (fig. 1) was examined by satellite observation and ship-based sampling by Warrick and others (2004b). These results suggest that approximately 90 percent of the fine sediment is rapidly removed from the buoyant plume within 1 km of the river mouth during storm discharge (fig. 20). We note that the Santa Clara River discharges suspended sediment at much higher concentrations than the Eel River, possibly resulting in the enhanced settling rates discussed above. Seabed coring by Drake (1972) after the largest recorded storm discharges in the history of the Santa Clara River (~40 Mt during winter 1968–69) showed that most fine sediment was emplaced near the river mouth in deposits more than 15 cm thick (fig. 21). During the next year, however, this sediment continued to be transported seaward, as evidenced by a shift in the position of the sediment deposit. This observation indicates that the fine sediment discharged from the Santa Clara River may be resuspended and transported for many months after a discharge event, much like on the Eel River shelf.

An example of a study of fine-sediment transport in which the sediment source is not a river is the Palos Verdes margin (fig. 1), where effluent and landslide-derived sediment have mixed to create recent shelf deposits (Lee and Wiberg, 2002). Movement of this effluent-derived sediment is important because it is contaminated with DDT-degradation products (fig. 22). Fine-sediment dispersal from the wastewater outfall is influenced by resuspension by waves and ambient currents (Noble and others, 2002; Sherwood and others, 2002; Wiberg and Harris, 2002; Wiberg and others, 2002). Resuspension of this material occurs an average of 10 times per

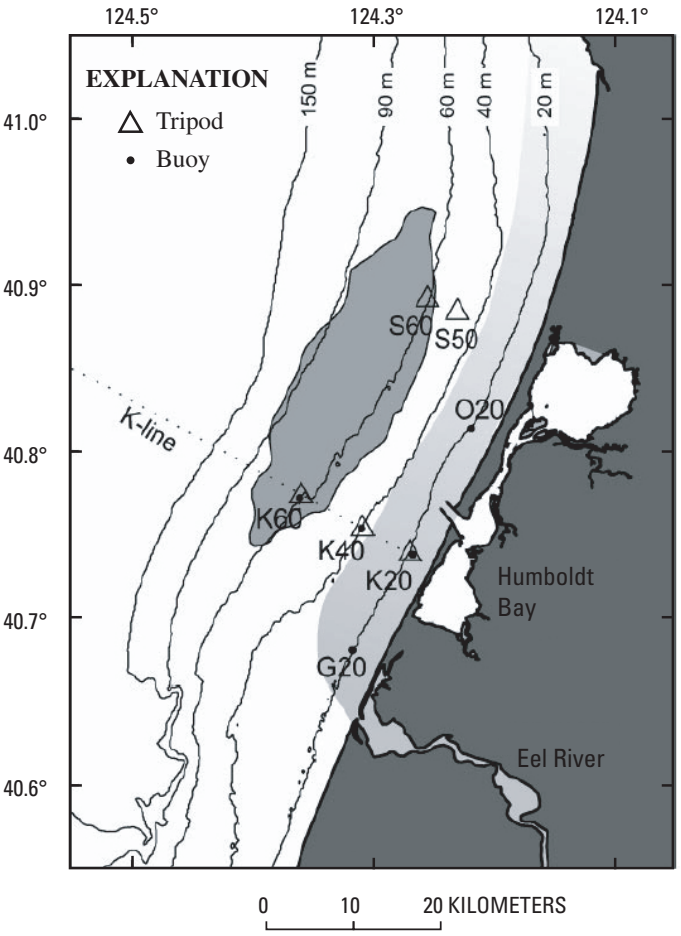

Figure 17. Eel River-Humboldt Bay area (fig. 1), showing locations of turbid buoyant plume during storm event (light-gray area) and poststorm flood deposit (dark-gray area; from Traykovski and others, 2000). A clear spatial discrepancy exists between plume, which occurs inshore of 40-m isobath, and deposit, which is centered between 60- and 90-m isobaths. Dots and triangles represent tripods and buoys instrumented to measure sediment-transport rates.

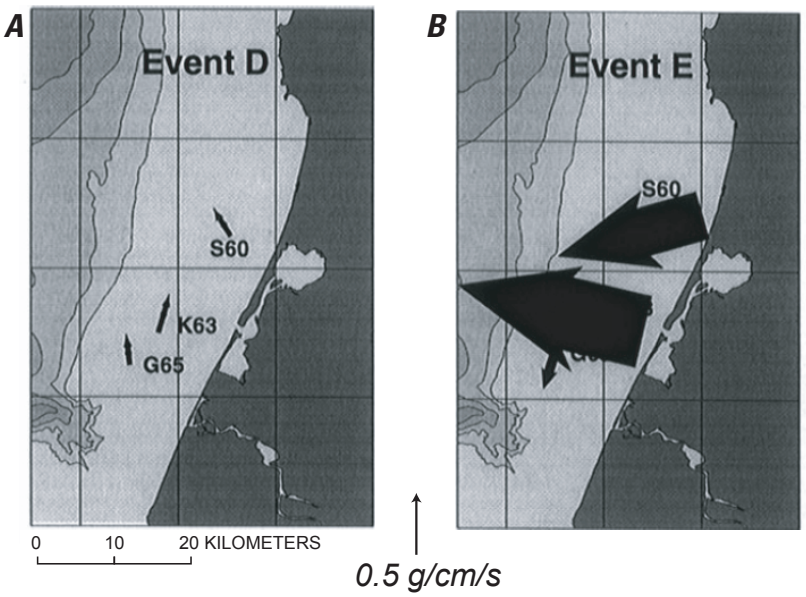

Figure 18. Eel River area (fig. 1), showing magnitude and direction of suspended-sediment transport along seabed offshore of river mouth during two storm events (D, fig. 18*A*; E, fig. 18*B*) in winter 1996–97 (after Ogston and others, 2000). Measurements were made at approximately 60-m water depth, and suspended-sediment transport was calculated as an integrated flux within 1.2 m above seabed. In both events, sediment transport during medium wave events peaked at 4-m wave height, although event E followed a river discharge with a peak flow of more than 11,000 m^3/s.

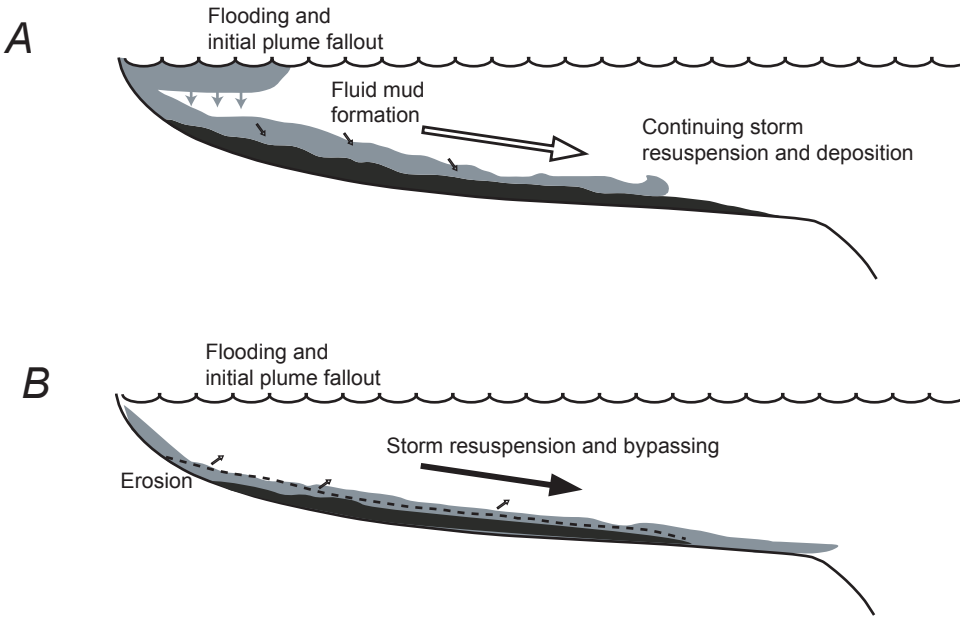

Figure 19. Fan and others' (2004) model for fine-sediment transport offshore of the Eel River (fig. 1), constructed from integrated results of STRATAFORM project (Nittrouer, 1999). Two transport regimes are identified: a high-concentration regime (*A*) that prevails during and immediately after flood events which introduce exceptional amounts of fine sediment, and a poststorm low-concentration regime (*B*) that prevails when shelf is no longer receiving flood-sediment input. During low-concentration regime, storm conditions resuspend sediment and transport it offshore, displacing flood deposit farther offshore.

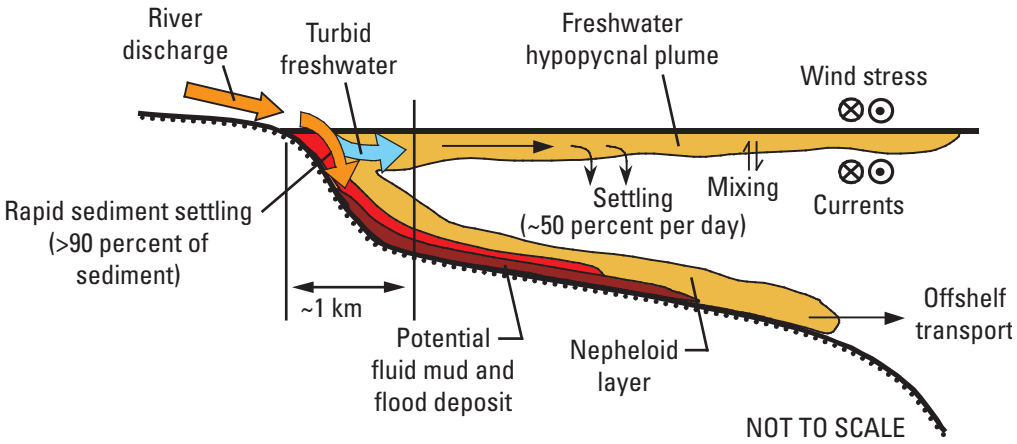

Figure 20. Model for fine-sediment-dispersal pathways during flood-event discharge from the Santa Clara River (fig. 1; after Warrick and others, 2004a).

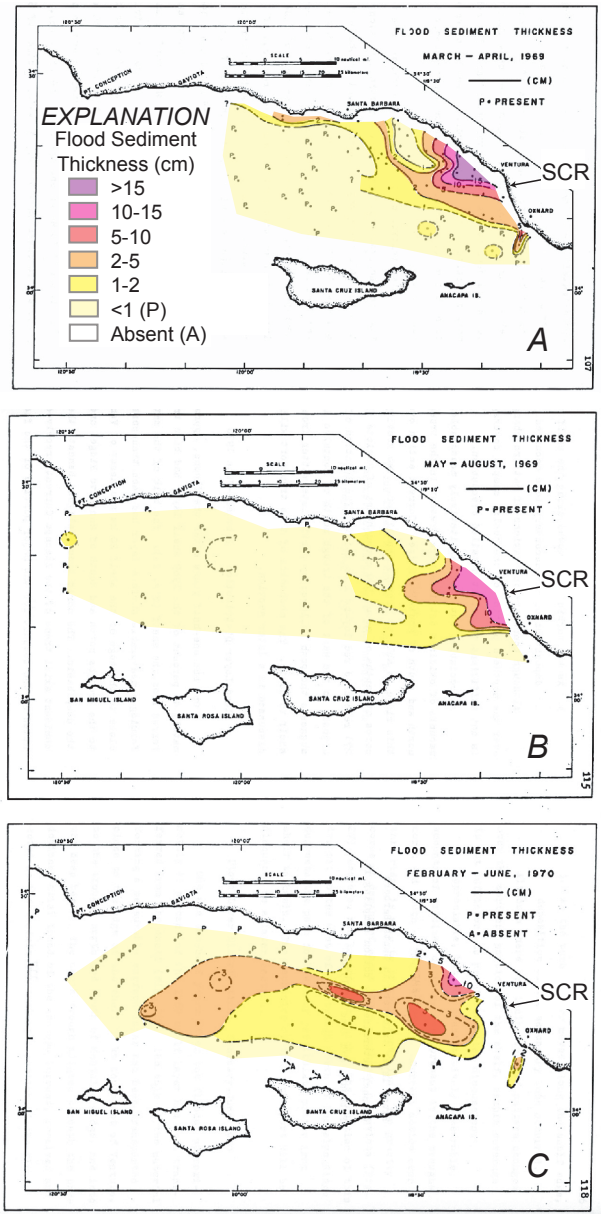

Figure 21. Time series of flood-layer thickness (in centimeters) in the Santa Barbara Channel offshore of the Santa Clara River (SCR; see fig. 1 for location) after massive flood in January–February 1969 (after Drake, 1972). *A*, March–April 1969. *B*, May–August 1969. *C*, February–June 1970. Dots, box cores. A, flood layer absent; P, flood layer present.

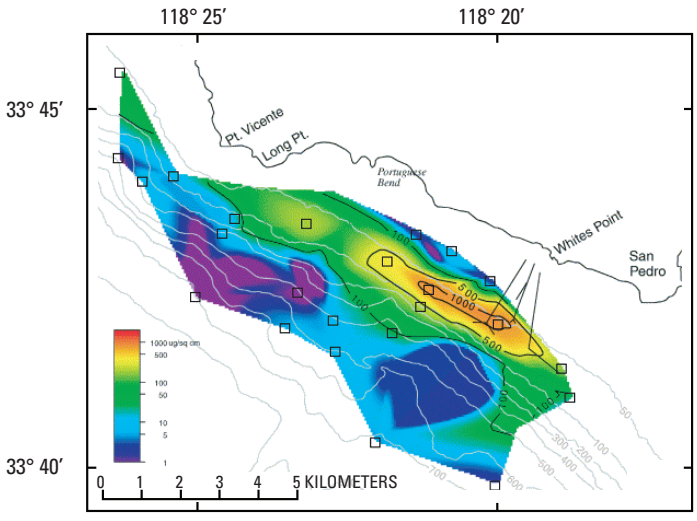

Figure 22. Distribution of p,p′-dichlorodiphenyldichloroethylene (p,p′-DDE, a DDT-degradation product) on the continental shelf offshore of the Palos Verdes peninsula (from Lee and others, 2002), plotted as integrated mass per unit area from sediment cores in upper 1 m of seabed (squares). Whites Point outfalls were dominant source of p,p′-DDE.

year at 60-m water depth and 3 times per year at 90-m water depth (Wiberg and others, 2002). The transport direction of this sediment, which is strongly influenced by the dominantly northwestward currents along this part of the continental shelf, results in deposition of contaminated sediment to the northwest of the outfall (fig. 22; Lee and others, 2002; Noble and others, 2002). This example of a nonriver setting reveals the effect of wave resuspension and ambient currents on fine-sediment dispersal on the California coastal margin.

Lastly, evidence exists that fine sediment can be resuspended and transported by ocean processes, such as internal bores related to tidal currents (for example, Noble and Xu, 2003). These processes appear to be focused on the continental shelf slope break, however, where internal tidal bores can shoal. Understanding of these processes across the California coastal margin is incomplete, largely owing to their nonlinearity and limited observations.

Research Questions

River sediment is clearly delivered to California coastal waters during winter storms, and so it is relevant to examine whether these storms impart unique environmental forcings on the coastal waters that cause sediment transport at rates or water depths not observed at other times of the year. Here we examine whether the oceanographic conditions that occur during river-flood events are unique in comparison with the rest of the year. We analyze the three largest California coastal rivers with respect to sediment discharge: the Eel, Salinas, and Santa Clara Rivers (fig. 1), all of which coincidentally have National Oceanic and Atmospheric Administration (NOAA) weather buoys offshore of their mouths.

Techniques

We compared river-discharge data from USGS river gauges and oceanographic data from nearby NOAA National Data Buoy Center (NDBC) buoys (fig. 23) for the Eel, Salinas, and Santa Clara Rivers (fig. 1) to evaluate the characteristics of storm-discharge periods relative to the rest of the year. Hourly river-discharge, wind, and wave data were obtained and compared for all three regions. Discharge events were identified for each river on the basis of instantaneous river-discharge

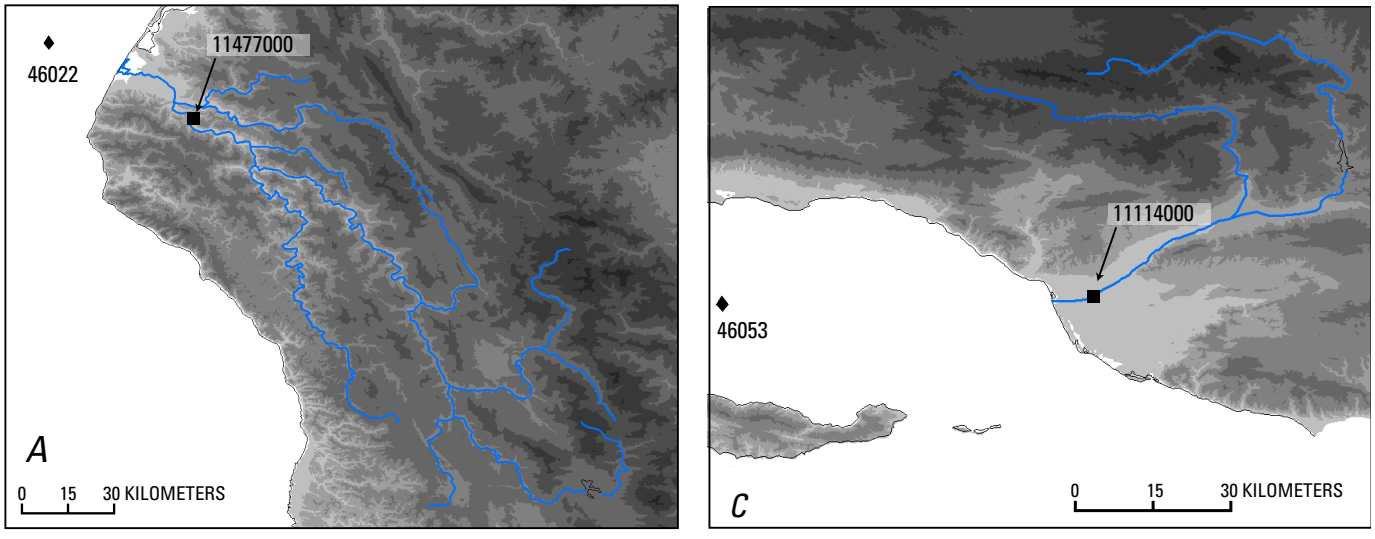

Figure 23. Drainage areas of the Eel River (*A*), the Salinas River (*B*), and the Santa Clara River (fig. 1), showing locations of National Oceanic and Atmospheric Administration's National Data Buoy Center buoys (diamonds) and U.S. Geological Survey gaging stations (squares) used in calculations.

measurements exceeding a threshold value, defined from the long-term discharge record at each gauge and encompassing all historical flood events on each river. This threshold value is equal to the rate at which more than 75 percent of the historical water discharge and 95 percent of the historical sediment discharge occurred. Threshold values of 500, 100, and 25 m^3/s were determined for the Eel, Salinas, and Santa Clara Rivers, respectively. Periods when instantaneous discharge (that is, 15-minute discharge records) exceeded these thresholds were identified, and the 48 hours before and after the peak discharge were considered the "prestorm" and "poststorm" periods. These 48-hour periods were conservatively long storm periods for a single event, given that the river discharge abated within hours after peak discharge and that longer periods could include multiple events from different storms. Event time series were compared for each system, and the mean and variance of these event time series were calculated for discharge, significant wave height (H_{mo}), and dominant wave period (T_{dom}). From these wave data, bottom-wave orbital velocities were calculated for the seabed at 20-m increments from 20- to 100-m water depth, based on linear wave theory (Dyer, 1986). These wave orbital velocities were compared with the critical threshold of particle entrainment (u_{cr}). A conservative u_{cr} value of 20 cm/s was used for fine sediment, based on the grain size of very fine sand (0.125 mm), to account for the minor cohesiveness of recently deposited fine sediment (Harris and Wiberg, 1997).

Results

Although geographic differences exist between the various systems, strong coupling is observed between river discharge, wind stress and direction, and wave climate at all sites. Below we detail the results by region from north to south, beginning with the Eel River (fig. 1).

Eel River

The Eel River discharges, on average, nearly 9.5 Mt of fine sediment annually to the coastal ocean. The initial fate of the sediment contained in this surface plume depends on surface currents set up by the wind before discharge (Pullen and Allen, 2000). On the Eel River shelf (fig. 1), the wind is generally from the north throughout the year; however, at significant times during the winter months the wind is from the south (figs. 24*A*, 24*B*). Immediately before and after times of peak discharge, winds are commonly strong and from the south (figs. 24*C*, 24*D*), setting up northward-moving surface currents that direct the river plume to the north, as discussed above (see fig. 17). After peak discharges, winds may be from the north and direct the tail end of the surface plume to the south (Pullen and Allen, 2000).

The sediment that is deposited on the seabed is then subjected to reworking by waves and currents. The influence of waves was examined to determine the potential for sediment resuspension and transport. Large discharge events (>500 m^3/s) on the Eel River coincided with significant increases in wave height and relatively stable wave periods (fig. 25). As river discharge decreased, wave height concurrently decreased. These patterns result in slightly higher bottom-wave orbital velocities during peak discharge. Thus, during large discharge events, conditions in the receiving waters for the Eel River shelf are energetic. This temporal connection leads to bottom-wave orbital velocities higher than the 20-cm/s threshold out to water depths of 80 to 100 m (fig. 25).

This energy regime is not unique, however, to times of large river discharge (fig. 26). On the Eel River shelf, bottom-wave orbital velocities exceed the 20-cm/s threshold approximately 30 percent of the time at 60-m water depth, only partly accountable for by times of large discharge events (fig. 26*A*). Thus, the rest of the fall and winter seasons provide plenty of opportunities when bottom-wave orbital velocities are high enough to resuspend fine sediment (fig. 26*B*). In the shallower waters (<60 m deep) of this energetic shelf, even the summer months allow for resuspension and transport of fine sediment.

Salinas River

The Salinas River (fig. 1) discharges, on average, nearly 2 Mt of fine sediment annually into Monterey Bay. Although this embayment is a different environment from that of the open Eel River shelf, similar forcings occur. Over the course of the year, dominant wind directions are from the northwest, with winter winds sometimes from the east-northeast (lighter) and south-southeast (stronger winds) (figs. 27*A*, 27*B*). Before river-flood discharge, however, winds are from a host of directions, although the strongest and most common winds are from the southeast. After river-flood events, winds are generally from the northwest (figs. 27*C*, 27*D*).

Any sediment initially deposited on the shelf offshore of the Salinas River mouth (fig. 1) is then subjected to reworking by waves and currents. Once again, patterns different from those on the Eel River shelf were observed. Wave heights peak before the arrival of river discharge and continue to fall over the course of the next 48 hours (fig. 28), although wave period varies little. Calculated bottom-wave orbital velocities show similar patterns to those of wave heights, with higher wave orbital velocities before peak discharge and falling during and after floods, leading to a decrease in sediment-resuspension potential during these flood events, reaching a maximum just before the influx of large amounts of sediment accompanying the peak discharge. This resuspension of fine sediment occurs to deeper than 60 m during the entire flood event (fig. 28*D*).

As on the Eel River shelf (fig. 1), wave energies high enough to resuspend material are not limited to flood events (fig. 29*A*). Sediment-resuspension potential is small during large river-discharge events and larger at other periods, though mostly during the energetic winter months (fig. 29*B*).

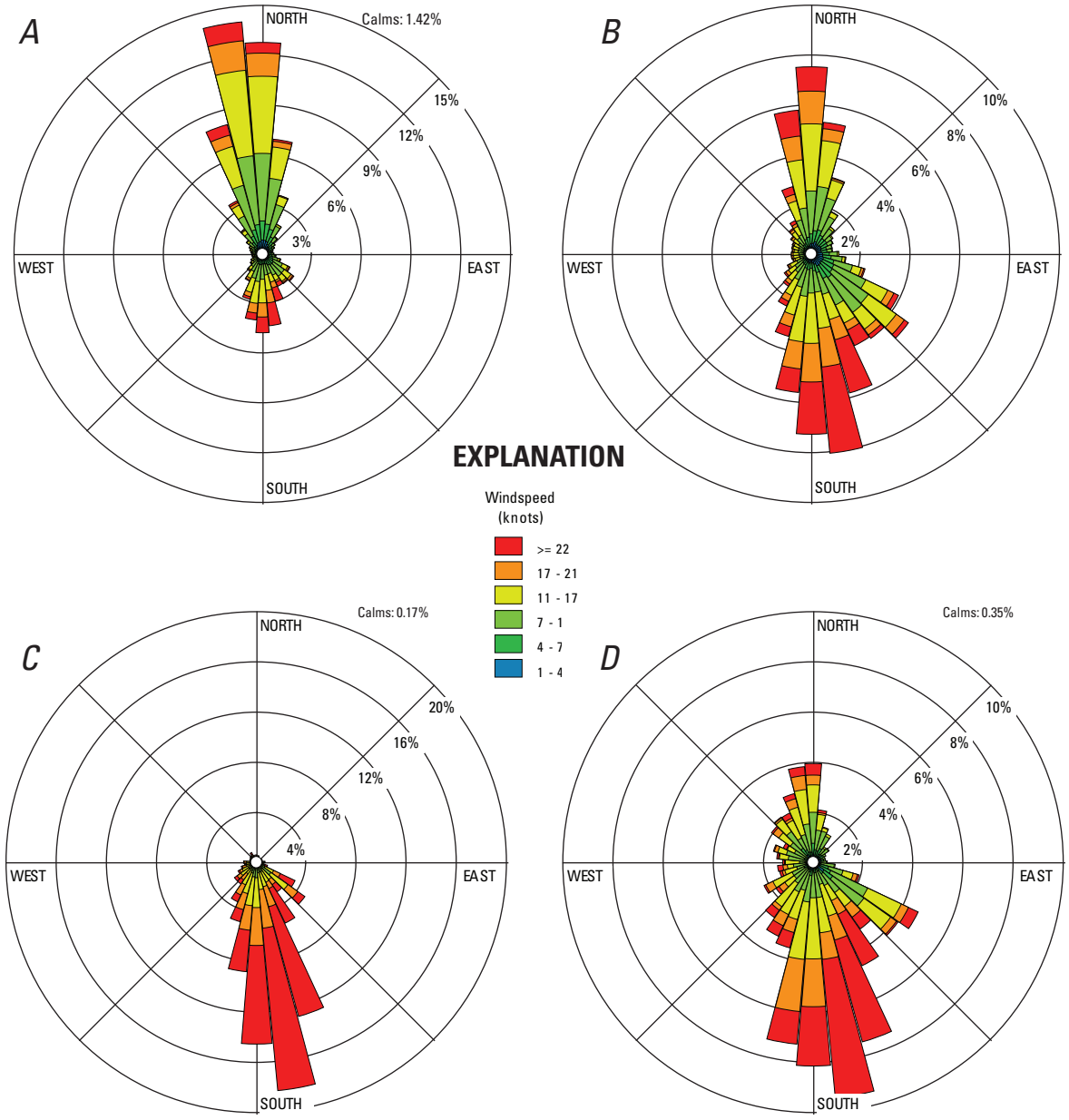

Figure 24. Rose diagrams of wind direction and windspeed generated from hourly data during period 1982–2005 at National Oceanic and Atmospheric Administration's National Data Buoy Center buoy 46022 (fig. 23A) near the Eel River (fig. 1). *A*, All hourly data. *B*, Winter (Dec.–Feb.) hourly data. *C*, Hourly data for 48 hours before peak flow. *D*, Hourly data for 48 hours after peak flow.

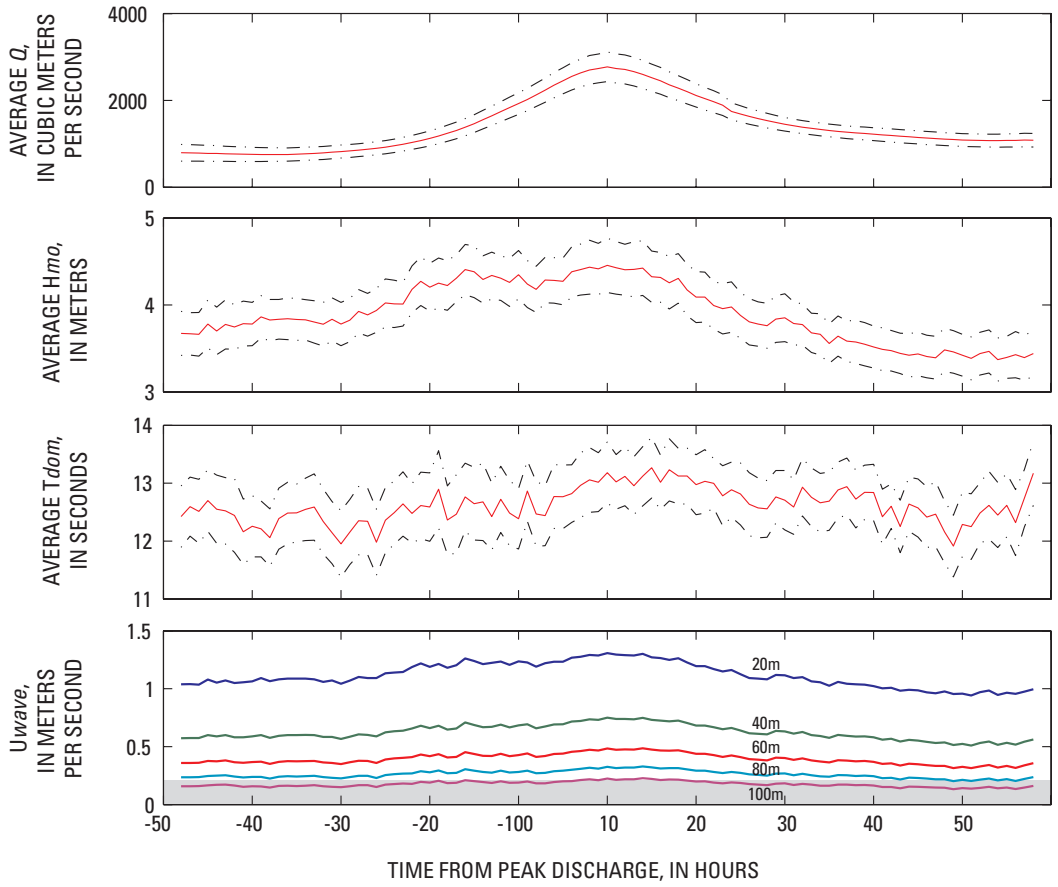

Figure 25. Average river discharge (*Q*), average significant wave height (H*mo*), average dominant wave period (T*dom*), and bottom-wave orbital velocity (U*wave*) at water depths of 20, 40, 60, 80, and 100 m for all discharge events (n=70) of Q>500 m^3/s from the Eel River (fig. 1). Solid curves, event-averaged values; dot-dashed curves, ±2σ deviations. Below U*wave*=0.2 m/s (gray area), resuspension of fine sediment is unlikely.

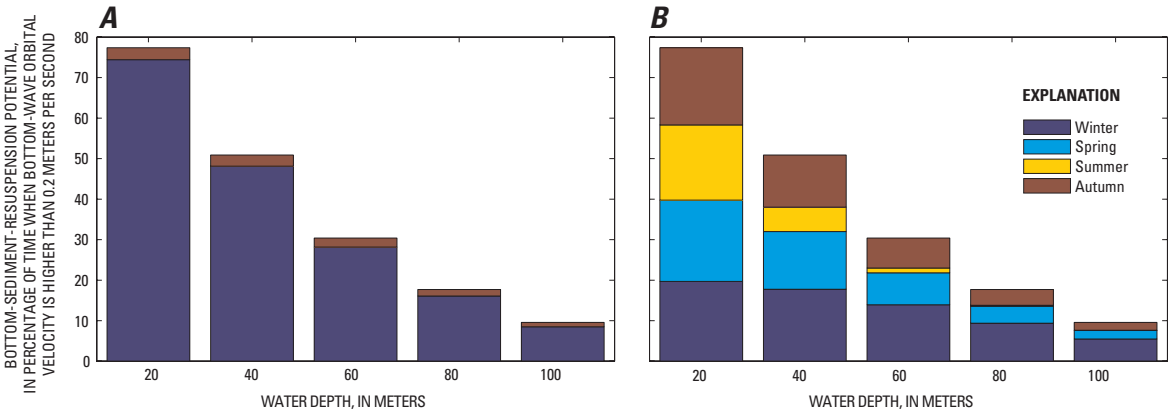

Figure 26. Bar charts showing fine-sediment-resuspension potential on the Eel River shelf (fig. 1), expressed as percentage of time when bottom-wave orbital velocity (U*wave*) is higher than 0.2 m/s, versus water depth. *A*, Fine-sediment-resuspension potential for nonflood periods (purple) and flood events (brown), defined as periods within 48 hours before and after peak flow. *B*, Fine-sediment-resuspension potential during winter (Dec.–Feb.), spring (Mar.–May), summer (June–Aug.), and autumn (Sept.–Nov.). Note that in shallower water, U*wave* values are high enough to resuspend sediment year round, whereas in deeper water U*wave* values are large enough almost exclusively in winter.

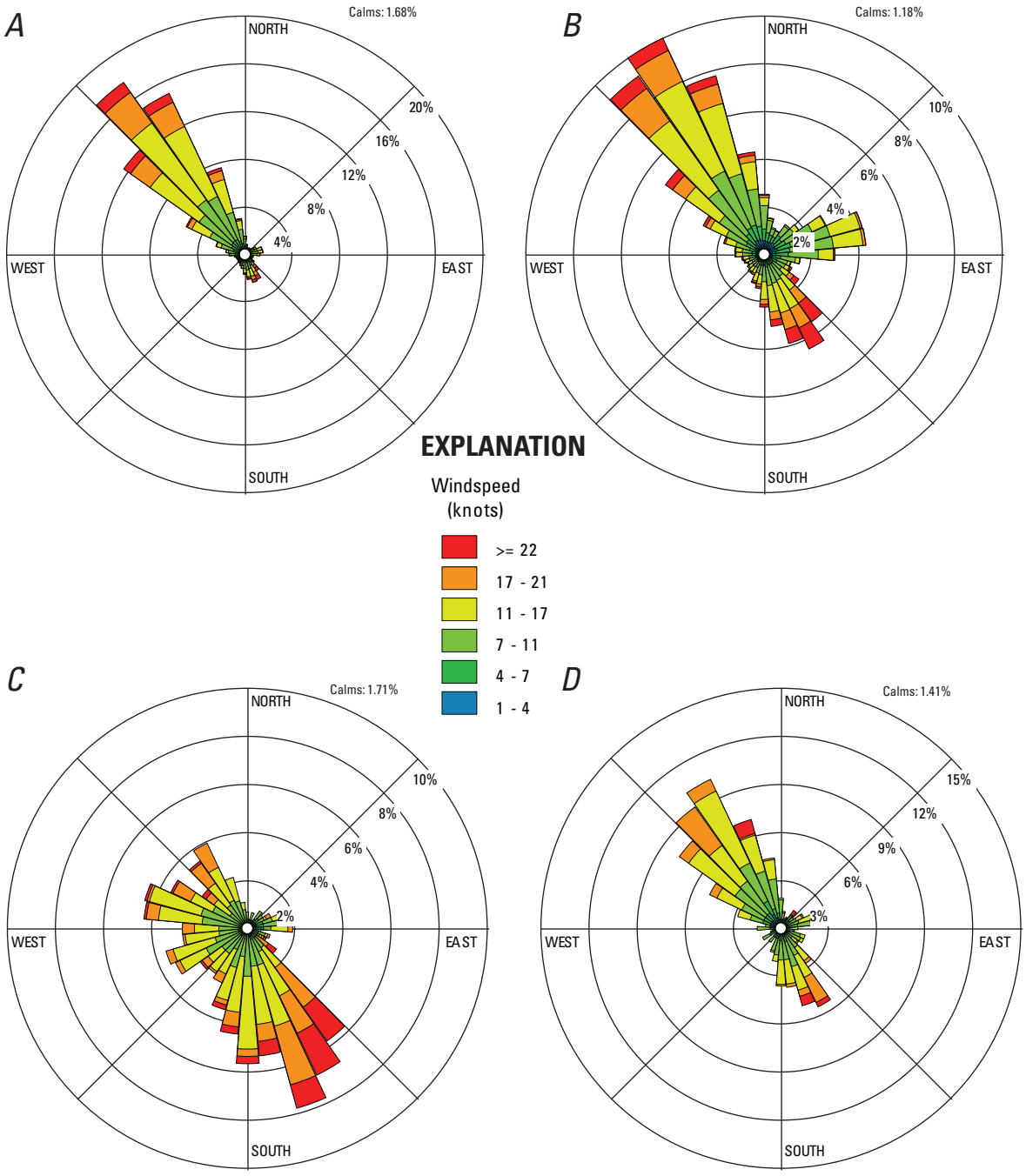

Figure 27. Rose diagrams of wind direction and windspeed generated from hourly data during period 1987–2005 at National Oceanic and Atmospheric Administration's National Data Buoy Center buoy 46042 (fig. 23B) near the Salinas River and Monterey Bay (fig. 1). *A*, All hourly data. *B*, Winter (Dec.–Feb.) hourly data. *C*, Hourly data for 48 hours before peak flow. *D*, Hourly data for 48 hours after peak flow.

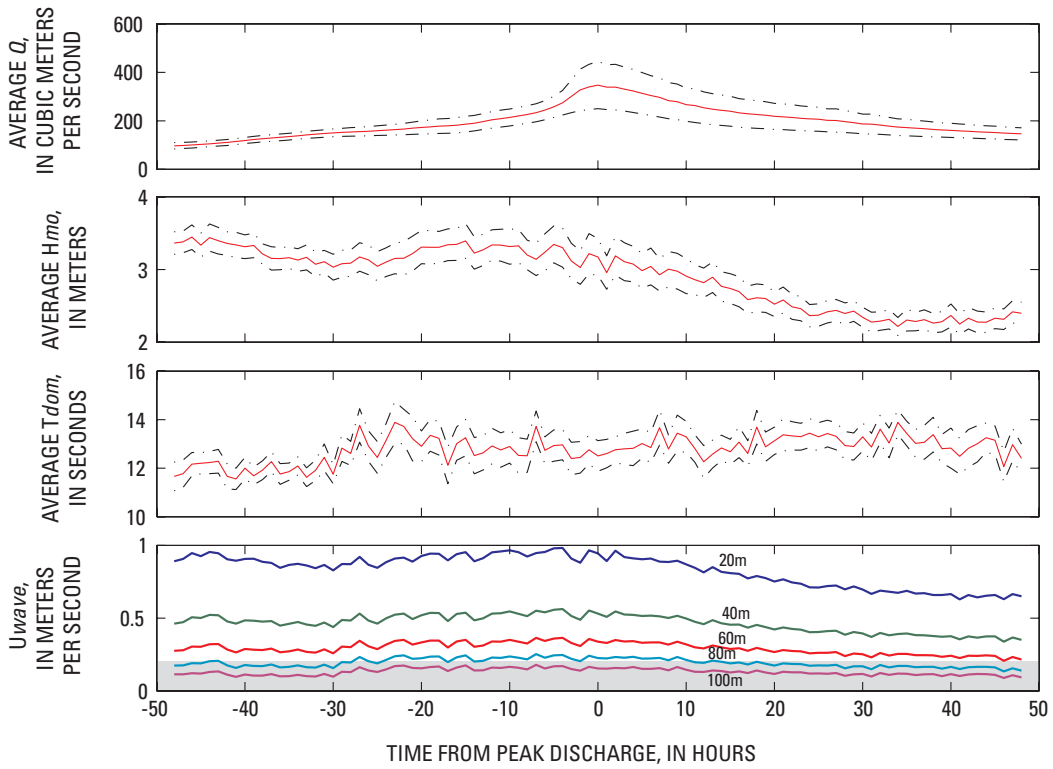

Figure 28. Average river discharge (*Q*), average significant wave height (H*mo*), average dominant wave period (T*dom*), and bottom-wave orbital velocity (U*wave*) at water depths of 20, 40, 60, 80, and 100 m for all discharge events (n=21) of Q>100 m^3/s from the Salinas River (fig. 1). Solid curves, event-averaged values; dot-dashed curves, ±2σ deviations. Below U*wave*=0.2 m/s (gray area), resuspension of fine sediment is unlikely.

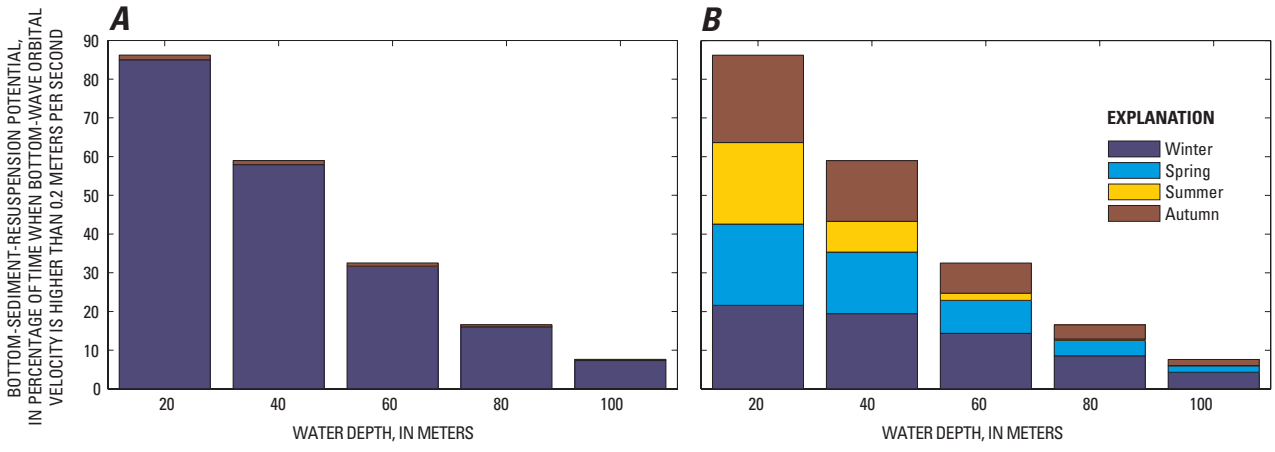

Figure 29. Bar charts showing fine-sediment-resuspension potential off the Salinas River in Monterey Bay (fig. 1), expressed as percentage of time when bottom-wave orbital velocity (U*wave*) is higher than 0.2 m/s, versus water depth. *A*, Fine-sediment-resuspension potential for nonflood periods (purple) and flood events (brown), defined as periods within 48 hours before and after peak flow. *B*, Fine-sediment-resuspension potential during winter (Dec.–Feb.), spring (Mar.–May), summer (June–Aug.), and autumn (Sept.–Nov.). Note that in shallower water, U*wave* values are high enough to resuspend sediment year round, whereas in deeper water U*wave* values are large enough almost exclusively in winter.

Santa Clara River

The Santa Clara River (fig. 1) provides yet another example of how physical forcings may control the dispersal of sediment from rivers on the California coast. The Santa Clara River discharges, on average, approximately 2 Mt of fine sediment annually, more than 90 percent of which is delivered over the course of just a few days a year. In the Santa Barbara Channel region near the mouth of the Santa Clara River, winds are dominantly from the west throughout the year (fig. 30*A*). During the winter, winds from east to east-southeast are commonly strong and associated with storm events (fig. 30*B*). The days before peak discharge are characterized by winds from the east-southeast (fig. 30*C*), immediately followed by winds from the west (fig. 30*D*). Thus, the Santa Clara River is unusual in that local winds are oriented east-west, and strong winds are from the west (that is, from upcoast) after river events.

Wave energies in the Santa Clara River mouth (fig. 1) are not as high as those off either the Salinas or Eel River (fig. 31). However, the significant wave height changes little during river events, whereas a depression is observed in the dominant wave period just before peak discharge (fig. 31), possibly owing to winds from the southeast and locally generated waves. Because of these patterns, bottom-wave orbital velocities peak within 15 hours of peak discharge (fig. 31), although this peak in bottom-wave orbital velocities does not extend to the same water depths offshore of the Eel or Salinas River systems, owing to the lower significant wave heights. Little sediment resuspension is observed offshore of the Santa Clara River deeper than 60 m during flood events (fig. 31).

Sediment-resuspension potential on the Santa Clara River shelf (fig. 1) due to high wave orbital velocities is much smaller than in the Eel and Salinas systems because of lower wave heights. Sediment-resuspension potential can be greater, however, during periods of insignificant river discharge, similar to the Eel and Salinas Rivers. Such periods of enhanced sediment-resuspension potential are most common in the winter and rarely affect water depths below 60 m (fig. 32).

Summary

The dispersal of fine sediment discharged onto the California continental shelf appears to occur in multiple resuspension-transport events that may continue over a period of weeks to more than a year. These resuspension/transport events occur dominantly during periods of large waves, which provide bottom-wave orbital velocities high enough to resuspend fine sediment from the seabed. Observations of sediment dispersal from river systems suggest that after somewhat brief advection in a buoyant plume (~hours), suspended-sediment transport along the seabed is the most important process for transporting fine sediment across the shelf. Although coherent temporal patterns exist in winds, waves, and river discharge, the potential to suspend and transport fine sediment during river floods is not unique to these events. Rather, periods when fine sediment may be resuspended and transported occurs almost entirely when river discharge is low. Thus, although most investigations of sediment transport and dispersal offshore of California have been in river-dominated settings, river floods by themselves have no unique sediment-transport forcings with respect to waves. We suggest that observations of the dispersal of fine sediment from rivers, especially transport along the seabed, may be applicable to the dispersal of sediment from other sources along the coast (for example, bluff erosion and sewer outfalls). This sediment transport will be influenced by the gradient in wave energy along the California coast, which is generally strongest in the north and weakest in the south. Local seabed topography, wave climate, currents, and sediment sources will greatly influence sediment transport in these coastal settings.

Fate and Accumulation of Fine Sediment

Introduction

Deposition, burial, and long-term accumulation of fine sediment mark the final stage of dispersal of sediment to the continental margin (Wright and Nittrouer, 1995). Sediment accumulates across the continental shelf and commonly into deeper parts of the ocean, as dictated by sediment sources, oceanographic processes, and coastal morphology. In coastal settings with an adequate supply of fine sediment, a sand-mud transition may occur over a narrow depth range (McCave, 1972; Stanley and others, 1983; George and others, 2006). The depth of this sand-mud transition is primarily related to wave height but also to sediment source and shelf geometry. Offshore of the sand-mud transition, fine sediment may accumulate within a region commonly called the midshelf mud belt (fig. 33). Midshelf mud belts have several distinguishing characteristics: high accumulation rates of fine sediment, elongate shape in the alongshore direction, and low slopes. Along the west coast of North America, mud belts have been described offshore of the Columbia, Eel, and Russian Rivers (Griggs and Hein, 1980; Nittrouer and Sternberg, 1981; Drake and Cacchione, 1985; Wheatcroft and others, 1997) and surrounding Monterey Bay (Edwards, 2002; Eittreim and others, 2002a).

Although midshelf mud belts are prevalent offshore of many Western U.S. rivers, the following two points should also be considered: (1) sand can also accumulate in these mud belts, and (2) mud belts are not the only sites of fine-sediment accumulation. An example of interbedding of sand and fine sediment in the mud belt offshore of the Eel River (fig. 1) was described by Fan and others (2004), as illustrated in figure 34. Clay-rich beds are deposited after river-flood-influenced transport events (or the “high-concentration regime”), whereas sand-rich beds are deposited after nonflood events (or the “low-concentration regime”).

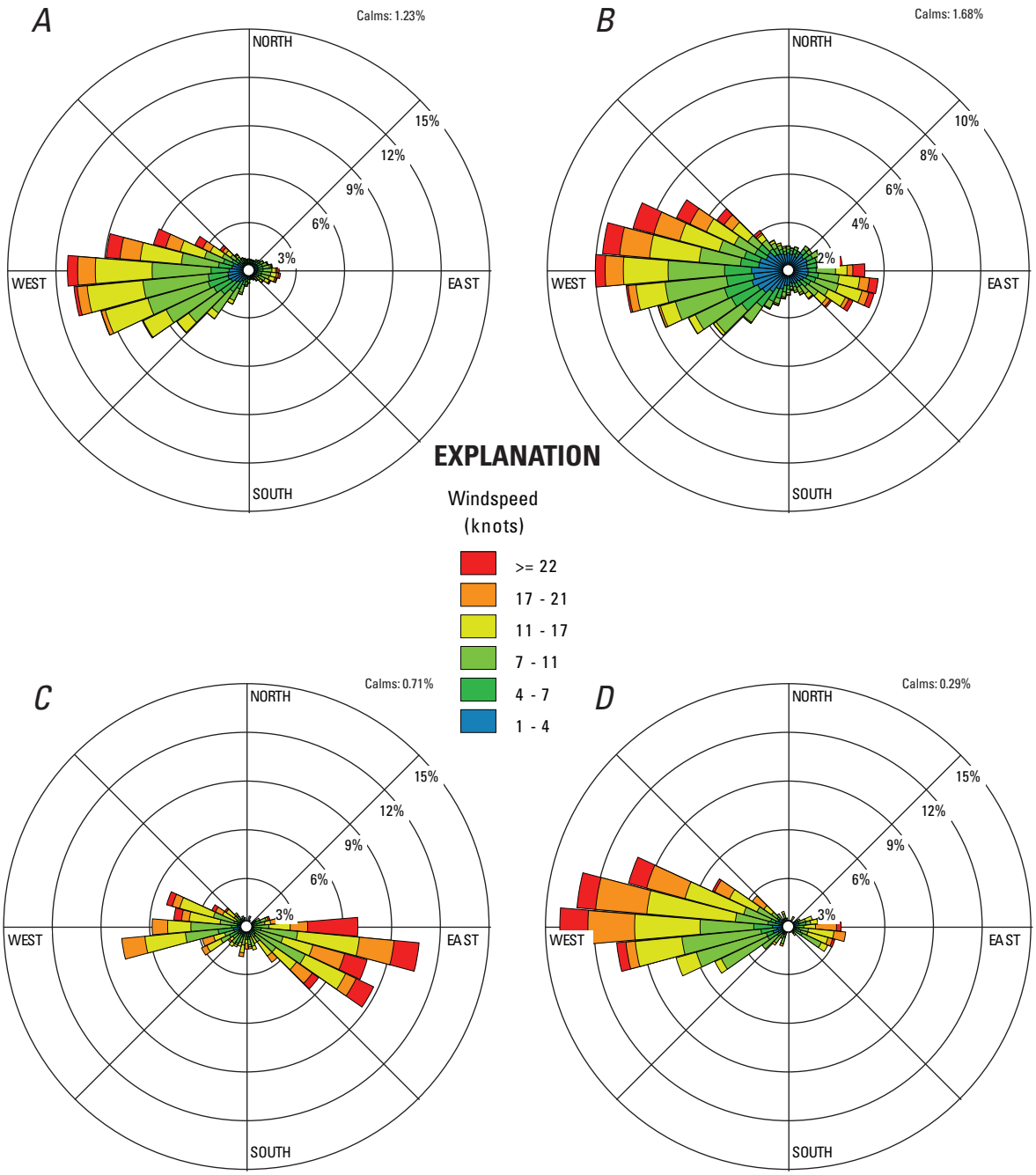

Figure 30. Rose diagrams of wind direction and windspeed generated from hourly data during period 1994–2004 at National Oceanic and Atmospheric Administration's National Data Buoy Center buoy 46053 (fig. 23C) near the Santa Clara River (fig. 1). *A*, All hourly data. *B*, Winter (Dec.–Feb.) hourly data. *C*, Hourly data for 48 hours before peak flow. *D*, Hourly data for 48 hours after peak flow.

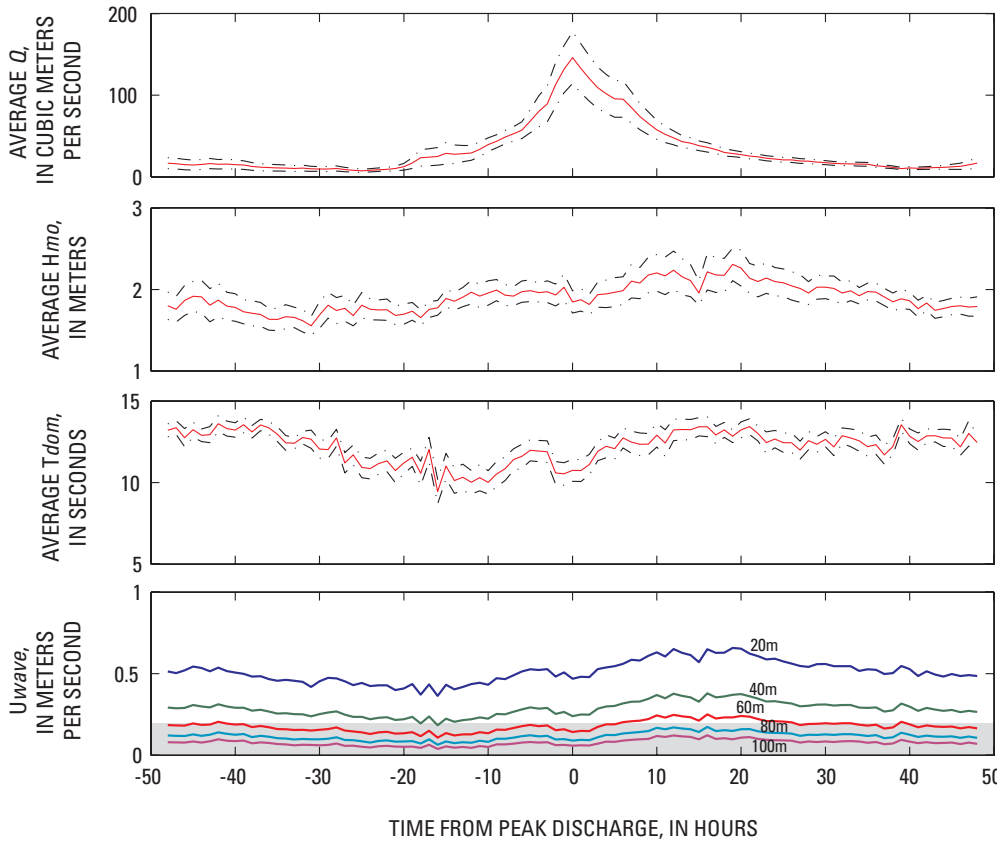

Figure 31. Average river discharge (*Q*), average significant wave height (H*mo*), average dominant wave period (T*dom*), and bottom-wave orbital velocity (U*wave*) at water depths of 20, 40, 60, 80, and 100 m for all discharge events (n=18) of Q>25 m^3/s from the Santa Clara River (fig. 1). Solid curves, event-averaged values; dot-dashed curves, ±2σ deviations. Below U*wave*=0.2 m/s (gray area), resuspension of fine sediment is unlikely.

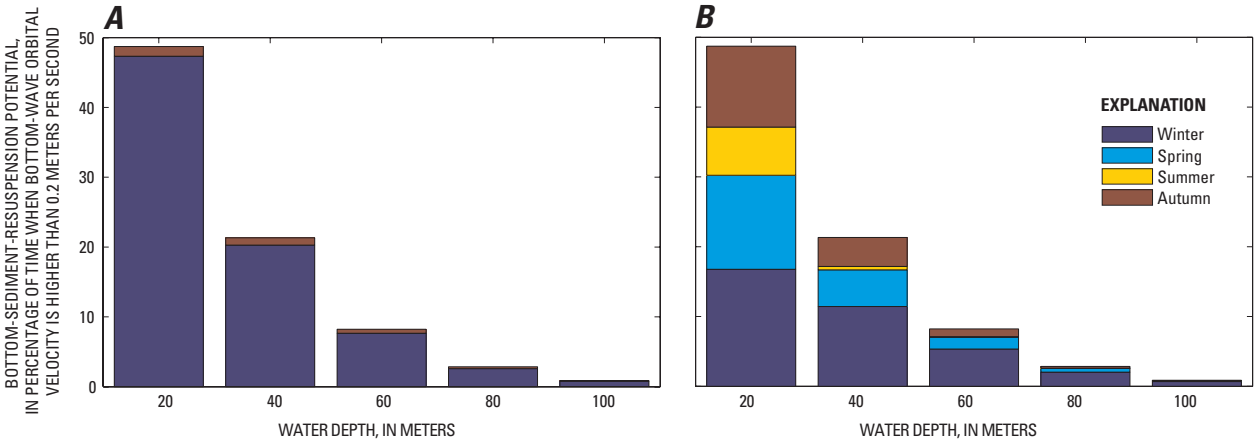

Figure 32. Bar charts showing fine-sediment-resuspension potential off the Santa Clara River (fig. 1), expressed as percentage of time when bottom-wave orbital velocity (U*wave*) is higher than 0.2 m/s, versus water depth. *A*, Fine-sediment-resuspension potential for nonflood periods (purple) and flood events (brown), defined as periods within 48 hours before and after peak flow. *B*, Fine-sediment-resuspension potential during winter (Dec.–Feb.), spring (Mar.–May), summer (June–Aug.), and autumn (Sept.–Nov.). Note that in shallower water, U*wave* values are high enough to resuspend sediment year round, whereas in deeper water U*wave* values are large enough almost exclusively in winter.

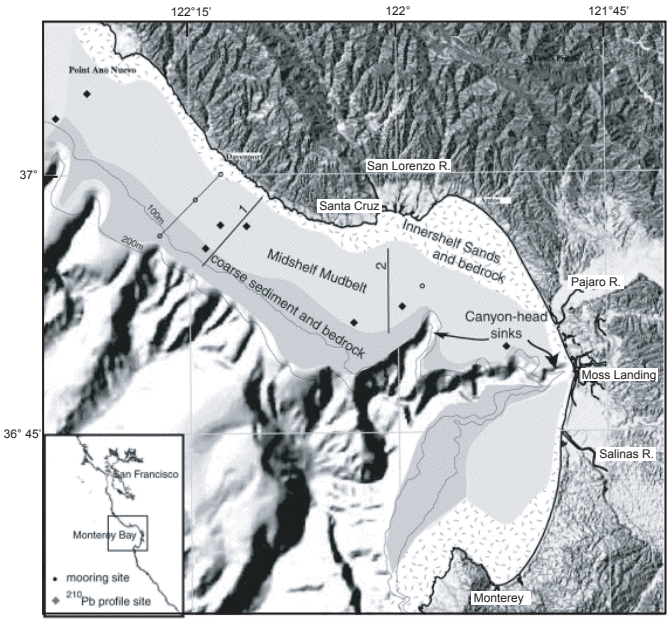

Figure 33. Monterey Bay area (fig. 1), showing location of midshelf mud belt (from Eittreim and others, 2000).

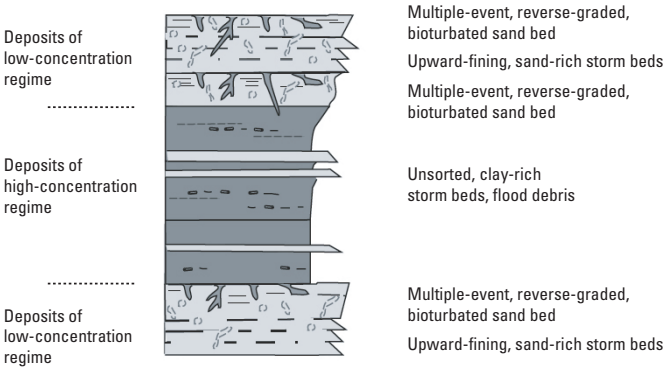

Figure 34. Generalized stratigraphic profile of sediment accumulation in mud belt offshore of the Eel River (fig. 1; from Fan and others, 2004). Beds of clay-rich sediment alternate with sandy beds, representing deposition after flood (high-concentration regime) and nonflood (low-concentration regime) events.

Ample evidence exists that midshelf mud belts are not the only sites of fine-sediment deposition. For example, the Eel River mud belt has been estimated to receive only 20–25 percent of the total fine-sediment discharge from the Eel River (fig. 1; Wheatcroft and others, 1997). The remaining fine sediment is either transported past the shelf break to the slope or through the Eel Canyon, or deposited on the Inner continental shelf. Crockett and Nittrouer (2004) estimated the inner-shelf deposition (defined as 20–55-m water depth) of fine sediment from the Eel River at 6–13 percent of the total fine-sediment load of the river. The total sedimentation rate on the inner shelf was estimated at 13 to 33 mm/yr since 1964, within which approximately 10 percent is fine sediment that occurs in both thin flood deposits and mixed into the sand (Crockett and Nittrouer, 2004). Thus, a mass balance of fine sediment for the Eel River margin suggests that approximately 10 percent accumulates on the inner shelf (<55-m water depth; Crockett and Nittrouer, 2004), approximately 20 percent on the mid-shelf and outer shelf (50–150-m water depth; Sommerfield and Nittrouer, 1999), and approximately 20 percent on the upper continental slope (150–600-m water depth; Alexander and Simoneau, 1999). The remaining approximately 50 percent of sediment load is likely transported down the Eel Canyon (Mullenbach and others, 2004) onto the Eel Fan or offshore of the upper continental slope.

In this section, we present a thorough analysis of grain-size distributions and sediment-accumulation rates on the California continental shelf. The purpose is to describe where fine sediment accumulates, how its location varies along the coast, and why such variation occurs. As described below, we used existing data from the USGS usSEABED database (URL *http://walrus.wr.usgs.gov/usseabed/*) and other published reports to describe the patterns of fine-sediment accumulation. Two tasks were addressed: (1) mapping and analysis of fine-sediment distributions offshore of California and (2) synthesis of published fine-sediment-accumulation rates in the study area (fig. 1).

Techniques

The grain size of the seabed was characterized by using physical and virtual (photographic and video) samples from seabed cores and grab samples summarized in the usSEABED database (Reid and others, 2006), which provides integrated numeric data based on existing small and large marine research efforts. This database includes surficial and sub-bottom numeric information on grain size, composition, and applied properties obtained from core logs, sample descriptions, photographs, and videos, as well as the more standard numeric data from laboratory analyses.

Here we use grain-size data from physical samples of the seabed surface contained in the usSEABED database. Two general types of seabed samples were used in our analyses: those with only verbal descriptions and those with laboratory grain-size analyses. Although laboratory data exist for many of the samples, exclusive use of these data would exclude nearly a third of the California coastline (fig. 35). Thus, for mapping purposes, we included both sample types, although for statistical analyses we only used the laboratory analyses. Grain-size information from verbal descriptions has been extracted (or "parsed") by using fuzzy-set theory, as explained by Reid and others (2006).

Sediment-accumulation data, which have been synthesized from available published records, were derived from either sediment cores or seismic-reflection surveys. Here

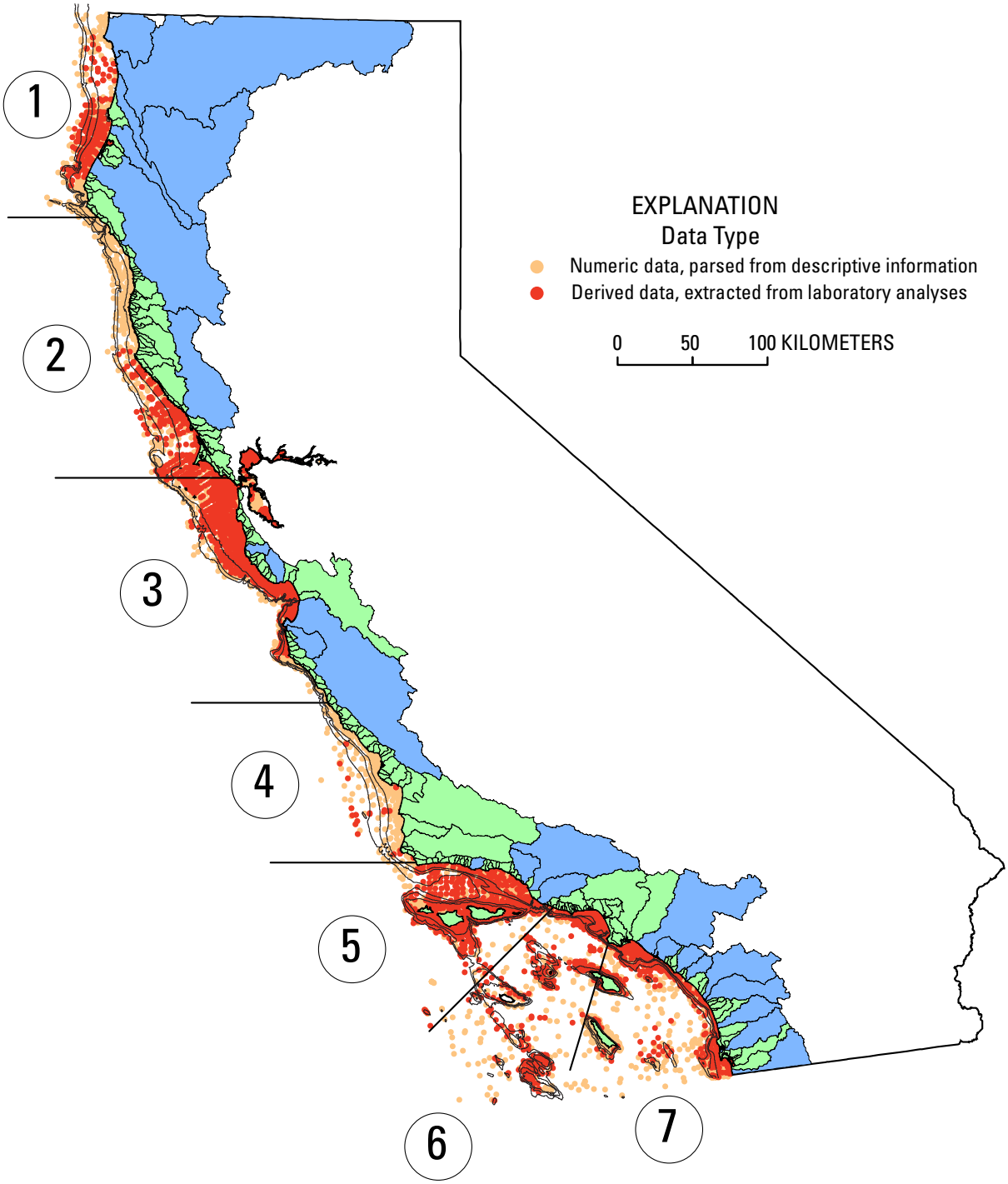

Figure 35. Outline map of California coast, showing distribution of sea-floor-sediment-sampling sites (dots; Reid and others, 2006) in regions 1 through 7. Dots, data types: yellow, numeric data parsed from descriptive information; red, derived data extracted from laboratory analyses.

we define "recent" (<100 yr) accumulation rates to be those derived largely from isotopic profiles of ^{210}Pb and (or) ^{137}Cs within sediment profiles, according to the techniques summarized by Nittrouer and others (1979) and Sommerfield and Nittrouer (1999). The "long term" (>1,000 yr) sediment-accumulation rates presented here are from either seismic profiles of the continental shelf, which use a strong basement reflector as the Holocene transgressive surface, or from ^{14}C dating of samples from within sediment cores (Schwalbach and Gorsline, 1985). Data have been summarized into three shelf regions on the basis of the water depth of the sample—inner shelf (<50-m depth), midshelf (50–100 m depth), and outer shelf (>100-m depth)—and into seven physiographic regions along the State (fig. 35).

Grain Size on the California Continental Shelf

Data on more than 19,200 grain-size samples from the seabed surface offshore of California are available in the usSEABED database, of which more than 7,650 records contain laboratory grain-size information (fig. 35). Fine sediment occurs throughout the sampled regions (1–7, fig. 35) but generally dominates the midshelf, especially offshore of major coastal rivers (fig. 36). The inner shelf generally has much-less fine sediment for most of California except in southern California, as discussed below. The continental shelf offshore of San Francisco Bay is notably devoid of fine sediment (fig. 36), whereas the interior of the bay is dominated by it. Below we present three examples from the continental shelf immediately offshore of the three rivers with the greatest sediment supply, the Eel, Salinas, and Santa Clara Rivers.

The grain size of sediment offshore of the Eel River (fig. 1) clearly reveals a transition from dominantly sand on the inner shelf to dominantly fine sediment on the midshelf to outer shelf (fig. 37*A*). The midshelf mud belt, which was the focus of the large research program STRATAFORM (Nittrouer, 1999), is observable to the north of the river mouth (fig. 37*A*), and fine sediment is present on much of the outer shelf and continental slope offshore of the mud belt. These grain-size relations with water depth can be observed in a statistical summary of the samples (fig. 38*A*). Sediment inshore of 50-m water depth is dominated by sand-size and coarser particles (fig. 38*A*). Below 50-m water depth, the seabed is much more likely to be dominated by fine sediment, except largely on the narrow, canyon-dominated shelves south of the river mouth (fig. 37*A*).

The continental shelf of Monterey Bay, which receives sediment inputs from the Salinas River and numerous small coastal rivers, displays similar sediment grain-size patterns to the Eel River shelf (figs. 1, 37*B*). The inner parts of the Monterey Bay shelf are dominated by sand, whereas a distinct fine-sediment region is present in the midshelf (fig. 37*B*), except in the southern most part of Monterey Bay, where the shelf is dominated by sand (fig. 37*B*). The outer shelf and upper continental slope have little fine sediment, in contrast to the muddy slope off the Eel River. These patterns are consistent with the interpretations by Eittreim and others (2002b), as illustrated in figure 33. Summarized by water depth, sand and coarser sediment dominates the sea floor inshore of 40-m water depth, whereas fine- sediment dominates the regions between 40- and 110-m water depth (fig. 38*B*). Below approximately 110-m water depth, the sediment is much coarser (fig. 38*B*).

The Santa Barbara Channel and Santa Monica Bay lie offshore of the Santa Clara River and several other small rivers in southern California (figs. 1, 37*C*). The grain-size distributions of this region differ considerably from those in northern and central California, as discussed above. Fine sediment is observed to dominate the seabed throughout the region, but little depth control is observed in these data (figs. 37*C*, 38*C*). Unlike the other systems discussed above, fine sediment is observed to dominate some of the samples from above 30-m water depth (fig. 38*C*). Sand-dominated regions of the shelf occur on the southern Ventura shelf, near Point Conception, and around the offshore islands. Southern California has no clear and consistent sand-mud transition (fig. 37*C*), likely because of variations in wave energy, sediment sources, currents, and shelf morphology.

An important characteristic of all three regions is that fine sediment is present in most seabed samples, even from the shallowest depths (fig. 38), a result consistent with the observations of Crockett and Nittrouer (2004) and suggesting that although relatively distinct sand-mud transitions can occur on the continental shelf, significant amounts of fine sediment lie inshore of these transitions. This characteristic appears to be especially important in southern California, where wave energy is significantly smaller than in northern California and where more fine sediment has been measured on the inner shelf (fig. 38*C*). Local variations in grain size may be related to temporal changes in the sediment deposited by either burial, erosion, or winnowing, as observed in grain-size samples from the Eel River shelf (fig. 37*A*). Assessment of the three years with the greatest amount of sampling indicates that seabed samples collected in 1998 contained less fine sediment than in 1995 or 1997 (fig. 39), consistent with the conceptual model of Fan and others (2004), as illustrated in figure 34, and with the sampling results of Drake (1972), as illustrated in figure 21, suggesting that the grain size of the seabed can be dynamic and respond to external forcing of river inputs and ocean conditions.

Fine-Sediment-Accumulation Rates

Sediment that is deposited on the continental shelf and buried by subsequent deposition forms the geologic record that can be evaluated for such characteristics as accumulation rates. Rates of fine-sediment accumulation offshore California have been estimated by using both isotopic records within sediment cores and seismic-reflection data, as plotted in figure 40 and summarized in table 5. For this summary, we divided

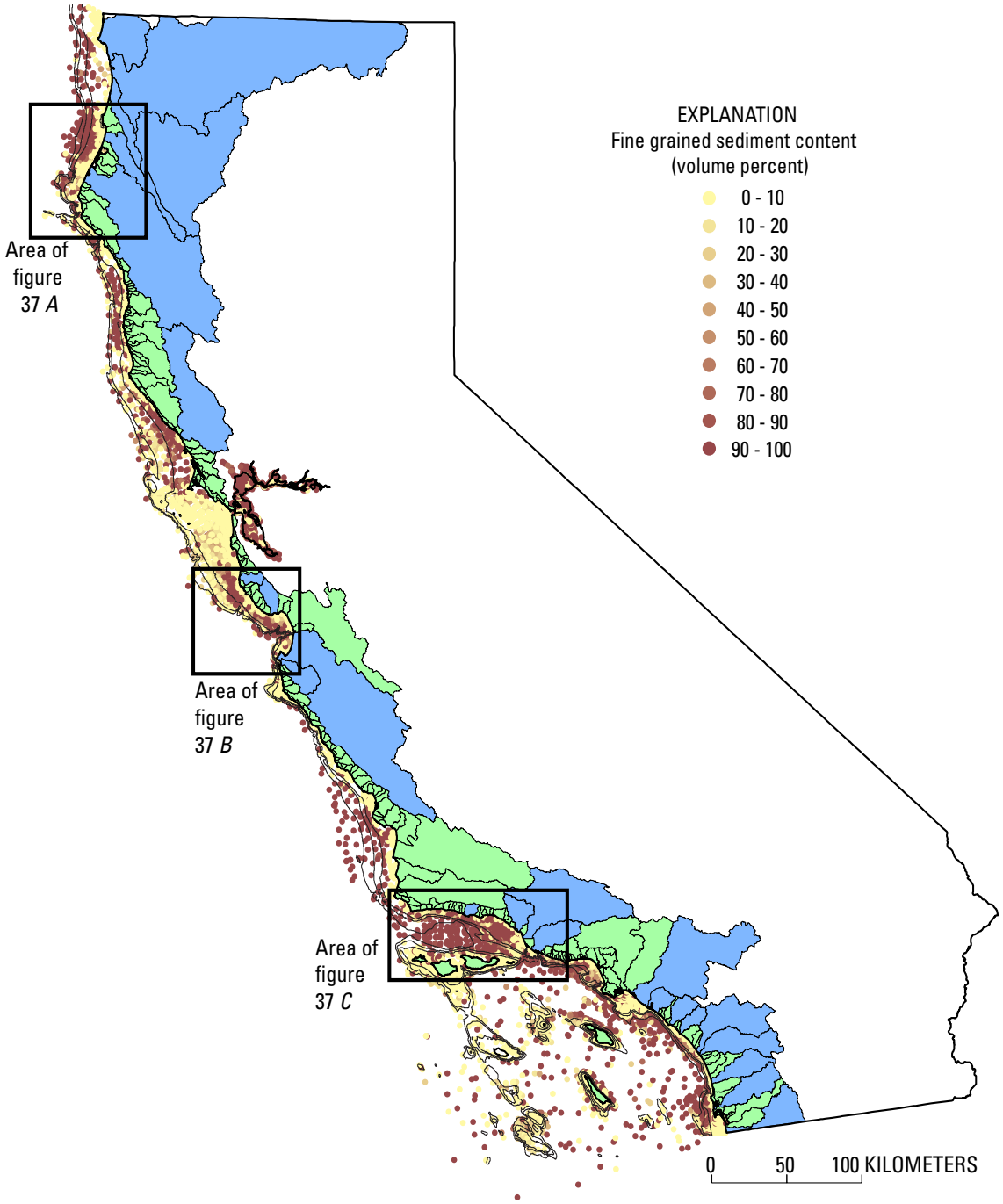

Figure 36. Outline map of California coast, showing distribution of fine-sediment content from sea-floor-sediment-sampling sites (dots) in usSEABED.

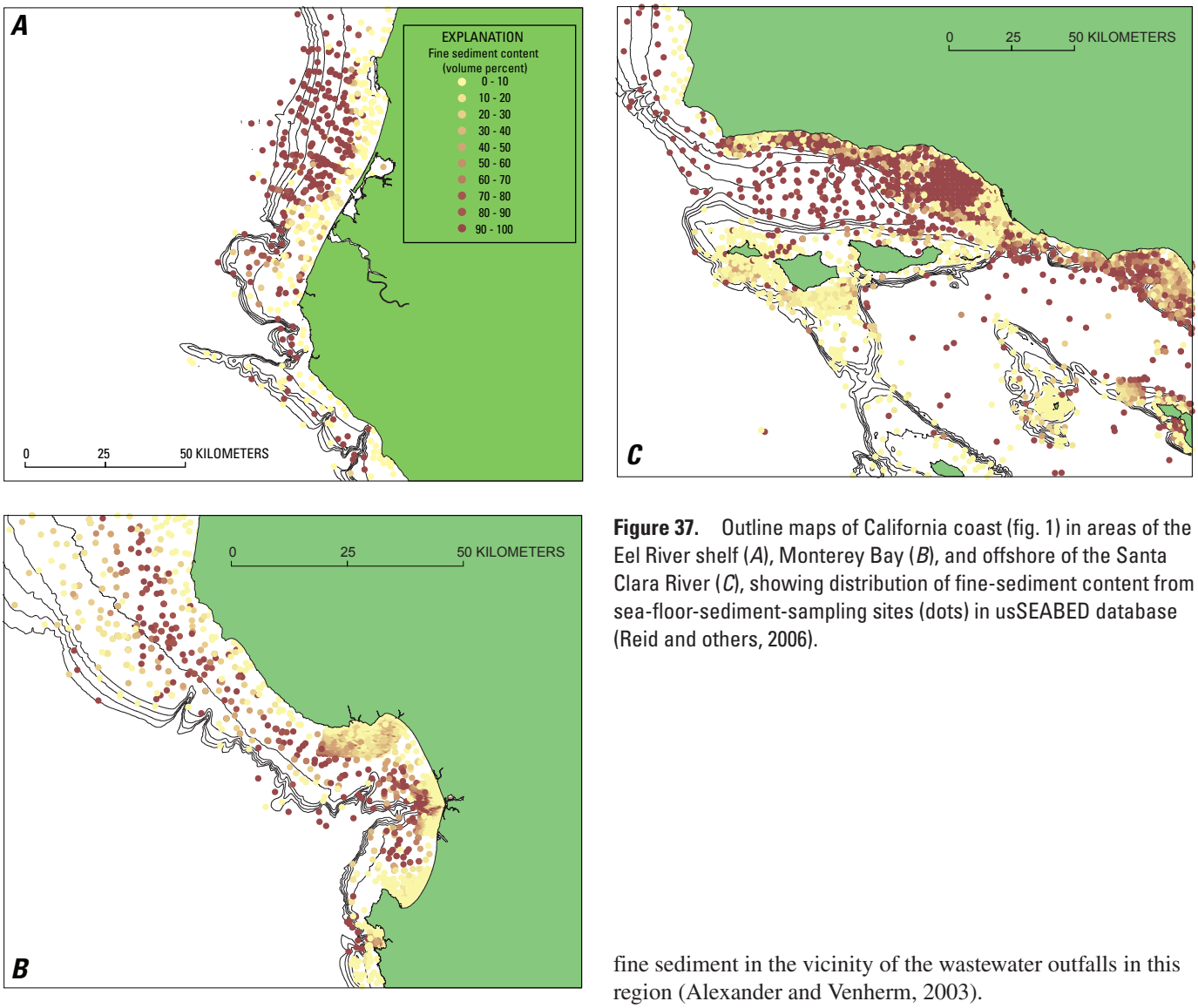

Figure 37. Outline maps of California coast (fig. 1) in areas of the Eel River shelf (*A*), Monterey Bay (*B*), and offshore of the Santa Clara River (*C*), showing distribution of fine-sediment content from sea-floor-sediment-sampling sites (dots) in usSEABED database (Reid and others, 2006).

California into seven regions that represent the sites of major studies. The most thorough investigations have been on the Eel River shelf (region 1, fig. 35) and in the Santa Monica Bay (region 6), whereas the other regions have received only localized or no investigations (table 5).

Sediment-accumulation rates are generally highest on the inner shelf (<50-m water depth) and decrease with depth, most obviously on the Eel River shelf and in Santa Monica Bay (regions 1 and 6, respectively, fig. 35), although this result is consistent across all regions (fig. 40). The highest sediment-accumulation rates anywhere on the shelf were observed offshore of the Eel River (region 1), which also receives the greatest sediment input of the study area (fig. 40). Sediment-accumulation rates on the Russian River shelf and in Monterey Bay (regions 2 and 3, respectively) are significantly lower (fig. 40). Elevated rates are also observed in Santa Monica Bay (region 6), which are partly related to sediment inputs from Transverse Range rivers and the thick accumulation of fine sediment in the vicinity of the wastewater outfalls in this region (Alexander and Venherm, 2003).

The long-term (>1,000 yr) sediment-accumulation rates are generally consistent with recent (<100 yr) rates (fig. 40; table 5). Long-term rates should be expected to be somewhat lower than recent rates, owing to infrequent periods of accumulation hiatuses and (or) erosion, as discussed by Sadler (1999) and Sommerfield (2006). This discrepancy is greatest in Santa Monica Bay (region 6), where long-term sediment-accumulation rates are 5 to 10 times lower than recent rates (fig. 40). Although the higher sediment-accumulation rates measured during recent years may be related to increases in fluvial discharge during the past 100 years (for example, Sommerfield and others, 2002), wastewater-outfall inputs (especially in some of the samples from Santa Monica Bay), or other anthropogenic sources, the longer-term records may be stratigraphically incomplete, as described by Sommerfield (2006), producing different sediment-accumulation rates over different measurement periods. We note that our results for Santa Monica Bay (region 6) differ from those of Sommerfield (2006), owing to our focus on the shelf and his focus on the deeper basins that receive much less sediment.

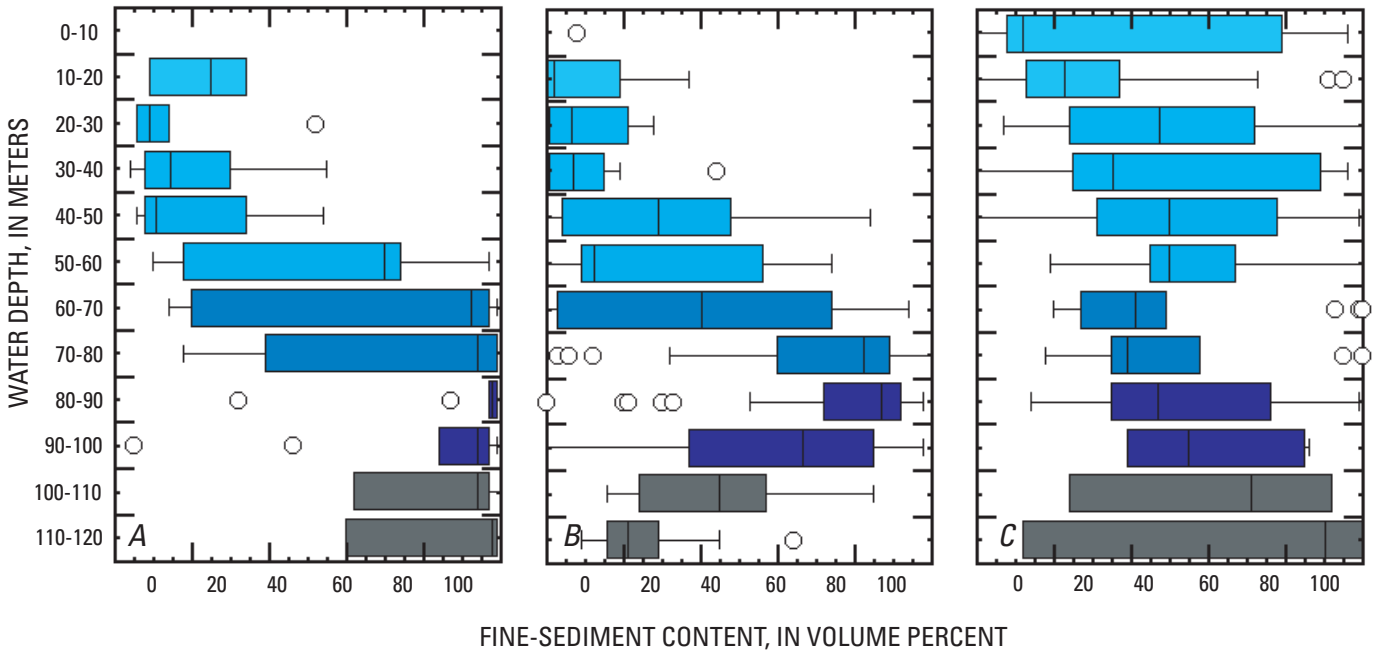

Figure 38. Water depth versus sea-floor-sediment grain size offshore of the Eel River shelf (*A*), Monterey Bay (*B*), and offshore of the Santa Clara River (*C*) (figs. 1, 37). Boxes enclose 50 percent of grain-size data within each 10-m depth interval, with median shown as a vertical bar within each box. Vertical bars extending from horizontal lines to either side of box indicate maximum and minimum values within dataset that fall within an acceptable range, defined as 1.5 times interquartile distance; circles, outliers. Data extracted from laboratory analyses reported in usSEABED database (Reid and others, 2006).

Table 5. Regional sediment accumulation rates on the California continental shelf.

[All values in millimeters per year. ND, no data]

Region (fig. 35)	Inner shelf (<50-m depth)	Midshelf (50–100-m depth)	Outer shelf (>100-m depth)	Long-term rate
1	13–33[1]	4.2–8[2,3]	1.5–6.4[2,3]	1–5[4]
2	ND	3.7–4.8[2]	1.5–2.4[2,5]	ND
3	ND	1–3.9[6]	ND	2.2–3.5[7,8,9]
4	ND	ND	ND	ND
5	ND	ND	0.5–0.9[10]	0.6–1.2[10,13]
6	1.8–9.7[11]	1–6[11]	0.9–4.9[11]	0.15–0.9[12,13]
7	ND	1–2[14]	ND	~3[15]

Notes: [1]Crockett and Nittrouer (2004), [2]Wheatcroft and Sommerfield (2005), [3]Sommerfield and Nittrouer (1999), [4]Sommerfield, and others (2002), [5]Demirpolat (1999), [6]Lewis and others (2002), [7]Greene (1977), [8]Mullins and others (1985), [9]Chin and others (1988), [10]Schwalbach and Gorsline (1985), [11]Alexander and Venherm (2003), [12]Sommerfield and Lee (2003), [13]Sommerfield and Lee (2004), [14]Lee and others (2002), [15]Hampton and others (2002).

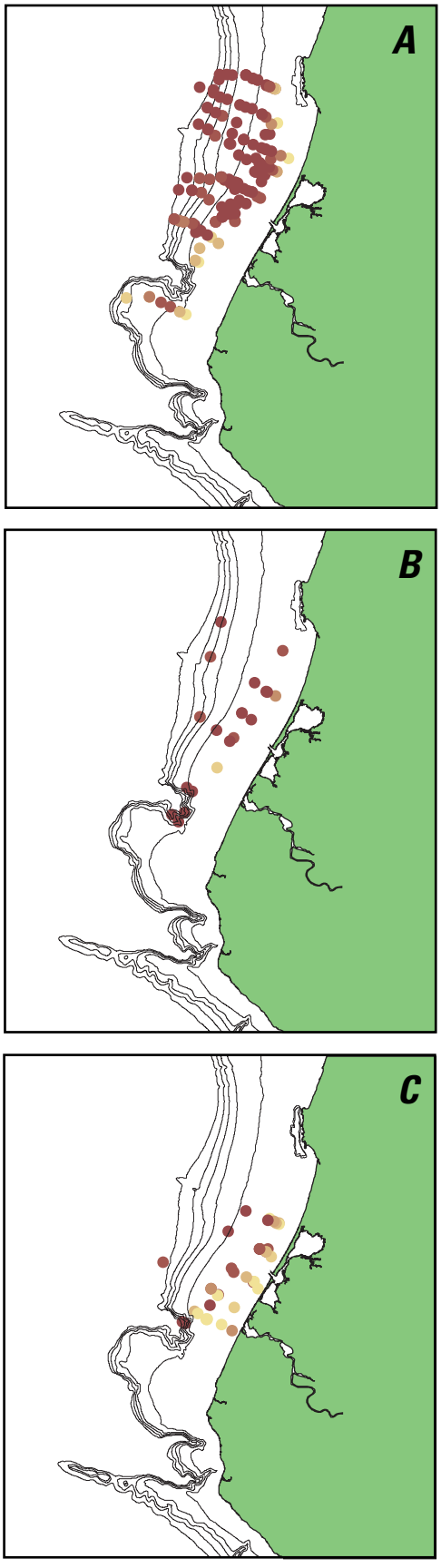

Figure 39. Outline maps of California coast (fig. 1) in area of the Eel River shelf, showing distribution of fine-sediment content from sea-floor-sediment-sampling sites (dots) in usSEABED database (Reid and others, 2006) Dynamic characteristic of shelf is evident in changes in sediment composition in 1995 (*A*), 1997 (*B*), and 1998 (*C*). Contour interval, 100 m.

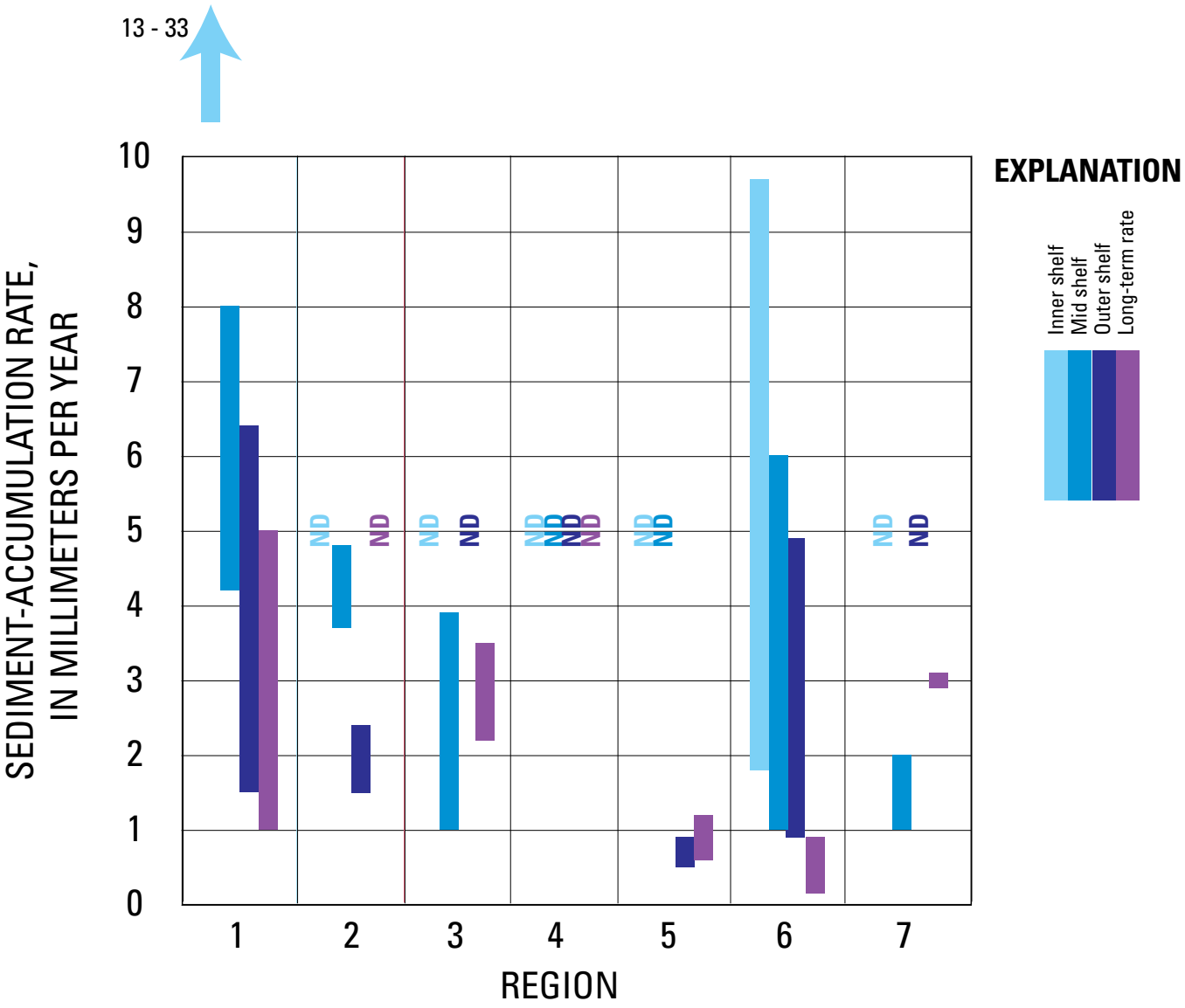

Figure 40. Regional modern and Holocene sediment-accumulation rates on the California continental shelf in regions 1 through 7 (fig. 35). ND, no data. See table 5 for data sources.

Summary

Fine sediment is deposited on the seabed along the California coast and forms thick (maximum of tens of meters) deposits on the continental shelf (table 5). Fine sediment typically dominates the seabed offshore of large river-sediment sources and in midshelf water depths; however, significant amounts of fine sediment are observed along the inner shelf, where it can represent a significant portion of the fine-sediment budget (for example, ~10 percent of Eel River discharge; Crockett and Nittrouer, 2004), especially in southern California, where fine sediment is not subject to strong depth control, presumably owing to the lower wave energy of this region. Sediment-accumulation rates appear to be highest offshore of large river-sediment sources, such as the Eel River, and consistently higher in shallower water depths. Long-term sediment-accumulation rates are generally consistent with recent accumulation rates except in southern California, where a tenfold discrepancy exists.

Conclusions

The results of this study suggest that large amounts of fine sediment are supplied to California coastal waters and that the source of this sediment is dominantly coastal rivers. Significant spatial and temporal variation exists in the supplies of sediment, which are related to the geographic province of the watersheds and the intensity of winter storms, respectively. The dispersal of sediment occurs primarily as suspended transport related to bottom-wave orbital velocities. This transport may be enhanced by downslope gravity flows of fluid mud when sufficient amounts of suspended sediment are available. Fine sediment has been observed to be initially deposited and resuspended during storms over a progression of events before final deposition and burial. In fact, most periods when waves are able to resuspend fine sediment on the continental shelf occur outside of times of river-flood events. Although midshelf mud belts are a conspicuous feature of fine-sediment accumulation, we note that significant amounts of fine sediment are also deposited and retained on the shelf both inshore and offshore of these mud belts. Inner-shelf accumulation of sediment appears to be greater in southern California than in central or northern California, owing to differences in wave climate and, possibly, shelf morphology.

Acknowledgments

This project was supported by the USGS Coastal and Marine Geology Program and the California Resources Agency under a Coastal Impact Assistance Program grant for the California Sediment Master Plan (California Sediment Management Workshop, 2006) being formulated by the CSMW and the California Department of Boating and Waterways (DBW). The manuscript was prepared with input from CSMW personnel but does not necessarily represent the official position of member agencies. We thank Patrick Barnard (USGS), Amy Draut (USGS), Clif Davenport (CSMW), Mark Johnsson (California Coastal Commission), Homa Lee (USGS), Jane Reid (USGS), Arthur Shak (USACE), and Kim Sterrett (DBW) for their reviews of the manuscript.

References Cited

Alexander, C.R., and Simoneau, A.M., 1999, Spatial variability in sedimentary processes on the Eel continental slope: Marine Geology, v. 154, no. 1–4, p. 243–254.

Alexander, C.R., and Venherm, C., 2003, Modern sedimentary processes in the Santa Monica, California continental margin; sediment accumulation, mixing and budget: Marine Environmental Research, v. 56, no. 1–2, p. 177–204.

Anchor Environmental CA L.P., 2003, Literature review of effects of resuspended sediments due to dredging operations: Los Angeles, Contaminated Sediment Task Force, 87 p.

Andrews, E.D., Antweiler, R.C., Neiman, P.J., and Ralph, F.M., 2004, Influence of ENSO on flood frequency along the California coast: Journal of Climate, v. 17, p. 337–348.

Asselman, N.E.M., 2000, Fitting and interpretation of sediment rating curves: Journal of Hydrology, v. 234, no. 3–4, p. 228–248.

Benumof, B.T., and Griggs, G.B., 1999, The relationships between seacliff erosion rates, cliff material properties, and physical processes, San Diego, California: Shore and Beach, v. 67, no. 4, p. 29–41.

Boggs, S., 1987, Principles of sedimentology and stratigraphy: New York, Macmillan, 784 p.

Bruland, K.W., Rue, E.L., and Smith, G.J., 2001, Iron and macronutrients in California coastal upwelling regimes; implications for diatom blooms: Limnology and Oceanography, v. 46, no. 7, p. 1661–1674.

Buck, K.N., Lohan, M.C., Berger, C.J.M., and Bruland, K.W., 2007, Dissolved iron speciation in two distinct river plumes and an estuary; Implications for riverine iron supply: Limnology and Oceanography, v. 52, no. 2, p. 843–855.

California Department of Boating and Waterways and California Coastal Conservancy, 2002, California beach restoration study: Sacramento, California Department of Boating and Waterways, 280 p.

California Coastal Sediment Management Workgroup, 2006, Sediment Master Plan Status Report: URL *http://www.dbw.ca.gov/csmw/PDF/SMPSR_status_report.pdf*.

Campbell, F.B., and Bauder, H.A., 1940, A rating-curve method for determining silt-discharge of streams: Eos (American Geophysical Union Transactions), v. 21, p. 603–607.

Chin, J.L., Clifton, H.E., and Mullins, H.T., 1988, Seismic stratigraphy and late Quaternary shelf history, south-central Monterey Bay, California: Marine Geology, v. 81, no. 1–4, p. 137–157.

Cleveland, W.S., 1979, Robust locally weighted regression and smoothing scatterplots: American Statistical Association Journal, v. 74, no. 368, p. 829–836.

Crockett, J.S., and Nittrouer, C.A., 2004, The sandy inner shelf as a repository for muddy sediment; an example from Northern California: Continental Shelf Research, v. 24, no. 1, p. 55–73.

Curran, K.J., Hill, P.S., and Milligan, T.G., 2002, Fine-grained suspended sediment dynamics in the Eel River flood plume: Continental Shelf Research, v. 22, no. 17, p. 2537–2550.

Demirpolat, S., 1991, Surface and near-surface sediments from the continental shelf off the Russian River, northern California: Marine Geology, v. 99, no. 1–2, p. 163–173.

Drake, D.E., 1972, Distribution and transport of suspended matter, Santa Barbara Channel, California: Los Angeles, University of Southern California, Ph.D. thesis, 358 p.

Drake, D.E., 1999, Temporal and spatial variability of the sediment grain-size distribution on the Eel Shelf; the flood layer of 1995: Marine Geology, v. 154, no. 1–4, p. 169–182.

Drake, D.E., and Cacchione, D.A., 1985, Seasonal variation in sediment transport on the Russian River shelf, California: Continental Shelf Research, v. 4, no. 5, p. 495–514.

Drake, D.E., Eganhouse, R.P., and McArthur, W., 2002, Physical and chemical effects of grain aggregates on the Palos Verdes margin, southern California: Continental Shelf Research, v. 22, no. 6–7, p. 967–986.

Dyer, K.R., 1986, Coastal and estuarine sediment dynamics: New York, John Wiley and Sons, 342 p.

Edwards, B.D., 2002, Variations in sediment texture on the northern Monterey Bay National Marine Sanctuary continental shelf: Marine Geology, v. 181, no. 1–3, p. 83–100.

Eittreim, S.L., Anima, R., and Stevenson, A.J., 2002a, Seafloor geology of the Monterey Bay area continental shelf: Marine Geology, v. 181, no. 1–3, p. 3–34.

Eittreim, S.L., Edwards, B.D., and Anima, R.J., 2000, Mid-shelf mudbelt in northern Monterey Bay [abs.]: Eos (American Geophysical Union Transactions), v. 81, p. 682.

Eittreim, S.L., Xu, J.P., Noble, M., and Edwards, B.D., 2002b, Towards a sediment budget for the Santa Cruz shelf: Marine Geology, v. 181, no. 1–3, p. 235–248.

Fan, S., Swift, D.J.P., Traykovski, P., Bentley, S., Borgeld, J.C., Reed, C.W., and Niedoroda, A.W., 2004, River flooding, storm resuspension, and event stratigraphy on the northern California shelf; observations compared with simulations: Marine Geology, v. 210, no. 1–4, p. 17–41.

Ferguson, R.I., 1987, Accuracy and precision of methods for estimating river loads: Earth Surface Processes and Landforms, v. 12, no. 1, p. 95–104.

George, D.A., Hill, P.S., and Milligan, T., 2006, Flocculation, heavy metals (Cu, Pb, Zn) and the sand-mud transition on the Adriatic continental shelf, Italy: Continental Shelf Research, v. 27, no. 3–4, p.475–488.

Geyer, W.R., Hill, P., Milligan, T., and Traykovski, P., 2000, The structure of the Eel River plume during floods: Continental Shelf Research, v. 20, p. 2067–2093.

Geyer, W.R., Hill, P.S., and Kineke, G.C., 2004, The transport and dispersal of sediment by buoyant coastal flows: Continental Shelf Research, v. 27, no. 7–8, p. 927–949.

Greene, H.G., 1977, Geology of the Monterey Bay region: U.S. Geological Survey Open-File Report 77–718, 343 p.

Griggs, G.B., and Hein, J.R., 1980, Sources, dispersal, and clay mineral composition of fine-grained sediment off central and northern California: Journal of Geology, v. 88, no. 5, p. 541–566.

Guy, H.P., and Norman, V.W., 1970, Field methods for measurement of fluvial sediment, chap. C2 of Applications of hydraulics (book 3): U.S. Geological Survey Techniques of Water-Resources Investigation, 59 p.

Hadley, R.F., Lal, E., Onstad, C., Walling, D.E., and Yair, A., 1985, Recent developments in erosion and sediment yield studies: Paris, UNESCO, 127 p.

Hampton, M.A., Karl, H., and Murray, C.J., 2002, Acoustic profiles and images of the Palos Verdes Margin; implications concerning deposition from the White's Point outfall: Continental Shelf Research, v. 22, no. 6–7, p. 841–858.

Harris, C.K., Traykovski, P., and Geyer, W.R., 2005, Flood dispersal and deposition by near-bed gravitational sediment flows and oceanographic transport; a numerical modeling study of the Eel River shelf, northern California: Journal of Geophysical Research, v. 110, no. C9, doi:10.1029/2004JC002727.

Harris, C.K., and Wiberg, P.L., 1997, Approaches to quantifying long-term continental shelf sediment transport with an example from the northern California STRESS mid-shelf site: Continental Shelf Research, v. 17, no. 11, p. 1389–1418.

Hicks, D.M., Gomez, B., and Trustrum, N.A., 2000, Erosion thresholds and suspended sediment yields, Waipaoa River Basin, New Zealand: Water Resources Research, v. 36, no. 4, p. 1129–1142.

Hill, P.S., Milligan, T.G., and Geyer, W.R., 2000, Controls on effective settling velocity of suspended sediment in the Eel River flood plume: Continental Shelf Research, v. 20, no. 16, p. 2095–2111.

Hillel, D., 1982, Introduction to soil physics: San Diego, Calif., Academic Press, 364 p.

Inman, D.L., and Jenkins, S.A., 1999, Climate change and the episodicity of sediment flux of small California rivers: Journal of Geology, v. 107, no. 3, p. 251–270.

Inman, D.L., Jenkins, S.A., and Wasyl, J., 1998, Database for streamflow and sediment flux of California rivers: Scripps Institute of Oceanography Reference Series 98–9, 13 p.

Johnson, K.S., Chavez, F.P., and Friedrich, G.E., 1999, Continental-shelf sediment as a primary source of iron for coastal phytoplankton: Nature, v. 398, no. 6729, p. 697–700.

Kirk, J.T.O., 1996, Light and photosynthesis in aquatic ecosystems (2d ed.): Cambridge, U.K., Cambridge University Press, 509 p.

Komar, P.D., 1996, The budget of littoral sediments; concepts and applications: Shore and Beach, v. 64, no. 3, p. 18–26.

Komar, P.D., 1998, Beach processes and sedimentation (2d ed.): Upper Saddle River, N.J., Prentice Hall, 544 p.

Lee, H.J., Sherwood, C.R., Drake, D.E., Edwards, B.D., Wong, F.L., and Hamer, M., 2002, Spatial and temporal distribution of contaminated, effluent-affected sediment on the Palos Verdes margin, southern California: Continental Shelf Research, v. 22, no. 6–7, p. 859–880.

Lee, H.J., and Wiberg, P.L., 2002, Character, fate and biological effects of contaminated, effluent-affected sediment on the Palos Verdes margin, southern California; an overview: Continental Shelf Research, v. 22, no. 6–7, p. 835–840.

Lewis, R.C., Coale, K.H., Edwards, B.D., Marot, M., Douglas, J.N., and Burton, E.J., 2002, Accumulation rate and mixing of shelf sediments in the Monterey Bay National Marine Sanctuary: Marine Geology, v. 181, no. 1–3, p. 157–169.

Mantua, N.J., Haidvogel, D., Kushnir, Y., and Bond, N., 2002, Making the climate connections; bridging scales of space and time in the U.S. GLOBEC program: Oceanography, v. 15, no. 2, p. 75–86.

Mantua, N.J., and Hare, S.R., 2002, The Pacific Decadal Oscillation: Journal of Oceanography, v. 58, no. 1, p. 35–44.

McCave, I.N., 1972, Transport and escape of fine-grained sediment from shelf areas, in Swift, D.J.P., Duane, D., and Pilkey, O.H., eds., Shelf sediment transport; process and pattern: Stroudsburg, Pa., Dowden, Hutchinson and Ross, p. 225–248.

McCave, I.N., and Syvitski, J.P.M., 1991, Principles and methods of geological particle size analysis, in Syvitski, J.P.M., ed., Principles, methods, and application of particle size analysis: New York, Cambridge University Press, p. 3–21.

McCool, W.W., and Parsons, J.D., 2004, Sedimentation from buoyant fine-grained suspensions: Continental Shelf Research, v. 24, no. 10, p. 1129–1142.

Mertes, L.A.K., and Warrick, J.A., 2001, Measuring flood output from 110 coastal watersheds in California with field measurements and SeaWiFS: Geology, v. 29, no. 7, p. 659–662.

Milliman, J.D., and Syvitski, J.P.M., 1992, Geomorphic/tectonic control of sediment discharge to the ocean; the importance of small mountainous rivers: Journal of Geology, v. 100, no. 5, p. 525–544.

Mulder, T., and Syvitski, J.P.M., 1995, Turbidity currents generated at river mouths during exceptional discharges to the world oceans: Journal of Geology, v. 103, no. 3, p. 285–299.

Mullenbach, B.L., Nittrouer, C.A., Puig, P., and Orange, D.L., 2004, Sediment deposition in a modern submarine canyon; Eel Canyon, northern California: Marine Geology, v. 211, no. 1–2, p. 101–119.

Mullins, H.T., Nagel, D.K., and Dominguez, L.L., 1985, Tectonic and eustatic controls of late Quaternary shelf sedimentation along the central California (Santa Cruz) continental margin; high-resolution seismic stratigraphic evidence: Sedimentary Geology, v. 45, no. 3–4, p. 327–347.

Nittrouer, C.A., 1999, STRATAFORM; overview of its design and synthesis of its results: Marine Geology, v. 154, no. 1–4, p. 3–12.

Nittrouer, C.A., and Sternberg, R.W., 1981, The formation of sedimentary strata in an allochthonous shelf environment; the Washington continental shelf: Marine Geology, v. 42, no. 1–4, p. 201–232.

Nittrouer, C.A., Sternberg, R.W., Carpenter, R., and Bennet, J.T., 1979, The use of Pb-210 geochronology as a sedimentological tool; application to the Washington continental shelf: Marine Geology, v. 31, no. 3–4, p. 297–316.

Noble, M., Ryan, H.F., and Wiberg, P.L., 2002, The dynamics of subtidal poleward flows over a narrow continental shelf, Palos Verdes, CA: Continental Shelf Research, v. 22, no. 6–7, p. 923–944.

Noble, M., and Xu, J.P., 2003, Observations of large-amplitude cross-shore internal bores near the shelf break, Santa Monica Bay, CA: Marine Environmental Research, v. 56, no. 1–2, p. 127–149.

Ogston, A.S., Cacchione, D.A., Sternberg, R.W., and Kineke, G.C., 2000, Observations of storm and river flood-driven sediment transport on the northern California continental shelf: Continental Shelf Research, v. 20, no. 16, p. 2141–2162.

Patsch, K., and Griggs, G.B., 2007, Development of sand budgets for California's major littoral cells: Santa Cruz, University of California, Institute of Marine Sciences, 115 p.

Pullen, J.D., and Allen, J.S., 2000, Modeling studies of the coastal circulation off Northern California; shelf response to a major Eel River flood event: Continental Shelf Research, v. 20, no. 16, p. 2213–2238.

Rantz, S.E., compiler, 1982, Measurement and computation of streamflow: U.S. Geological Survey Water-Supply Paper 2175, 2 v.

Reid, J.A., Reid, J.M., Jenkins, C.J., Zimmermann, M., Williams, S.J., and Field, M.E., 2006, usSEABED; Pacific coast (California, Oregon, and Washington) offshore surficial-sediment data release: U.S. Geological Survey Data Series 182 [URL *http://pubs.usgs.gov/ds/2006/182/*].

Sadler, P.M., 1999, The influence of hiatuses on sediment accumulation rates: GeoResearch Forum, v. 5, p. 15–40.

Schoelhamer, D.H., Lionberger, M.A., Jaffe, B.E., Ganju, N.K., Wright, S.A., and Shellenbarger, G.G., 2005, Bay sediment budgets; sediment accounting 101, in Pulse of the estuary; monitoring and managing water quality in the San Francisco Estuary: Oakland, Calif., San Francisco Estuary Institute, p. 58–63.

Schwalbach, J.R., and Gorsline, D.S., 1985, Holocene sediment budgets for the basins of the California Continental Borderland: Journal of Sedimentary Petrology, v. 55, no. 6, p. 829–842.

Scott, K.M., and Williams, R.P., 1978, Erosion and sediment yields in the Transverse Ranges, southern California: U.S. Geological Survey Professional Paper 1030, 38 p.

Scully, M.E., Friedrichs, C.T., and Wright, L.D., 2002, Application of an analytical model of critically stratified gravity-driven sediment transport and deposition to observations from the Eel River continental shelf, Northern California: Continental Shelf Research, v. 22, no. 14, p. 1951–1974.

Sherwood, C.R., Drake, D.E., Wiberg, P.L., and Wheatcroft, R.A., 2002, Prediction of the fate of p,p′–DDE in sediment on the Palos Verdes shelf, California, USA: Continental Shelf Research, v. 22, no. 6–7, p. 1025–1058.

Sommerfield, C.K., 2006, On sediment accumulation rates and stratigraphic completeness; lessons from Holocene ocean margins: Continental Shelf Research, v. 26, p. 2225–2240.

Sommerfield, C.K., Drake, D.E., and Wheatcroft, R.A., 2002, Shelf record of climatic changes in flood magnitude and frequency, north-coastal California: Geology, v. 30, no. 5, p. 395–398.

Sommerfield, C.K., and Lee, H.J., 2003, Magnitude and variability of Holocene sediment accumulation in Santa Monica Bay, California: Marine Environmental Research, v. 56, no. 1–2, p. 151–176.

Sommerfield, C.K., and Lee, H.J., 2004, Across-shelf sediment transport since the Last Glacial Maximum, southern California margin: Geology, v. 32, no. 4, p. 345–348.

Sommerfield, C.K., and Nittrouer, C.A., 1999, Modern accumulation rates and a sediment budget for the Eel River shelf; a flood-dominated depositional environment: Marine Geology, v. 154, no. 1–4, p. 227–241.

Stanley, D.J., Addy, S.K., and Behrens, E.W., 1983, The mudline; variability of its position relative to shelfbreak, in Stanley, D.J., and Moore, G.T., eds., The shelfbreak; critical interface on continental margins: Tulsa, Okla., Society of Economic Paleontologists and Mineralogists Special Publication 33, p. 279–298.

Storlazzi, C.D., and Griggs, G.B., 2000, Influence of El Niño-Southern Oscillation (ENSO) events on the evolution of central California's shoreline: Geological Society of America Bulletin, v. 112, no. 2, p. 236–249.

Taylor, J.R., 1997, An introduction to error analysis (2d ed.): Sausalito, Calif., University Science Books, 327 p.

Thornton, E.B., Sallenger, A., Sesto, J.C., Egley, L., McGee, T., and Parsons, R., 2006, Sand mining impacts on long-term dune erosion in southern Monterey Bay: Marine Geology, v. 229, no. 1–2, p. 45–58.

Traykovski, P., Geyer, W.R., Irish, J.D., and Lynch, J.F., 2000, The role of wave-induced density-driven fluid mud flows for cross-shelf transport on the Eel River continental shelf: Continental Shelf Research, v. 20, no. 16, p. 2113–2140.

Trimble, S.W., 1997, Contribution of stream channel erosion to sediment yield from an urbanizing watershed: Science, v. 278, no. 21, p. 1442–1444.

Walling, D.E., 1977, Assessing the accuracy of suspended sediment rating curves for a small basin: Water Resources Research, v. 13, no. 3, p. 531–538.

Walling, D.E., and Moorehead, P.W., 1989, The particle size characteristics of fluvial suspended sediment; an overview: Hydrobiologia, v. 176–177, no. 1, p. 125–149.

Walling, D.E., and Webb, B.W., 1981, The reliability of suspended sediment load data, in Measurement of erosion and transport of sediments: IAHS-AISH Publication, v. 133, p. 177–194.

Warrick, J.A., Mertes, L.A.K., Washburn, L., and Siegel, D.A., 2004a, A conceptual model for river water and sediment dispersal in the Santa Barbara Channel, California: Continental Shelf Research, v. 24, no. 17, p. 2029–2043.

Warrick, J.A., Mertes, L.A.K., Washburn, L., and Siegel, D.A., 2004b, Dispersal forcing of southern California river plumes, based on field and remote sensing observations: Geo-Marine Letters, v. 24, no. 1, p. 46–52.

Warrick, J.A., and Milliman, J.D., 2003, Hyperpycnal sediment discharge from semiarid southern California rivers; implications for coastal sediment budgets: Geology, v. 31, no. 9, p. 781–784.

Warrick, J.A., and Rubin, D., 2007, Suspended-sediment rating curve response to urbanization and wildfire, Santa Ana River, California: Journal of Geophysical Research, v. 112, no. F2, doi:10.1029/2006JF000662.

Wass, P.D., and Leeks, G.J.L., 1999, Suspended sediment fluxes in the Humber catchment, UK: Hydrological Processes, v. 13, no. 7, p. 935–953.

Wheatcroft, R.A., and Butman, C.A., 1997, Spatial and temporal variability in aggregated grain-size distribution, with implications for sediment dynamics: Continental Shelf Research, v. 17, no. 4, p. 367–390.

Wheatcroft, R.A., and Sommerfield, C.K., 2005, River sediment flux and shelf sediment accumulation rates on the Pacific Northwest margin: Continental Shelf Research, v. 25, no. 3, p. 311–332.

Wheatcroft, R.A., Sommerfield, C.K., Drake, D.E., Borgeld, J.C., and Nittrouer, C.A., 1997, Rapid and widespread dispersal of flood sediment on the Northern California margin: Geology, v. 25, no. 2, p. 163–166.

Wiberg, P.L., Drake, D.E., Harris, C.K., and Noble, M., 2002, Sediment transport on the Palos Verdes shelf over seasonal to decadal time scales: Continental Shelf Research, v. 22, no. 6–7, p. 987–1004.

Wiberg, P.L., and Harris, C.K., 2002, Desorption of p,p′–DDE from sediment during resuspension events on the Palos Verdes shelf, California; a modeling approach: Continental Shelf Research, v. 22, no. 6–7, p. 1005–1023.

Willis, C.M., and Griggs, G.B., 2003, Reductions in fluvial sediment discharge by coastal dams in California and implications for beach sustainability: Journal of Geology, v. 111, no. 2, p. 167–182.

Wright, L.D., and Friedrichs, C.T., 2006, Gravity-driven sediment transport on continental shelves; a status report: Continental Shelf Research, v. 26, no. 17–18, p. 2092–2107.

Wright, L.D., and Nittrouer, C.A., 1995, Dispersal of river sediments in coastal seas; six contrasting cases: Estuaries, v. 18, no. 3, p. 494–508.

Young, A.P., and Ashford, S.A., 2006, Application of airborne LIDAR for seacliff volumetric change and beach sediment budget contributions: Journal of Coastal Research, v. 22, no. 2, p. 307–318.

Yu, B., 2000, A systematic over-estimation of flows: Journal of Hydrology, v. 233, no. 1–4, p. 258-262.

Appendix A. Grain-Size Information

The Wentworth scale divides sediment into size classes based on powers of 2. According to this scale, fine sediment is defined as the clay and silt components and includes all particles smaller than 0.0625 mm in diameter (table A1). Krumbein introduced the phi (ϕ) scale as an alternative measure of sediment size, related to grain size by the equation

$$\phi = -\log_2 d,$$

such that $d=2^{-\phi}$, where d is the grain diameter (in millimeters). Thus, larger phi units correspond to smaller grain sizes. The phi scale is commonly used throughout the sedimentological community.

Table A1. Wentworth-Krumbein scale of sediment-size classification.

Sediment size	Phi (ϕ) unit	Lower-bin grain diameter (mm)
Boulder	−8	256
Cobble	−6	64
Pebble	−2	4
Granular	−1	2
Very coarse sand	0	1
Coarse sand	1	0.5
Medium sand	2	0.25
Fine sand	3	0.125
Very fine sand	4	0.0625
Silt	8	0.004
Clay	12	0.00024

Appendix B. Sediment-Discharge Rating Curves for All Stations

The traditional local regression (loess) weighting function is the tricube (fig. B1):

$$w(x) = \begin{cases} (1 - |x|^3)^3 & \text{for } |x| < 1 \\ 0 & \text{for } |x| \geq 1. \end{cases}$$

The estimated suspended-sediment concentration is then obtained by evaluating the local polynomial fit. The entire loess fit is complete after the regression-function values have been calculated for each data point. The flexibility in this method is that the degree of the polynomial model and the width of the subset window (α, the fraction of the total number of samples) are user selectable. For this project, all fits were given a degree of 1 (linear); the weighting factors (α values) of the loess rating curves for all the U.S. Geological Survey gaging stations used in this study (fig. 1) are listed in table B1.

Table B1. Weighting factors (α values) of loess sediment-discharge rating curves for all the U.S. Geological Survey gaging stations used in this study, listed from north to south.

[USGS, U.S. Geological Survey]

Watershed (fig. 1)	USGS gaging station	α value
Smith River	11532500	0.20
Supply Creek	11530020	0.20
Trinity River	11530000	0.20
Klamath River	11523000	0.20
Redwood Creek	11482500	0.20
Mad River	11481000	0.20
Eel River	11477000	0.20
Russian River	11467000	0.20
Pine Creek	11460170	0.40
Pescadero Creek	11162500	0.20
San Lorenzo River	11160500	0.20
Salinas River	11152500	0.20
Carmel River	11143250	0.30
San Jose Creek	11120510	0.40
Ventura River	11118500	0.20
Santa Clara River	11114000	0.30
Calleguas Creek	11106550	0.30
Santa Ana River	11078000	0.30
San Juan Creek	11046550	0.30
San Mateo River	11046370	0.50
Santa Margarita River	11046000	0.40
San Luis Rey River	11042000	0.20
San Dieguito River	11030500	0.40
San Diego River	11022500	0.30
Tijuana River	11013500	0.30

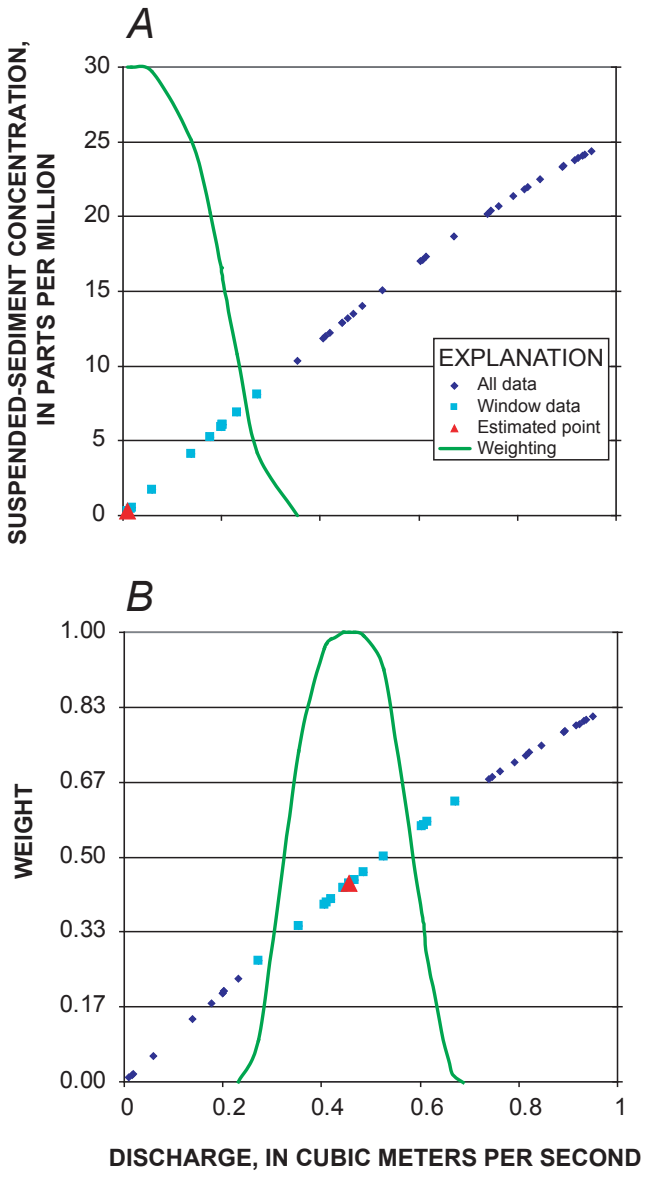

Figure B1. Example of loess rating-curve weighting function. *A*, Weighting function on outer edges of data, showing truncation of curve. *B*, Full weighting function for locally weighted regression.

Figure B2. Loess rating curves of suspended-sediment concentration versus discharge for watersheds used in this study (fig. 1). Top, instantaneous measured (green curve, left) and daily-reported (red curve, center) suspended-sediment concentration (in parts per million) versus discharge (in cubic meters per second), with a combined plot (right) of both datasets for comparison. Middle, vertically compressed plots of top two curves, with $\pm 2\sigma$ deviations of daily-reported suspended-sediment concentration (blue curves) added for reference. Bottom, residual analyses of weighted-least-squares fits to curves in middle plots.

A, Smith River (U.S. Geological Survey gaging sta. 11532500).

B, Supply Creek (U.S. Geological Survey gaging sta. 11530020).

C, Trinity River (U.S. Geological Survey gaging sta. 11530000).

D, Klamath River (U.S. Geological Survey gaging sta. 11523000).

E, Redwood Creek (U.S. Geological Survey gaging sta. 11482500).

F, Mad River (U.S. Geological Survey gaging sta. 11481000).

G, Eel River (U.S. Geological Survey gaging sta. 11477000).

H, Russian River (U.S. Geological Survey gaging sta. 11467000).

I, Pine Creek (U.S. Geological Survey gaging sta. 11460170).

J, Pescadero Creek (U.S. Geological Survey gaging sta. 11162500).

K, San Lorenzo River (U.S. Geological Survey gaging sta. 11160500).

L, Salinas River (U.S. Geological Survey gaging sta. 11152500).

M, Carmel River (U.S. Geological Survey gaging sta. 11143250).

N, San Jose Creek (U.S. Geological Survey gaging sta. 11120510).

O, Ventura River (U.S. Geological Survey gaging sta. 11118500).

P, Santa Clara River (U.S. Geological Survey gaging sta. 11114000).

Q, Calleguas Creek (U.S. Geological Survey gaging sta. 11106550).

R, Santa Ana River (U.S. Geological Survey gaging sta. 11078000).

S, San Juan Creek (U.S. Geological Survey gaging sta. 11046550).

T, San Mateo River (U.S. Geological Survey gaging sta. 11046370).

U, Santa Margarita River (U.S. Geological Survey gaging sta. 11046000).

V, San Luis Rey River (U.S. Geological Survey gaging sta. 11042000).

W, San Dieguito River (U.S. Geological Survey gaging sta. 11030500).

X, San Diego River (U.S. Geological Survey gaging sta. 11022500).

Y, Tijuana River (U.S. Geological Survey gaging sta. 11013500).

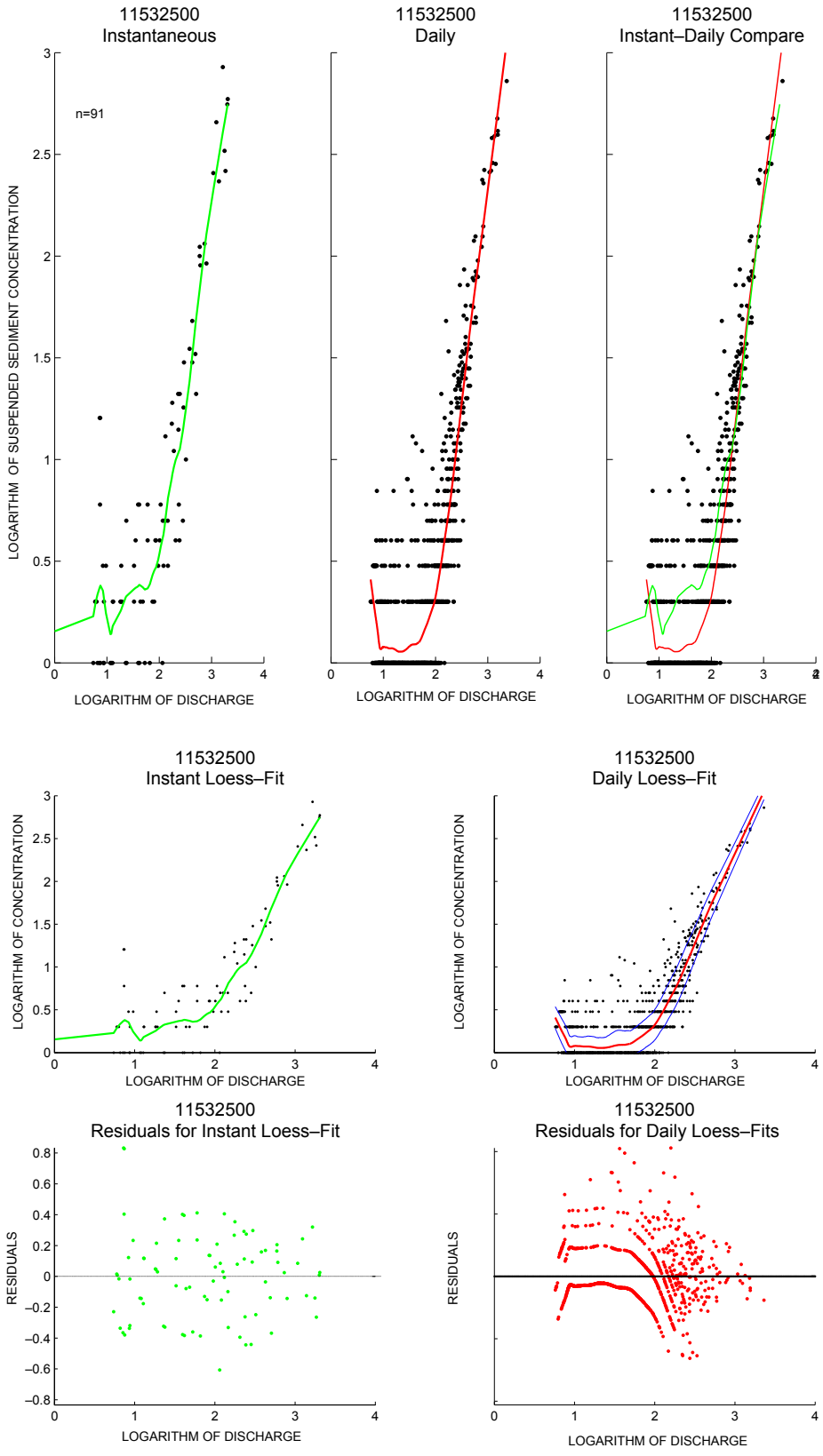

Figure B2. *A*, Smith River (U.S. Geological Survey gaging sta. 11532500).

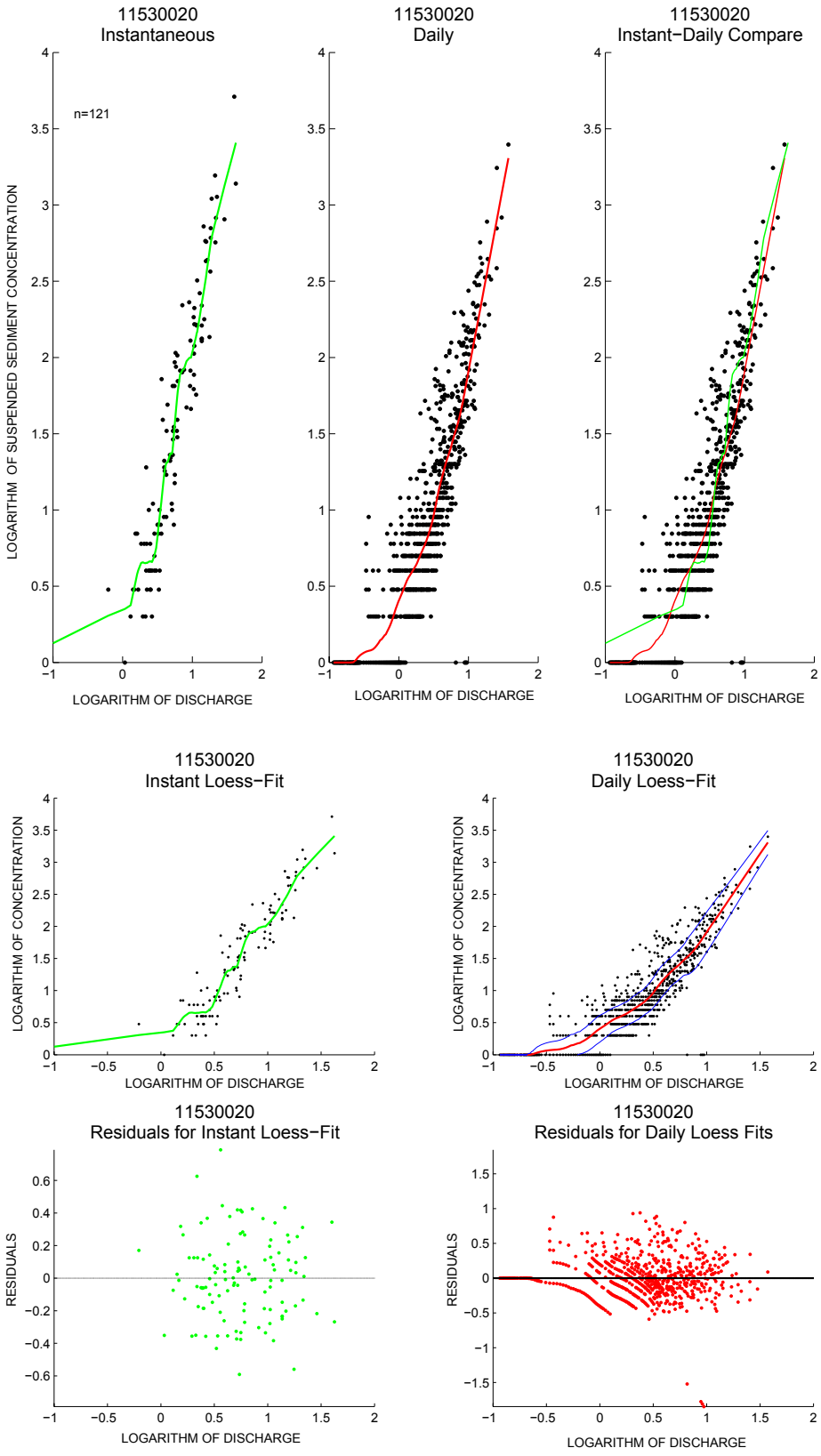

Figure B2 *B*, Supply Creek (U.S. Geological Survey gaging sta. 11530020)—Continued.

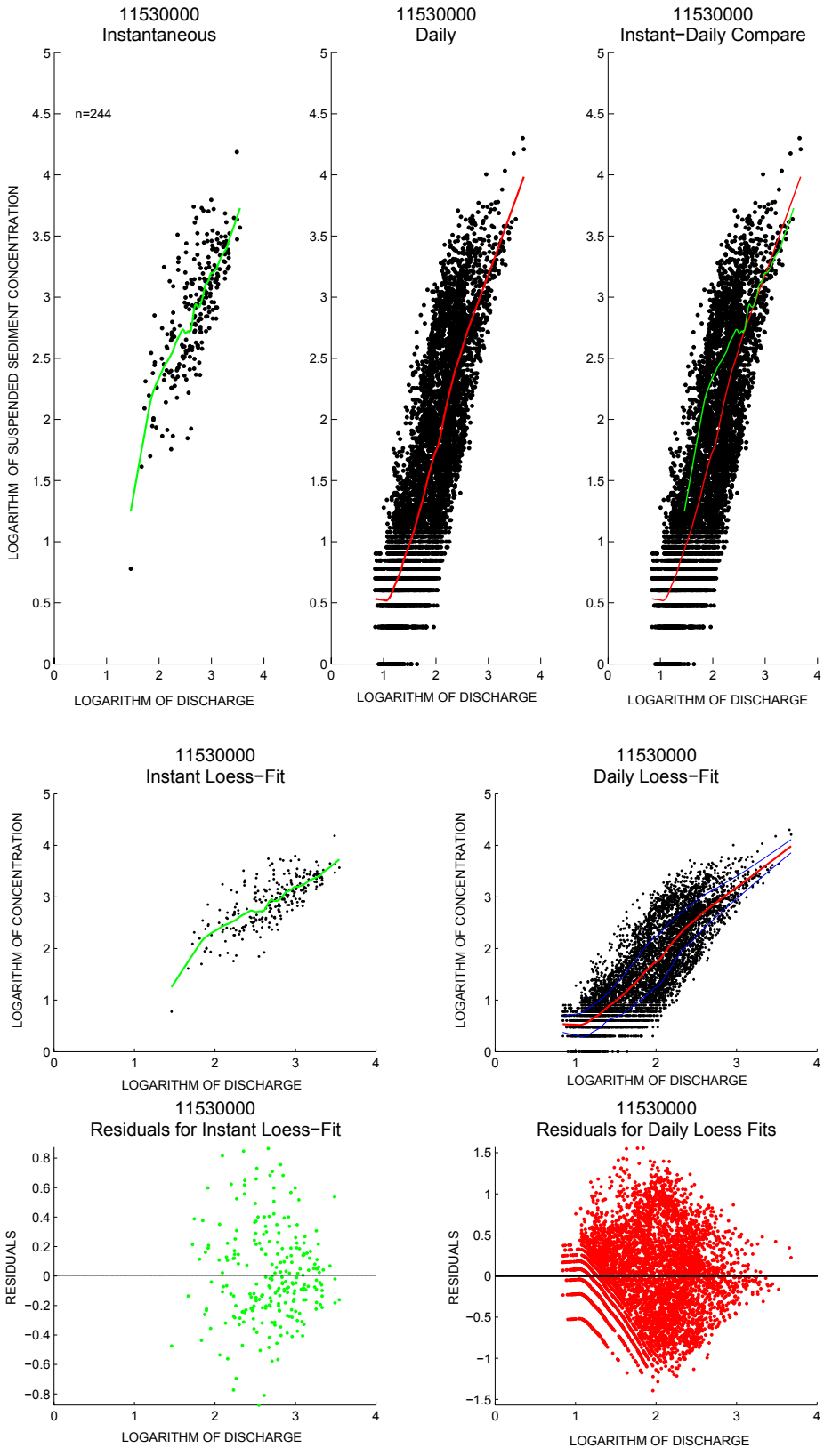

Figure B2 *C*, Trinity River (U.S. Geological Survey gaging sta. 11530000)—Continued.

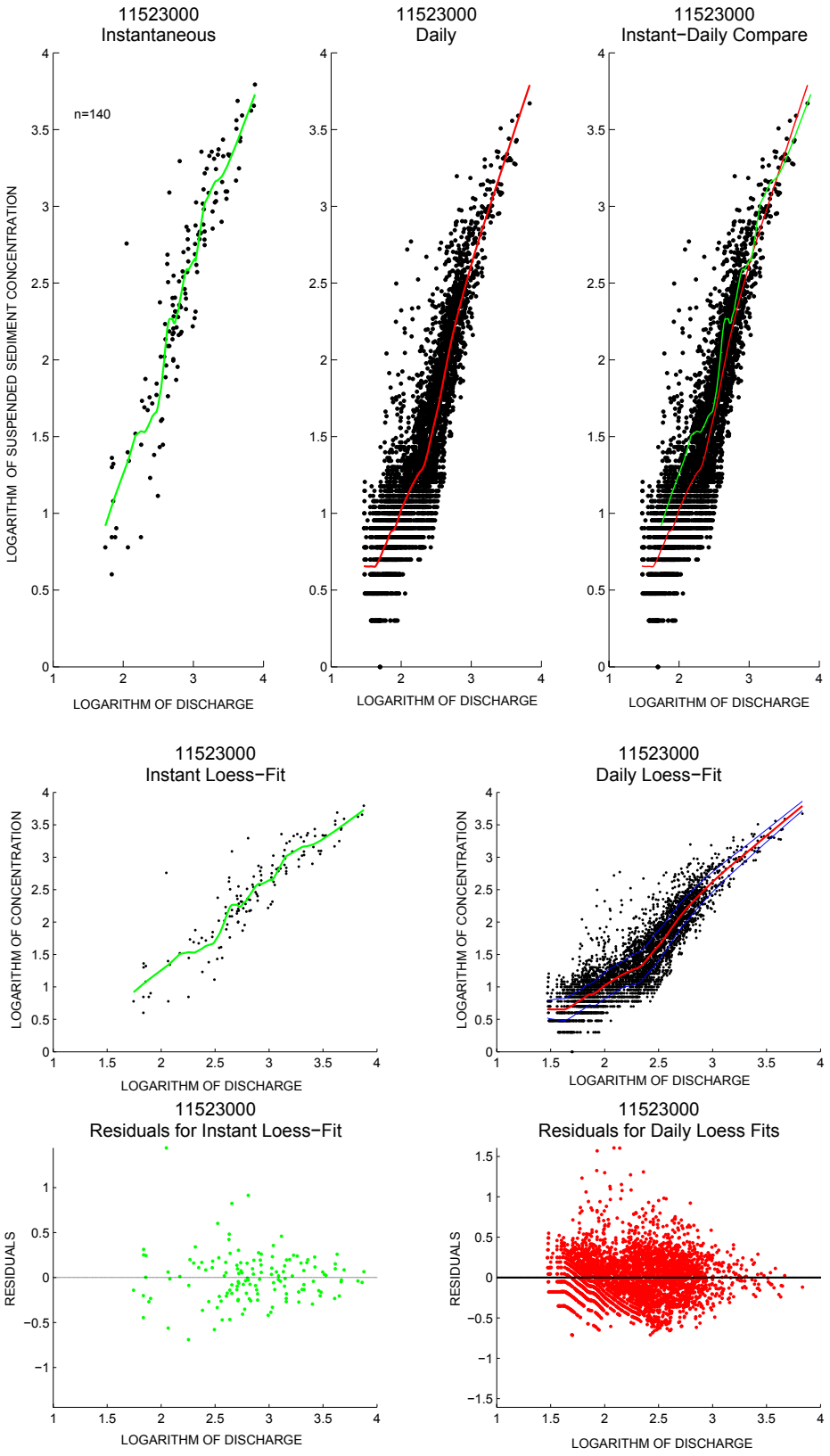

Figure B2 *D*, Klamath River (U.S. Geological Survey gaging sta. 11523000)—Continued.

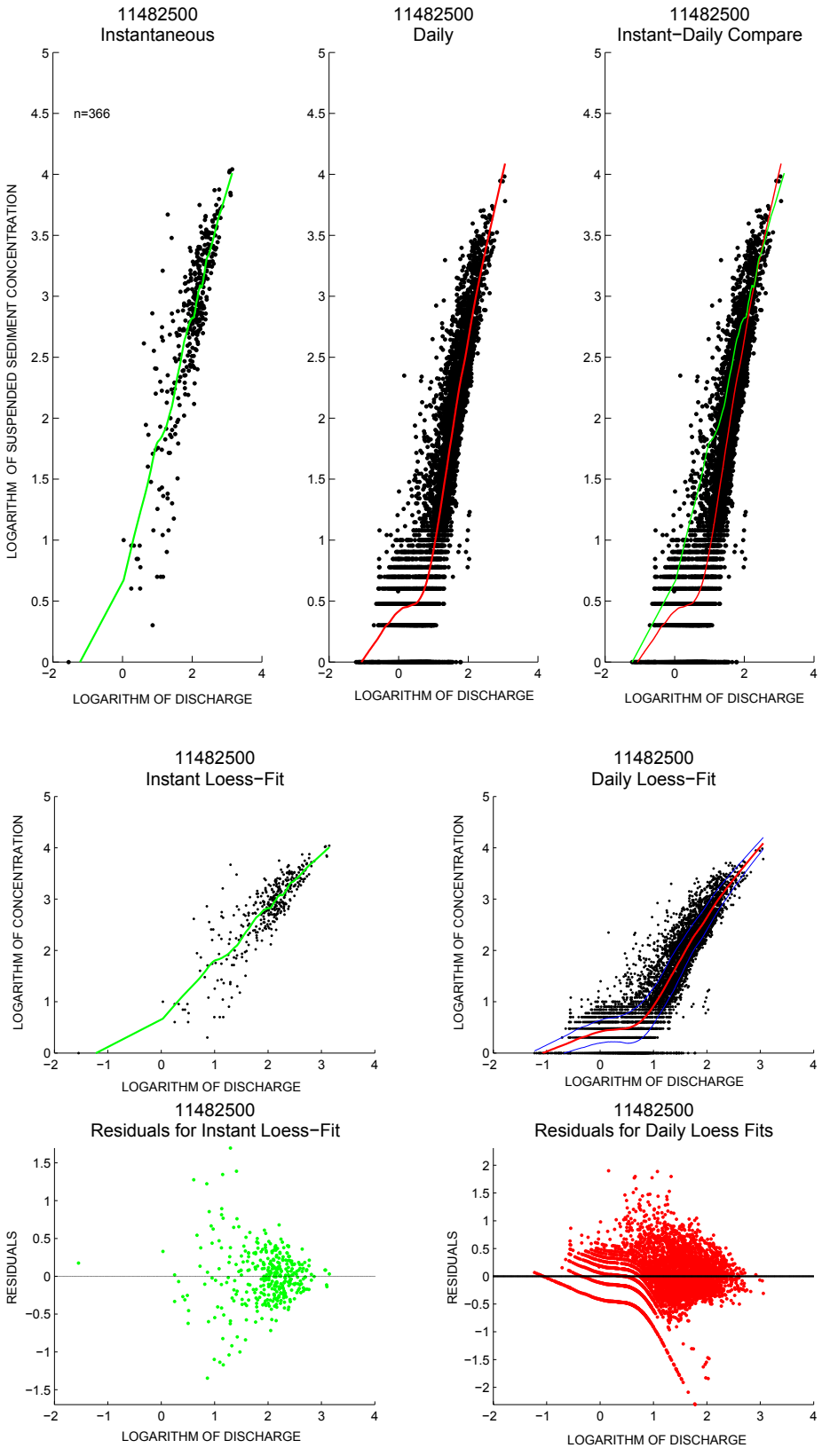

Figure B2 *E*, Redwood Creek (U.S. Geological Survey gaging sta. 11482500)—Continued.

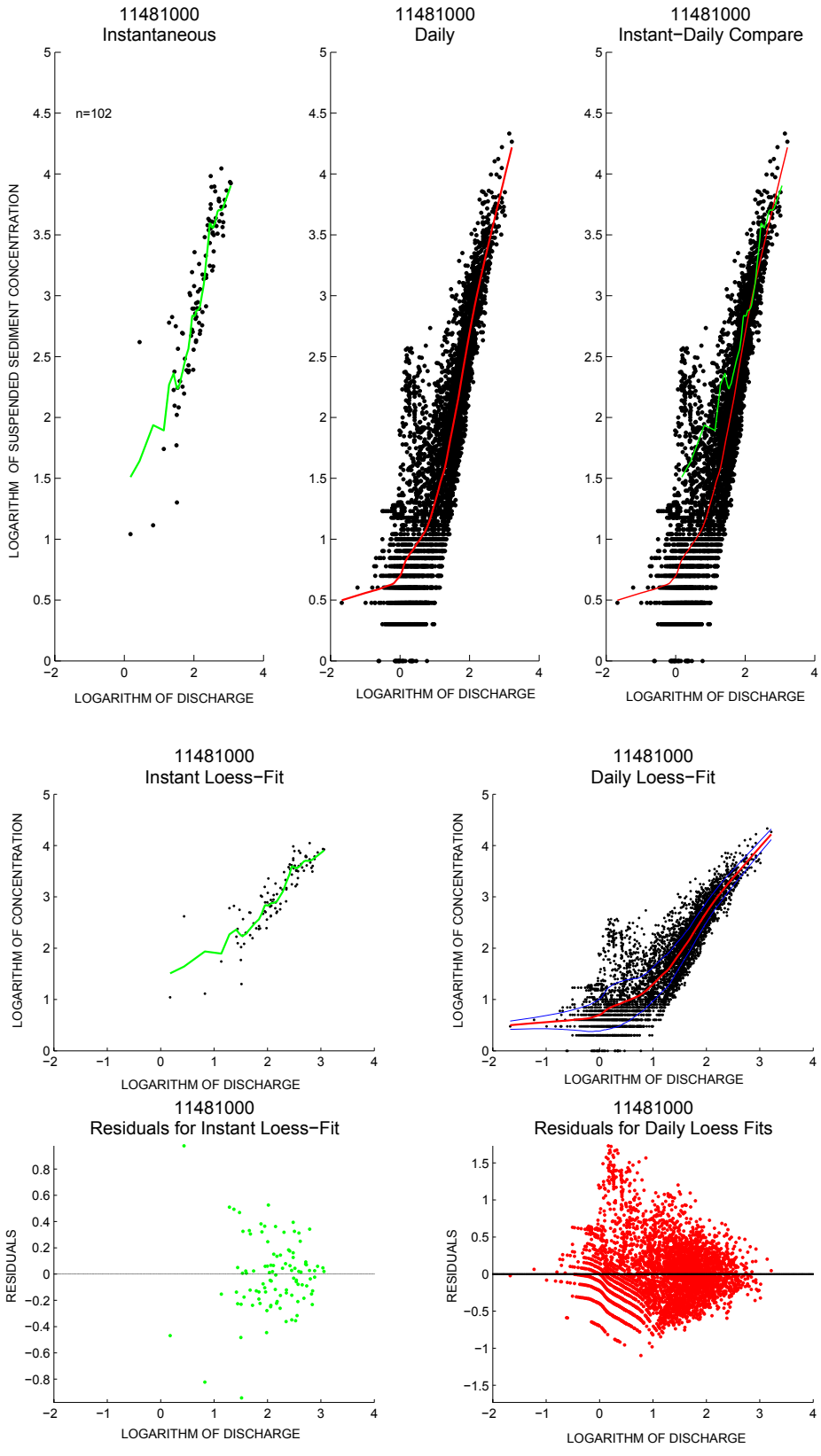

Figure B2 *F*, Mad River (U.S. Geological Survey gaging sta. 11481000)—Continued.

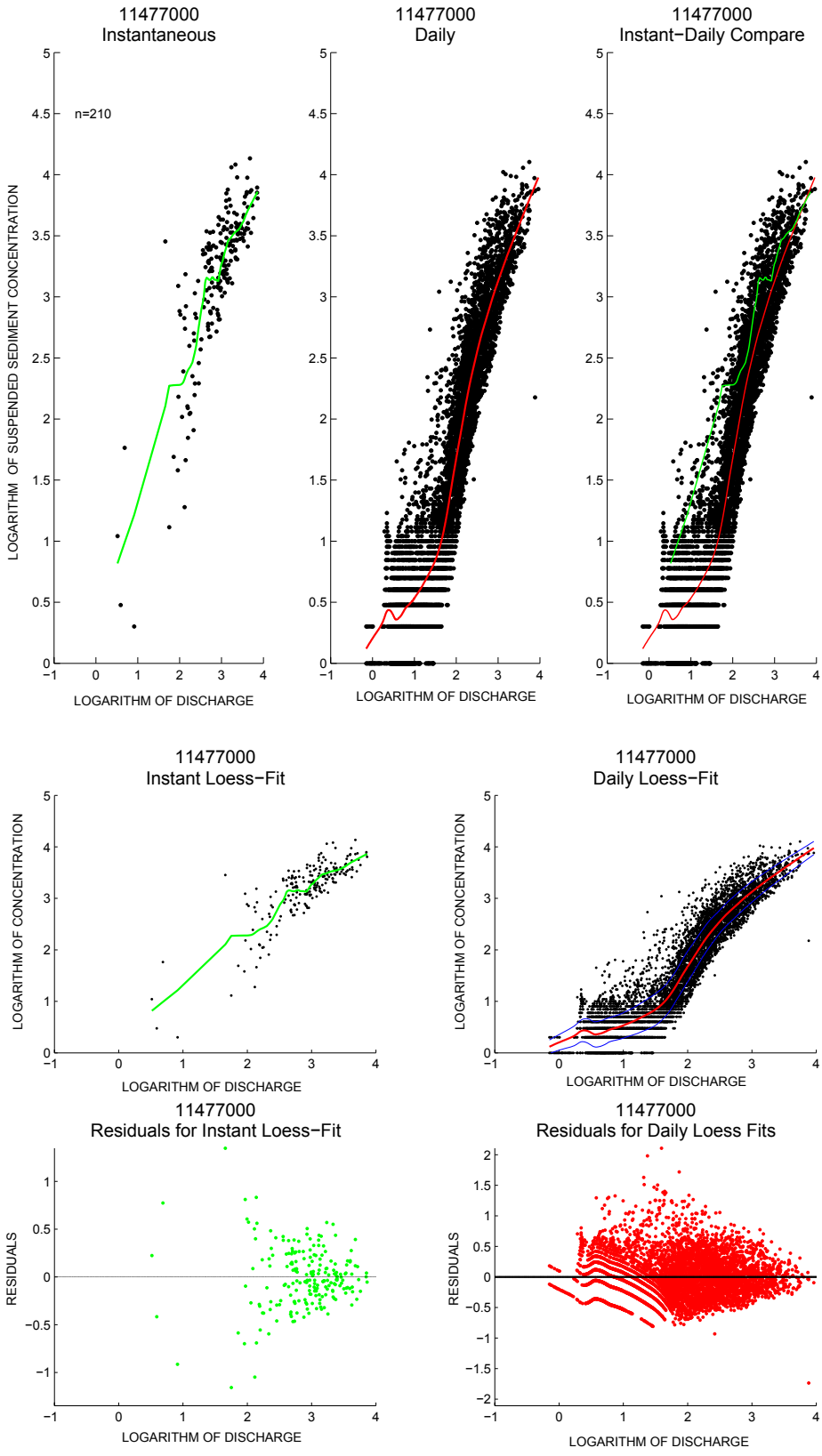

Figure B2 *G*, Eel River (U.S. Geological Survey gaging sta. 11477000)—Continued.

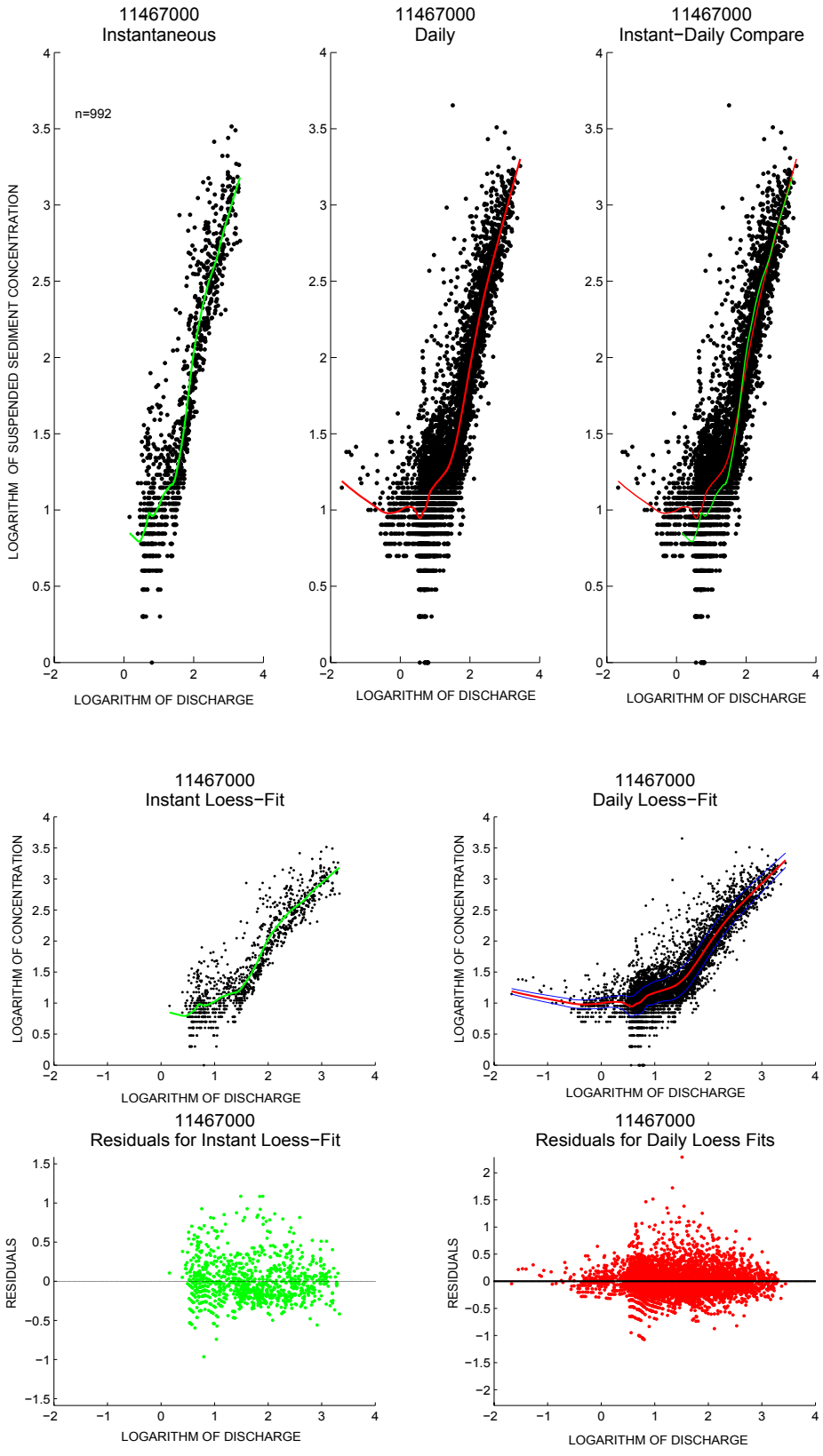

Figure B2 *H*, Russian River (U.S. Geological Survey gaging sta. 11467000)—Continued.

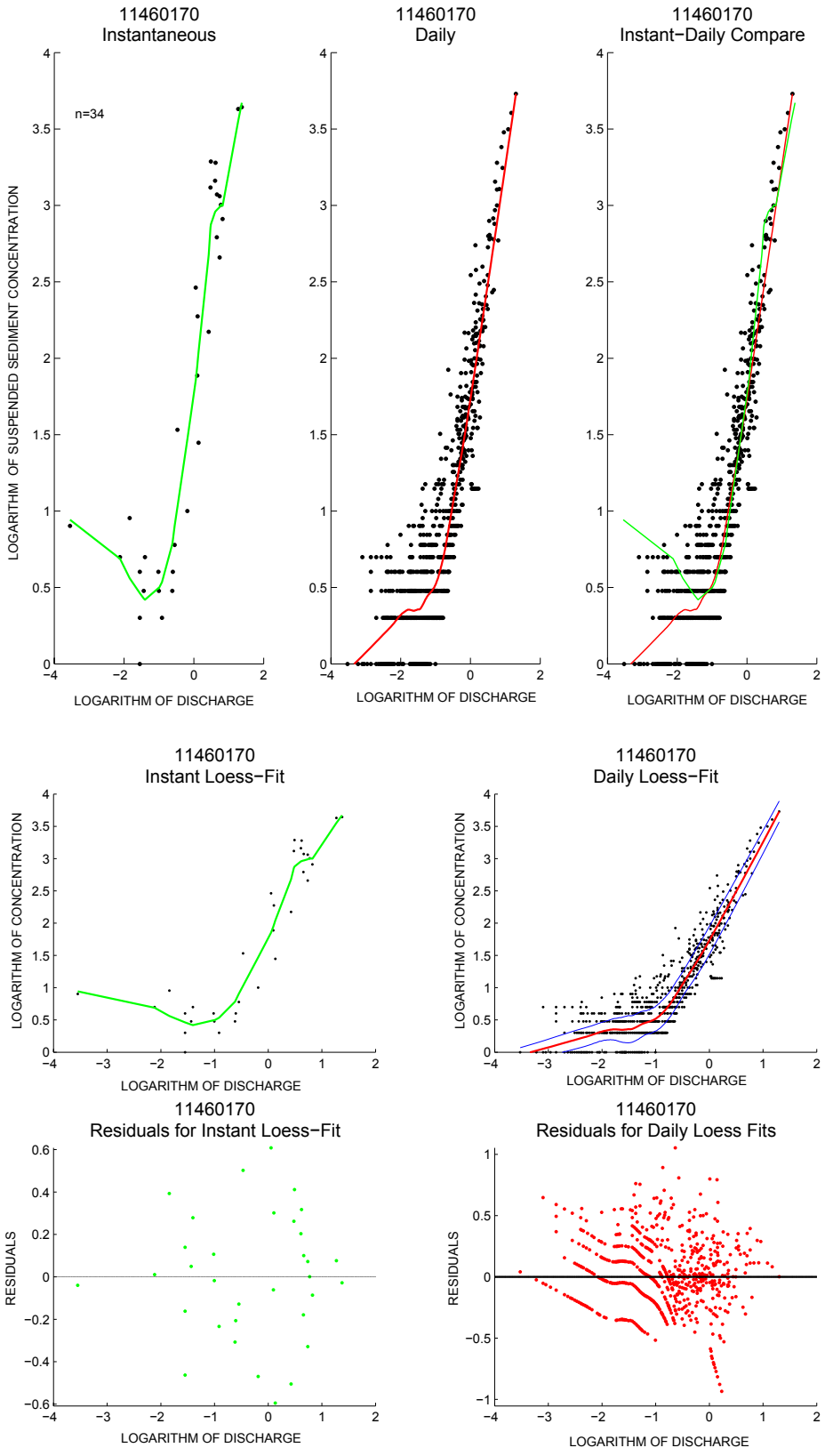

Figure B2 *I*, Pine Creek (U.S. Geological Survey gaging sta. 11460170)—Continued.

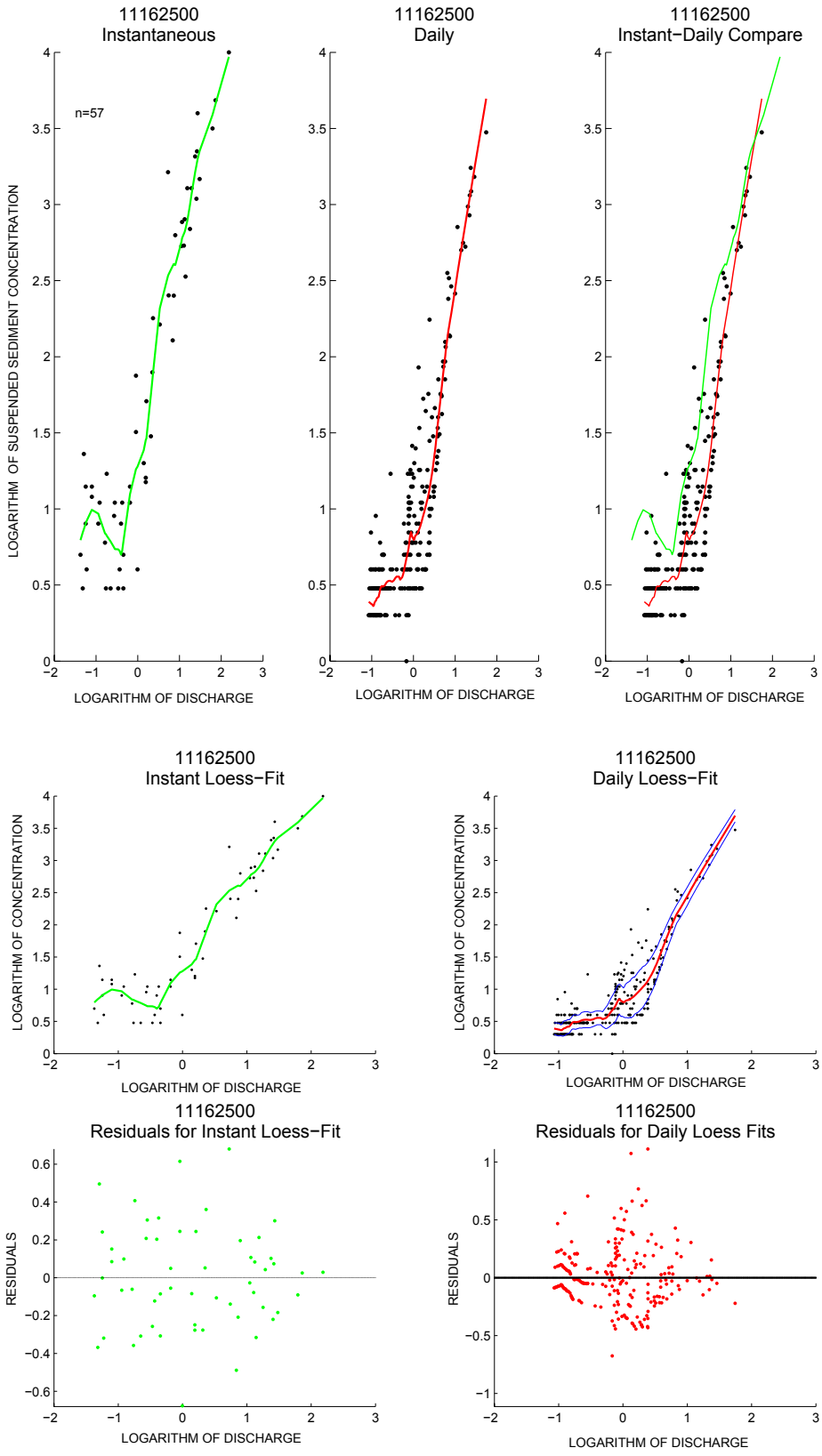

Figure B2 *J*, Pescadero Creek (U.S. Geological Survey gaging sta. 11162500)—Continued.

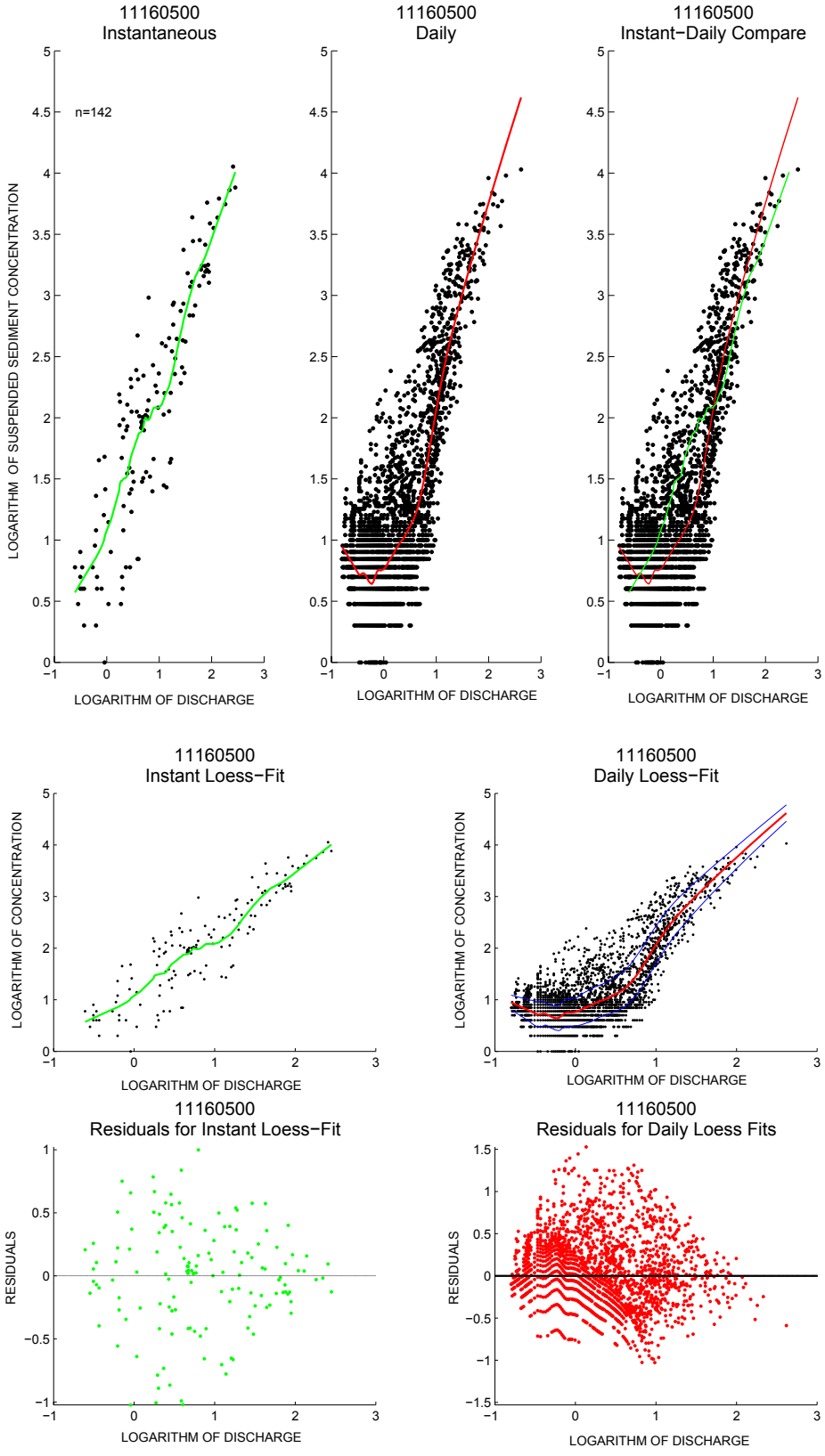

Figure B2 *K*, San Lorenzo River (U.S. Geological Survey gaging sta. 11160500)—Continued.

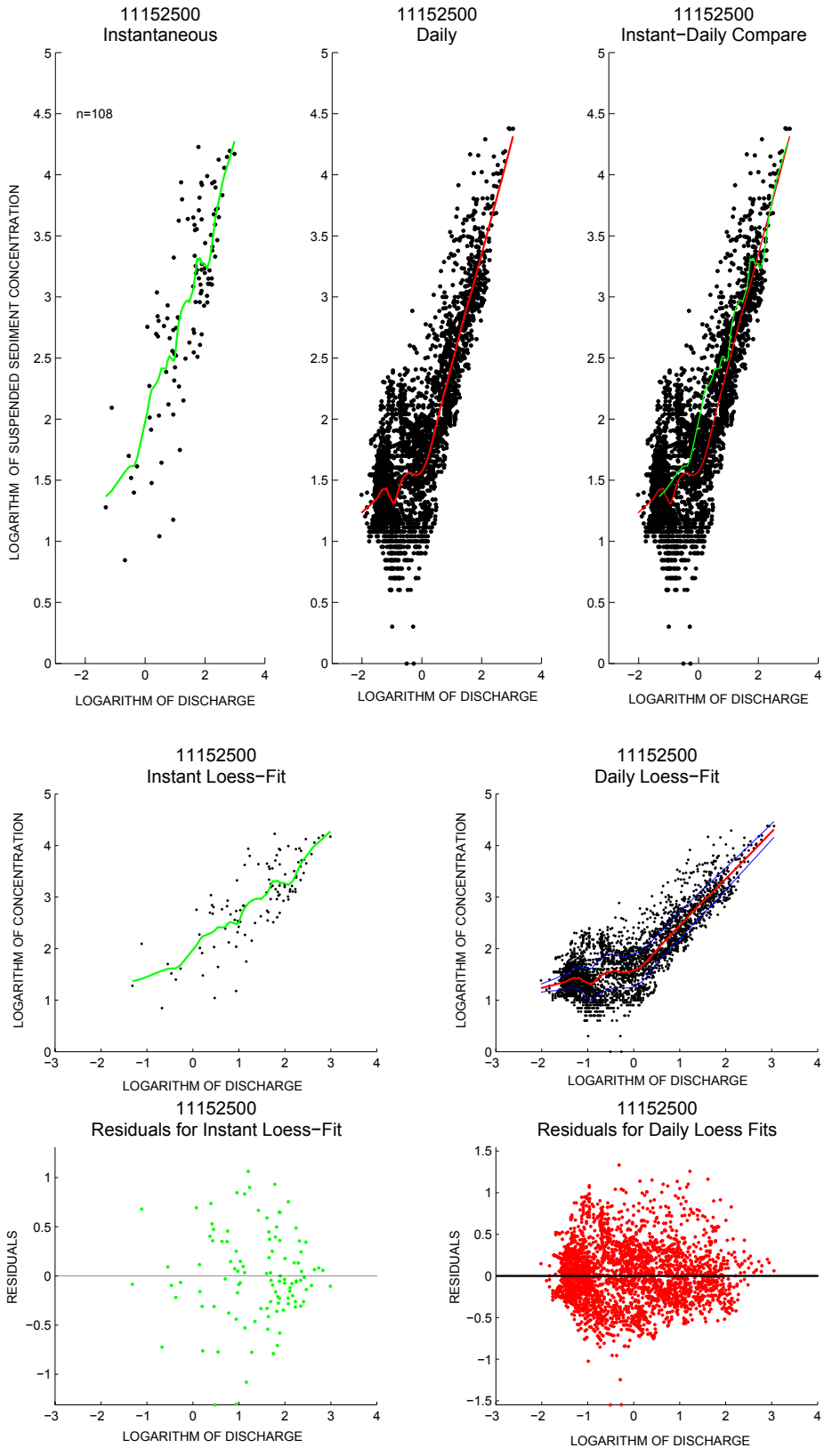

Figure B2 , Salinas River (U.S. Geological Survey gaging sta. 11152500)—Continued.

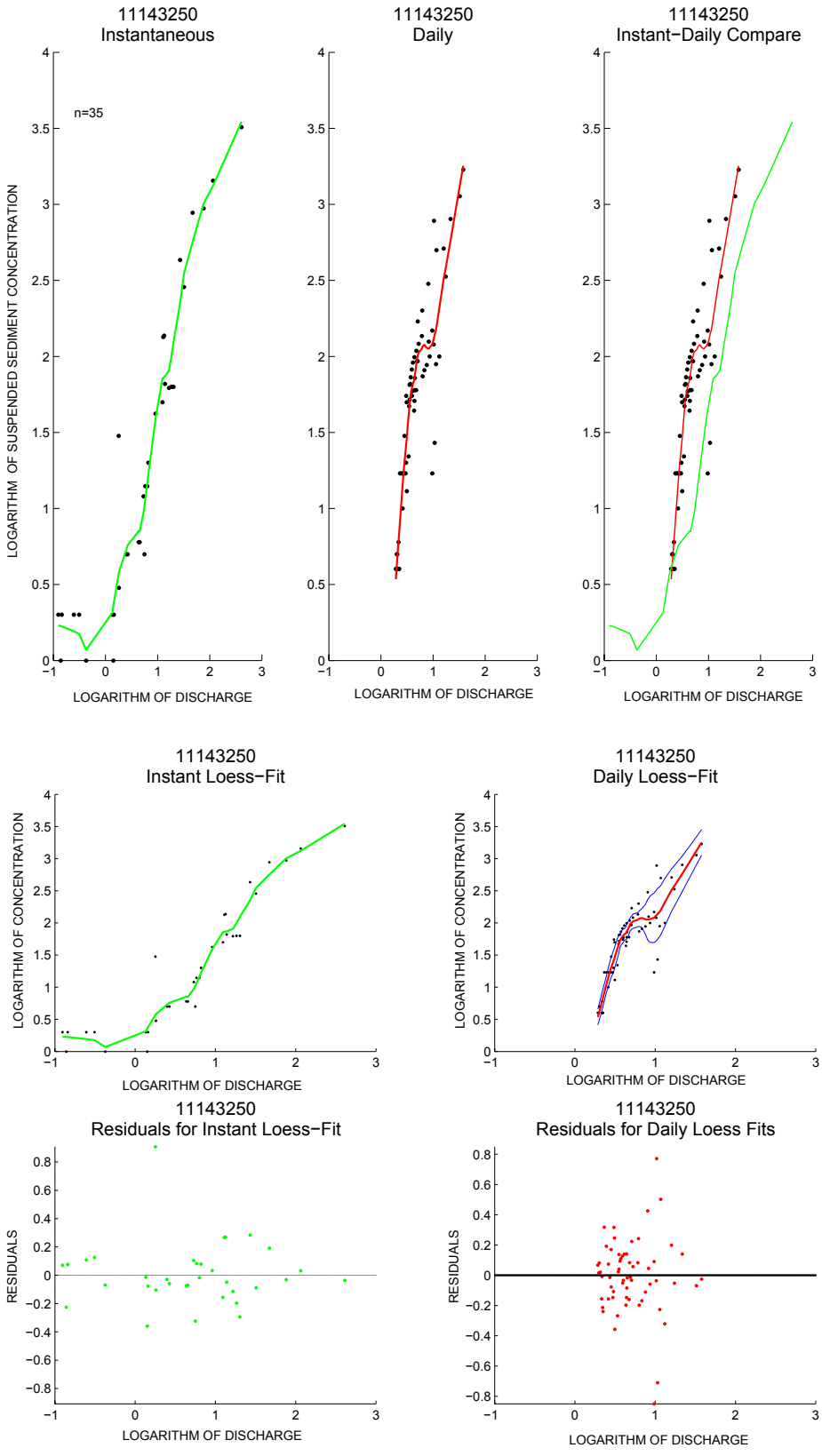

Figure B2 *M*, Carmel River (U.S. Geological Survey gaging sta. 11143250)—Continued.

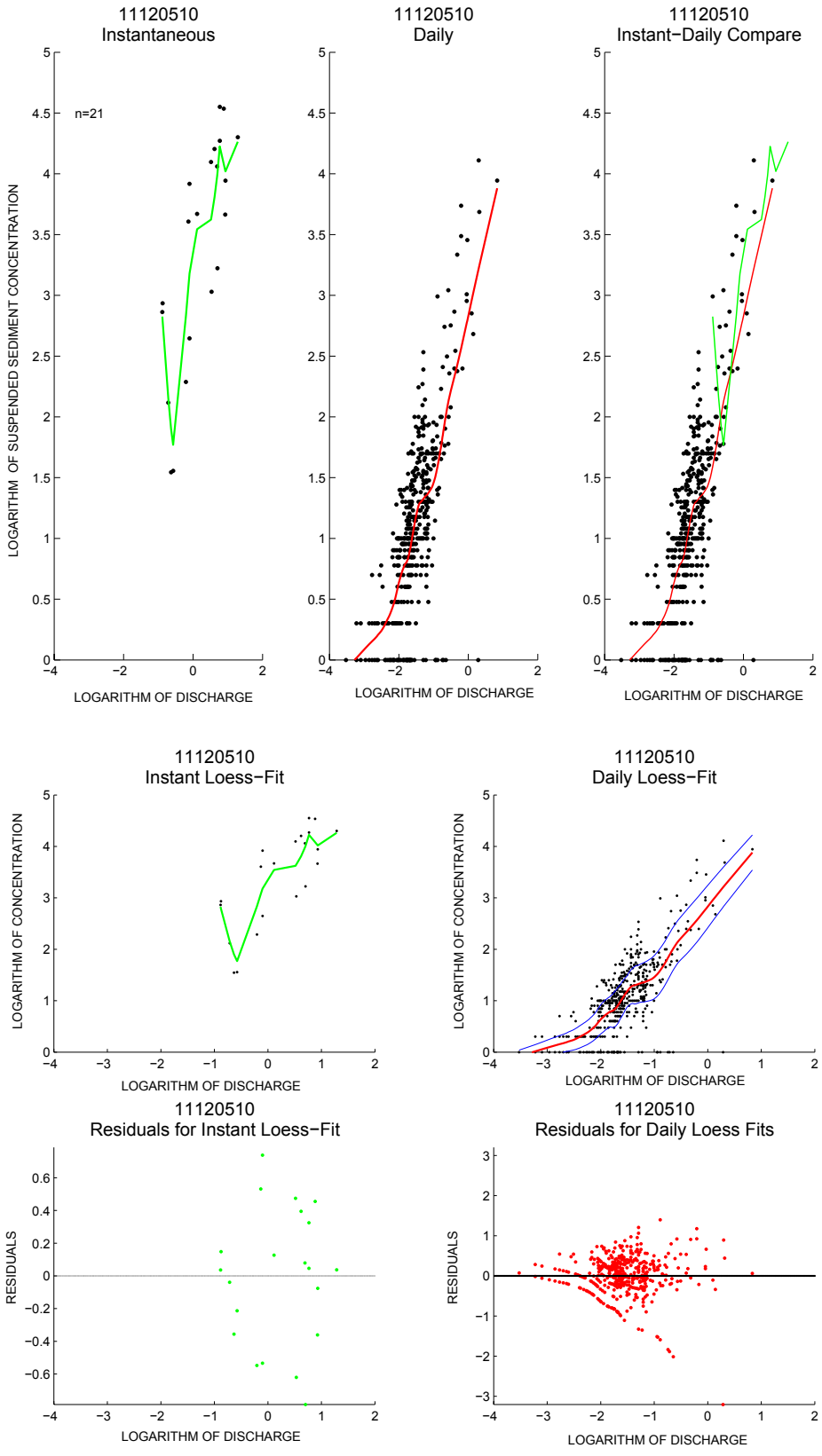

Figure B2 *N*, San Jose Creek (U.S. Geological Survey gaging sta. 11120510)—Continued.

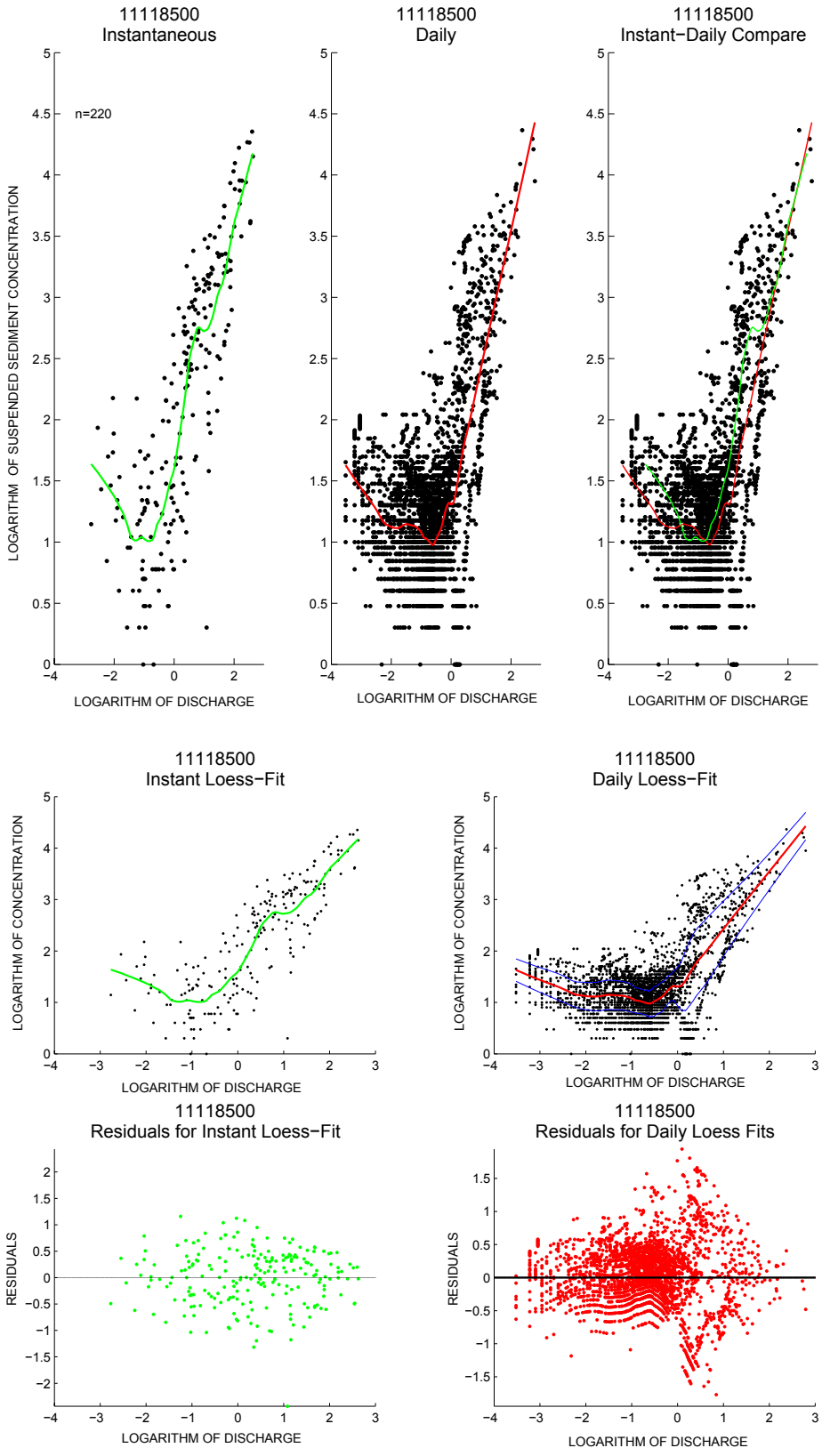

Figure B2 *O*, Ventura River (U.S. Geological Survey gaging sta. 11118500)—Continued.

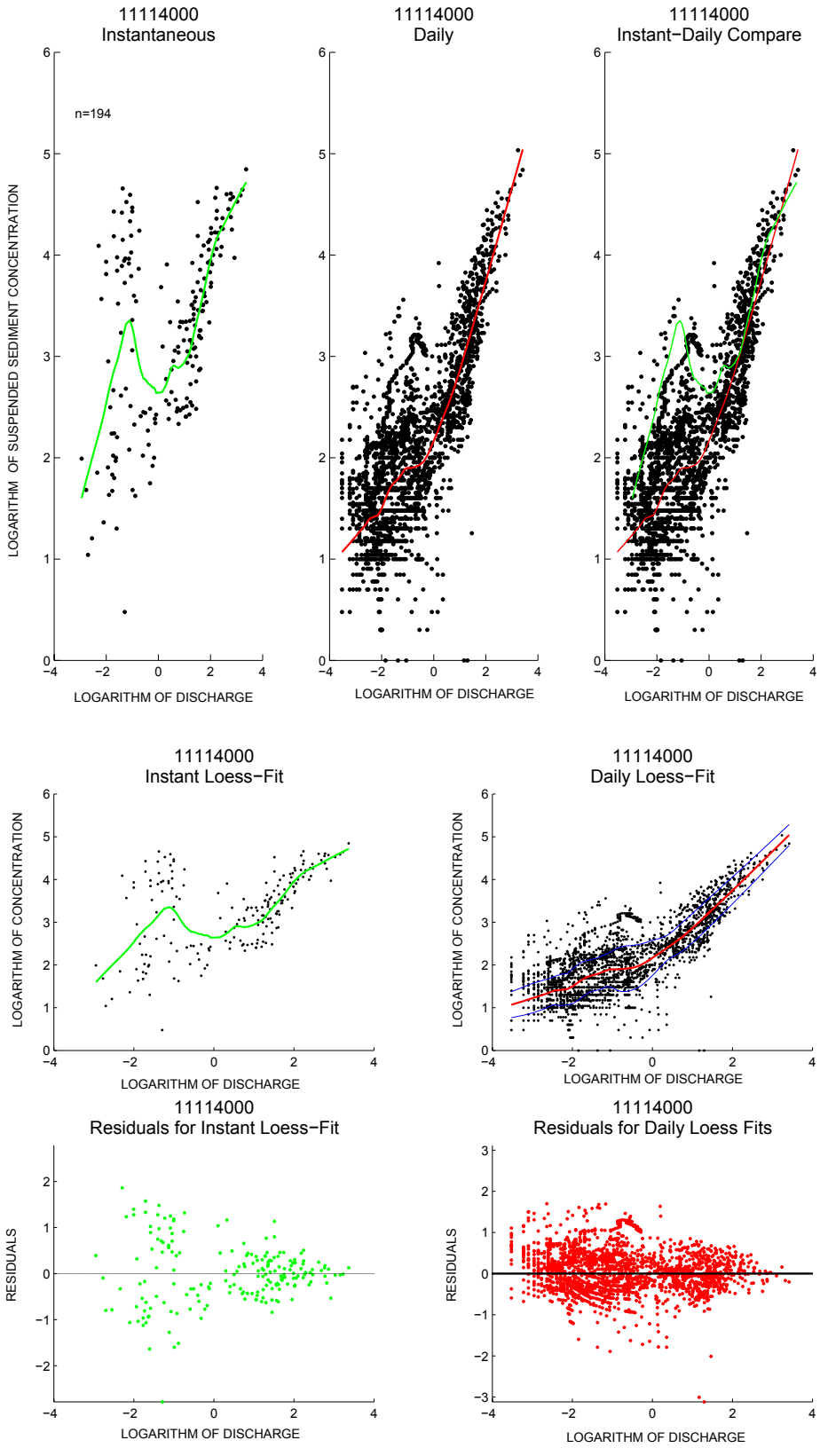

Figure B2 *P*, Santa Clara River (U.S. Geological Survey gaging sta. 11114000)—Continued.

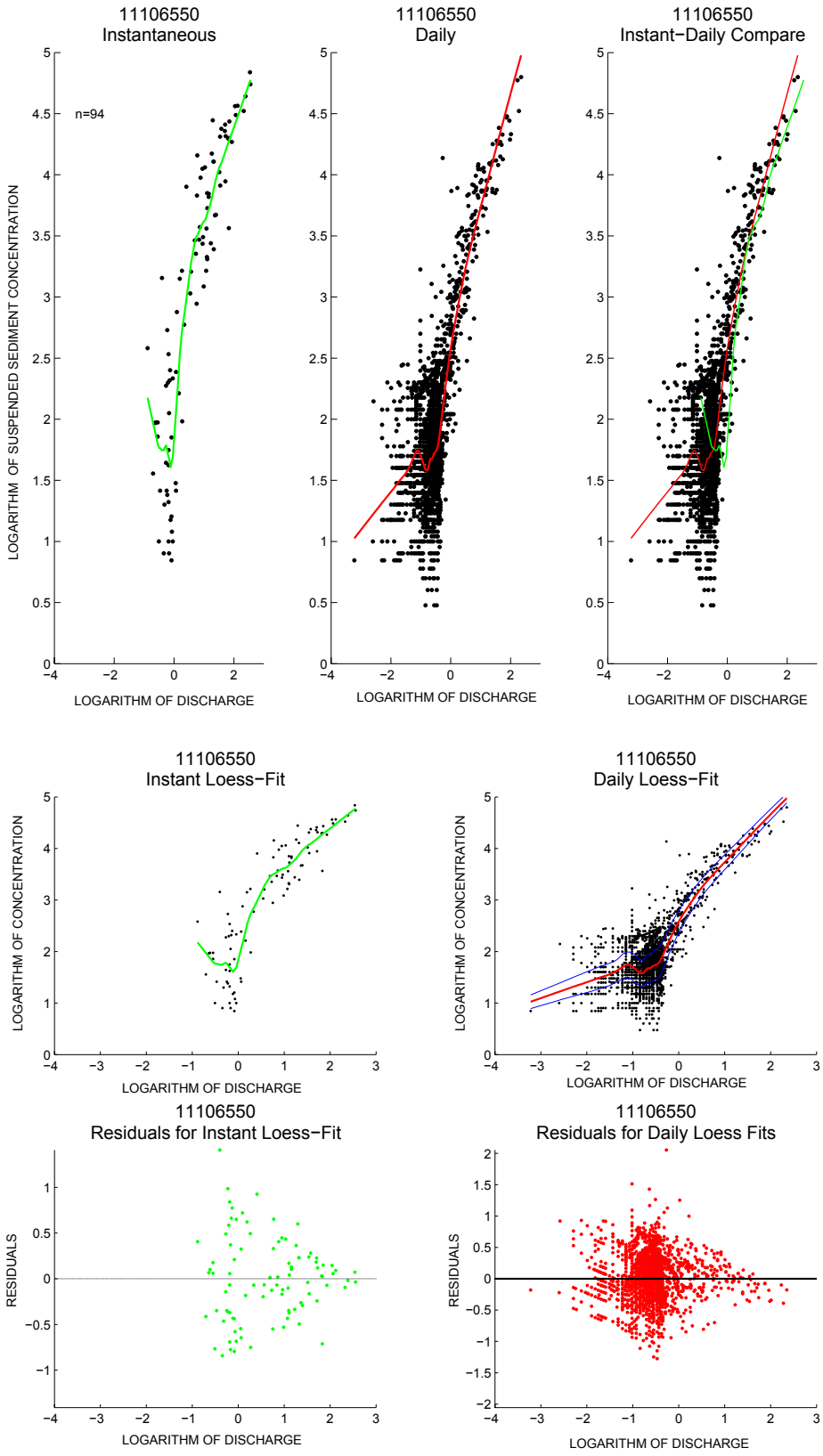

Figure B2 *Q*, Calleguas Creek (U.S. Geological Survey gaging sta. 11106550)—Continued.

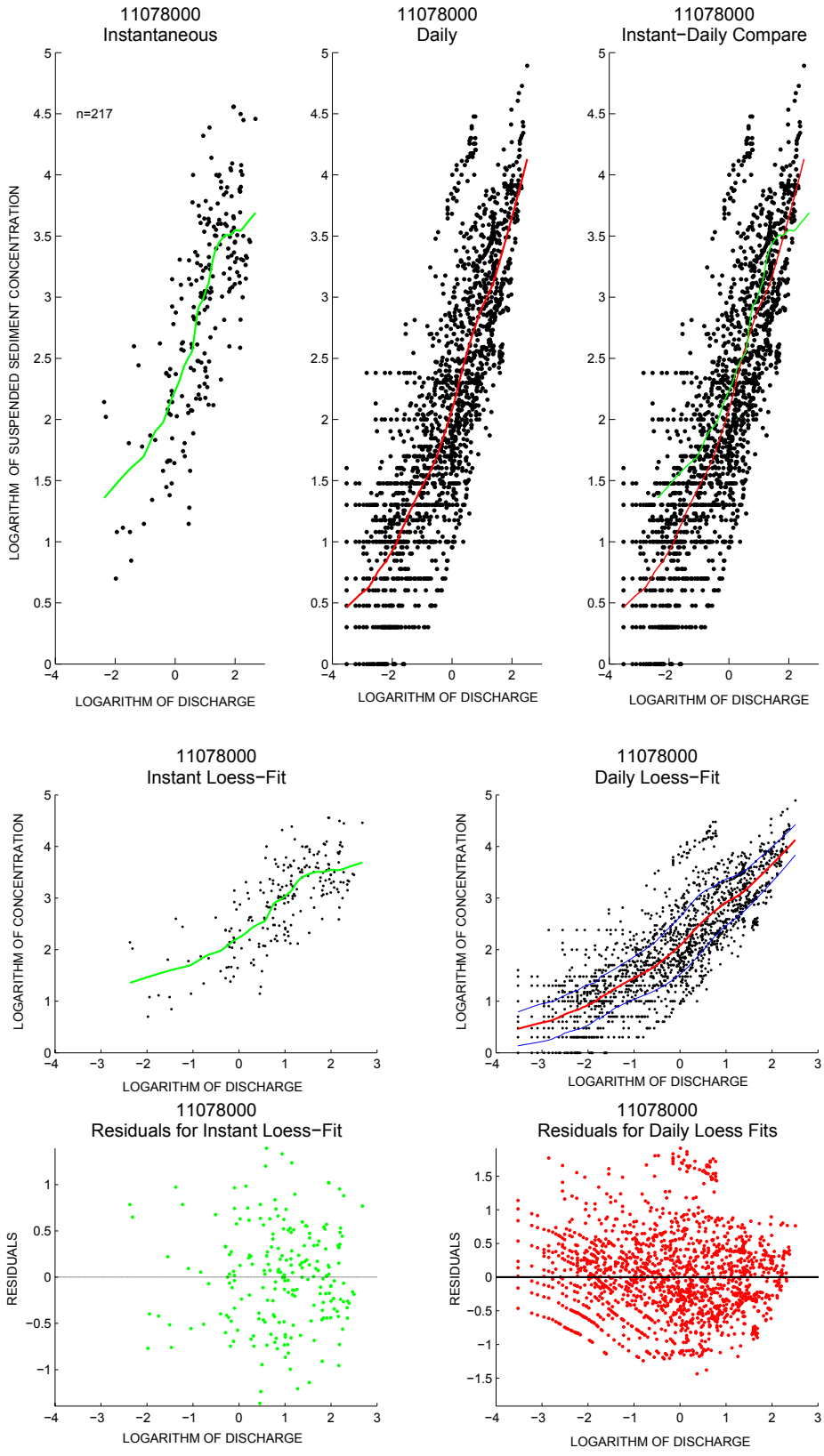

Figure B2 *R*, Santa Ana River (U.S. Geological Survey gaging sta. 11078000)—Continued.

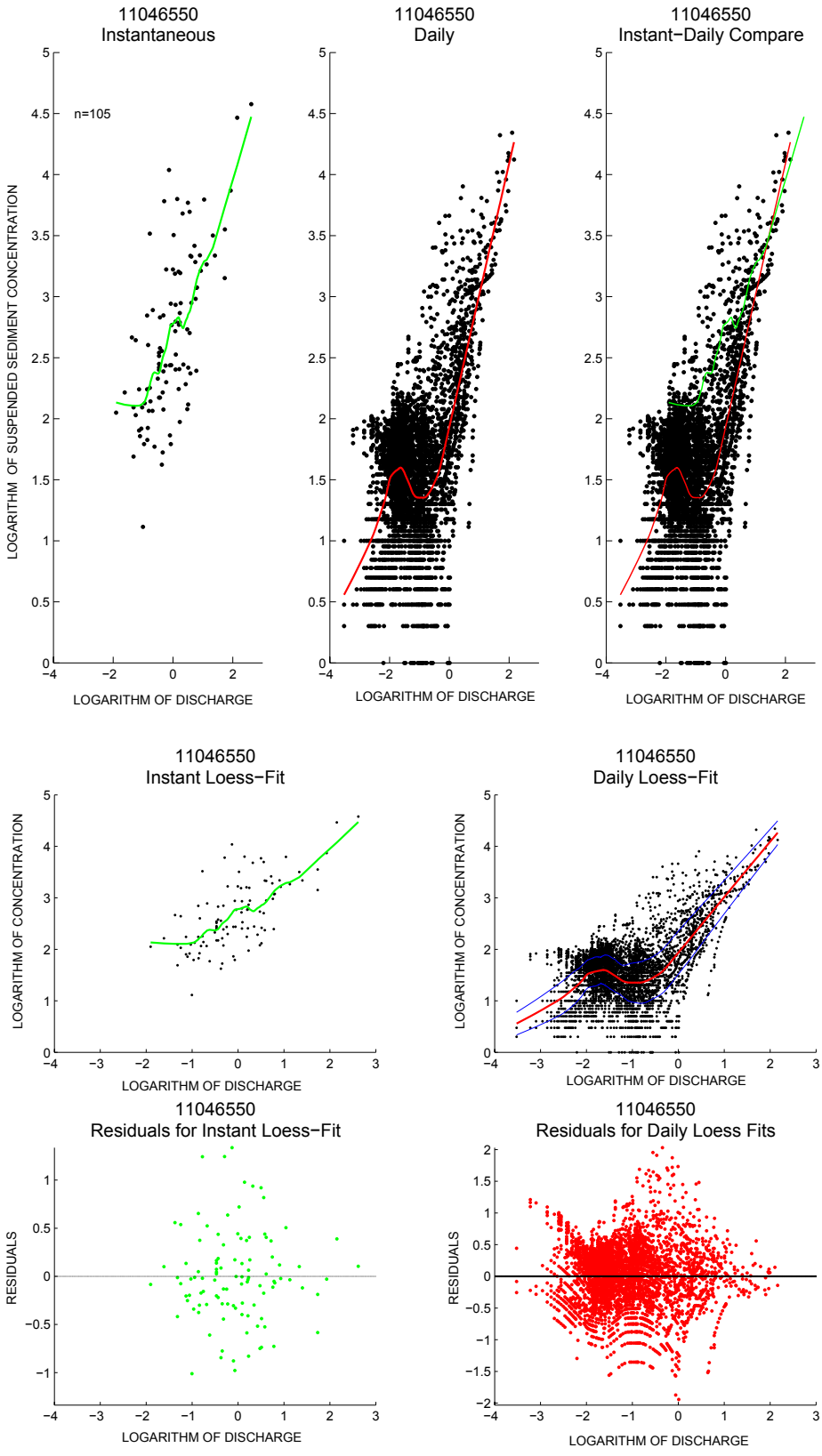

Figure B2 *S*, San Juan Creek (U.S. Geological Survey gaging sta. 11046550)—Continued.

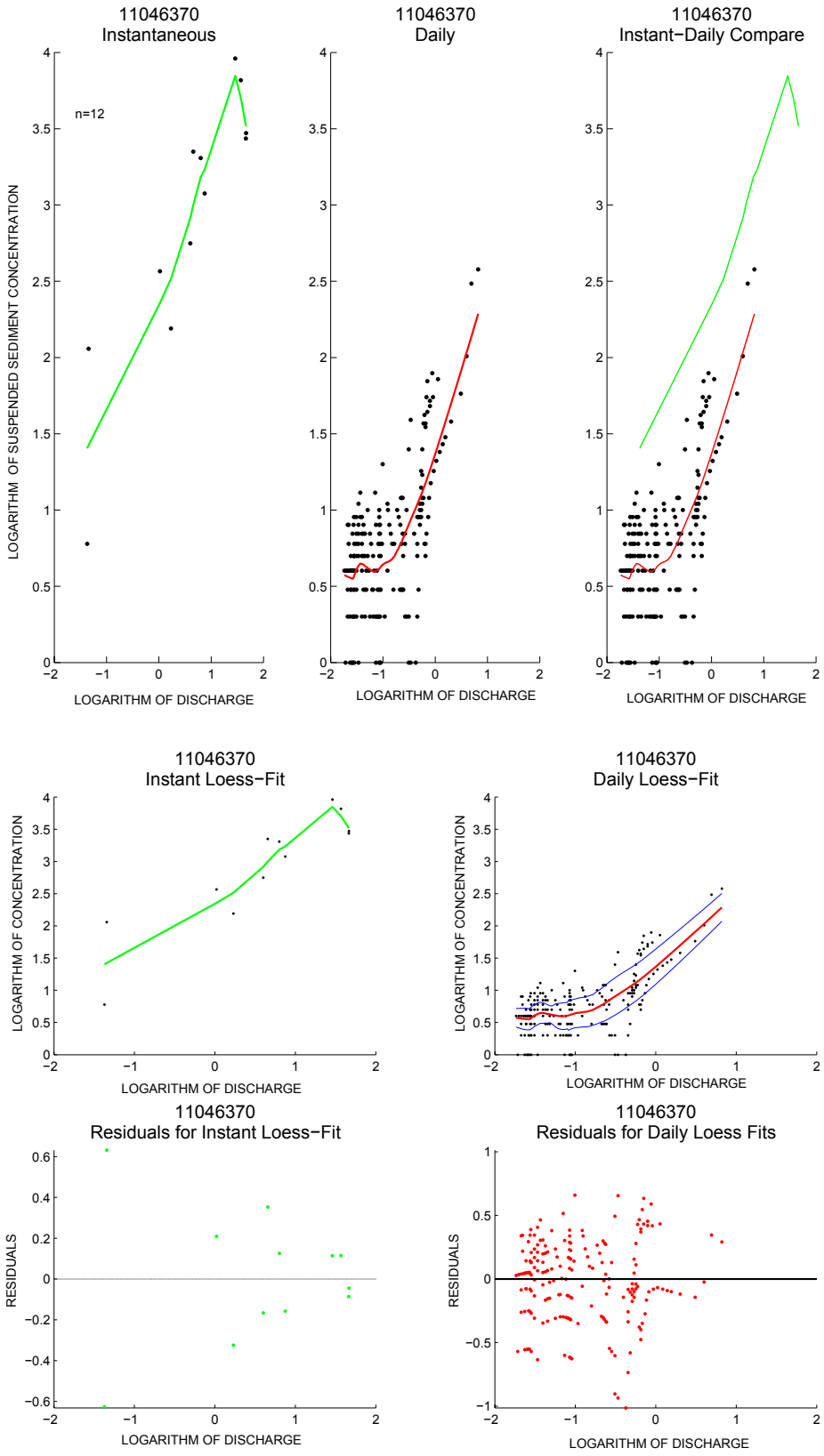

Figure B2 T, San Mateo River (U.S. Geological Survey gaging sta. 11046370)—Continued.

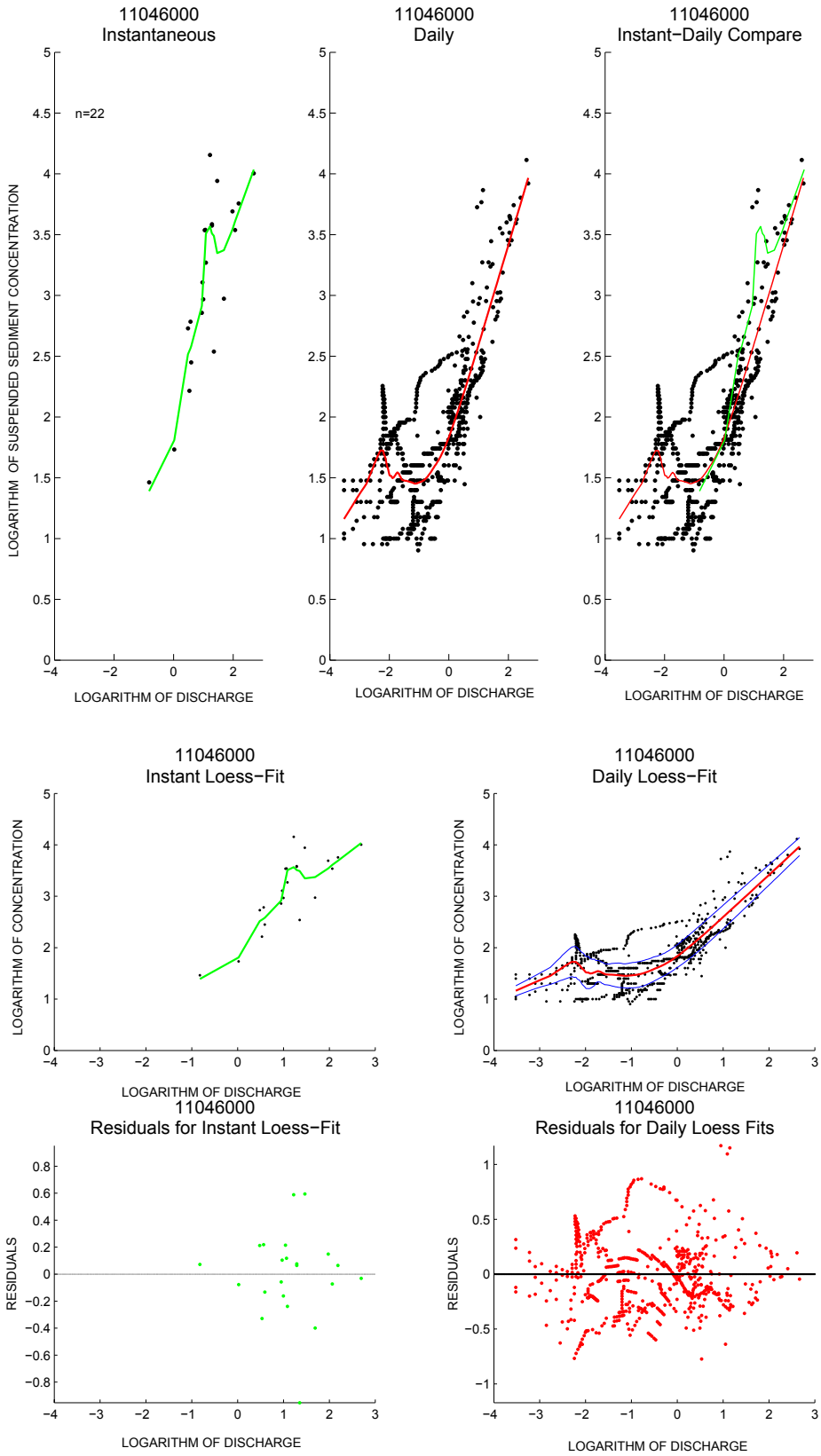

Figure B2 *U*, Santa Margarita River (U.S. Geological Survey gaging sta. 11046000)—Continued.

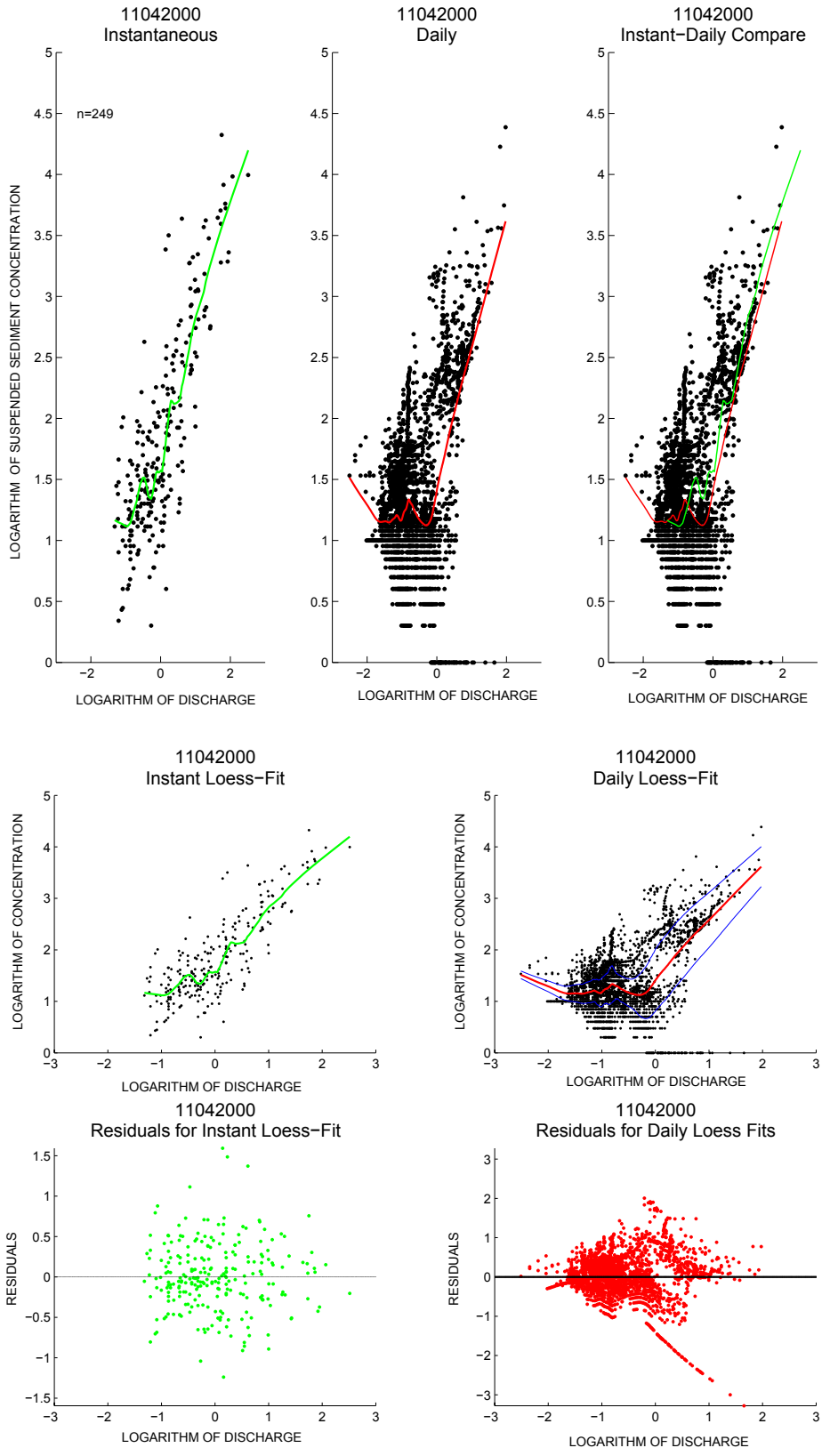

Figure B2 *V*, San Luis Rey River (U.S. Geological Survey gaging sta. 11042000)—Continued.

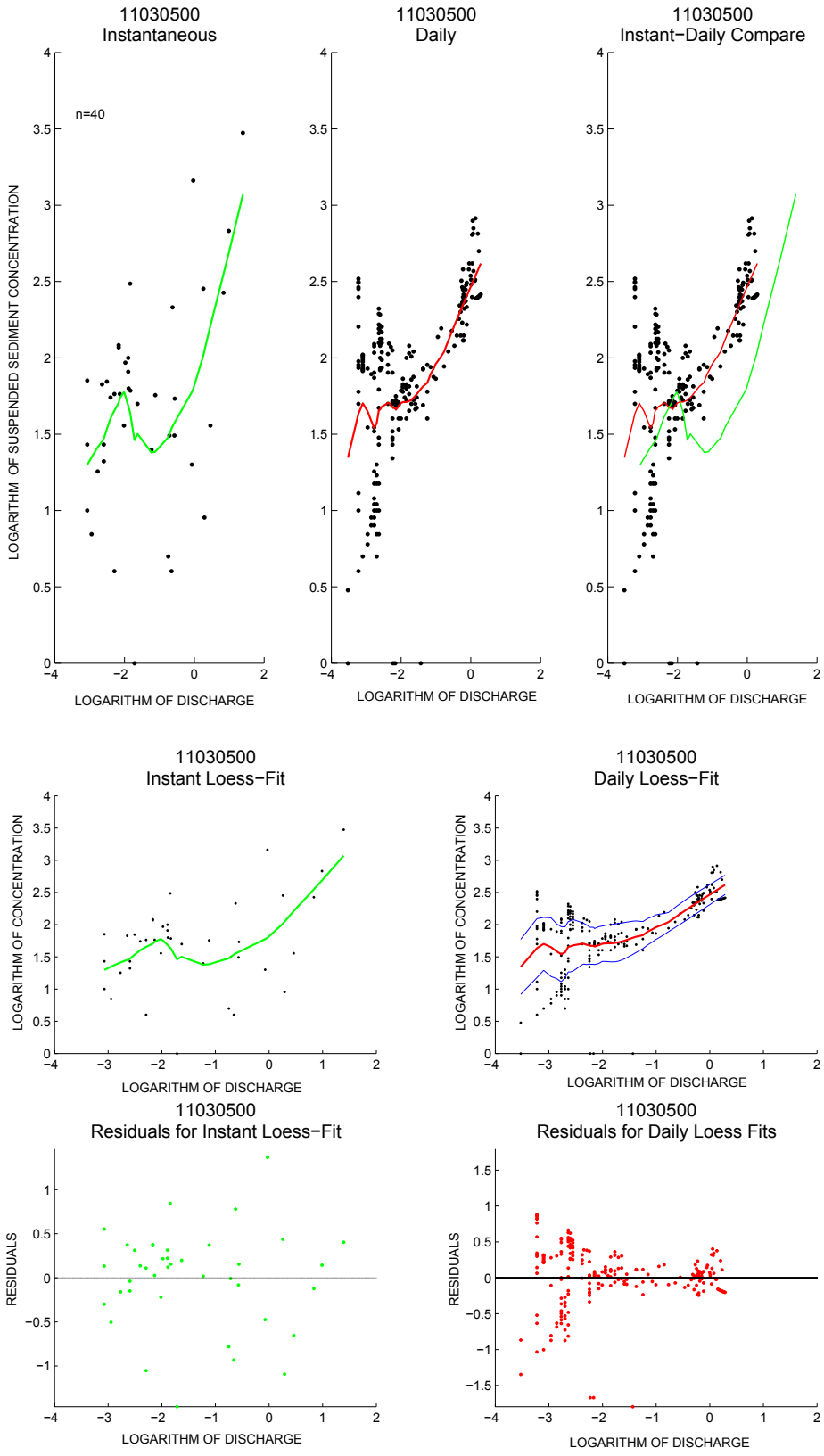

Figure B2 *W*, San Dieguito River (U.S. Geological Survey gaging sta. 11030500)—Continued.

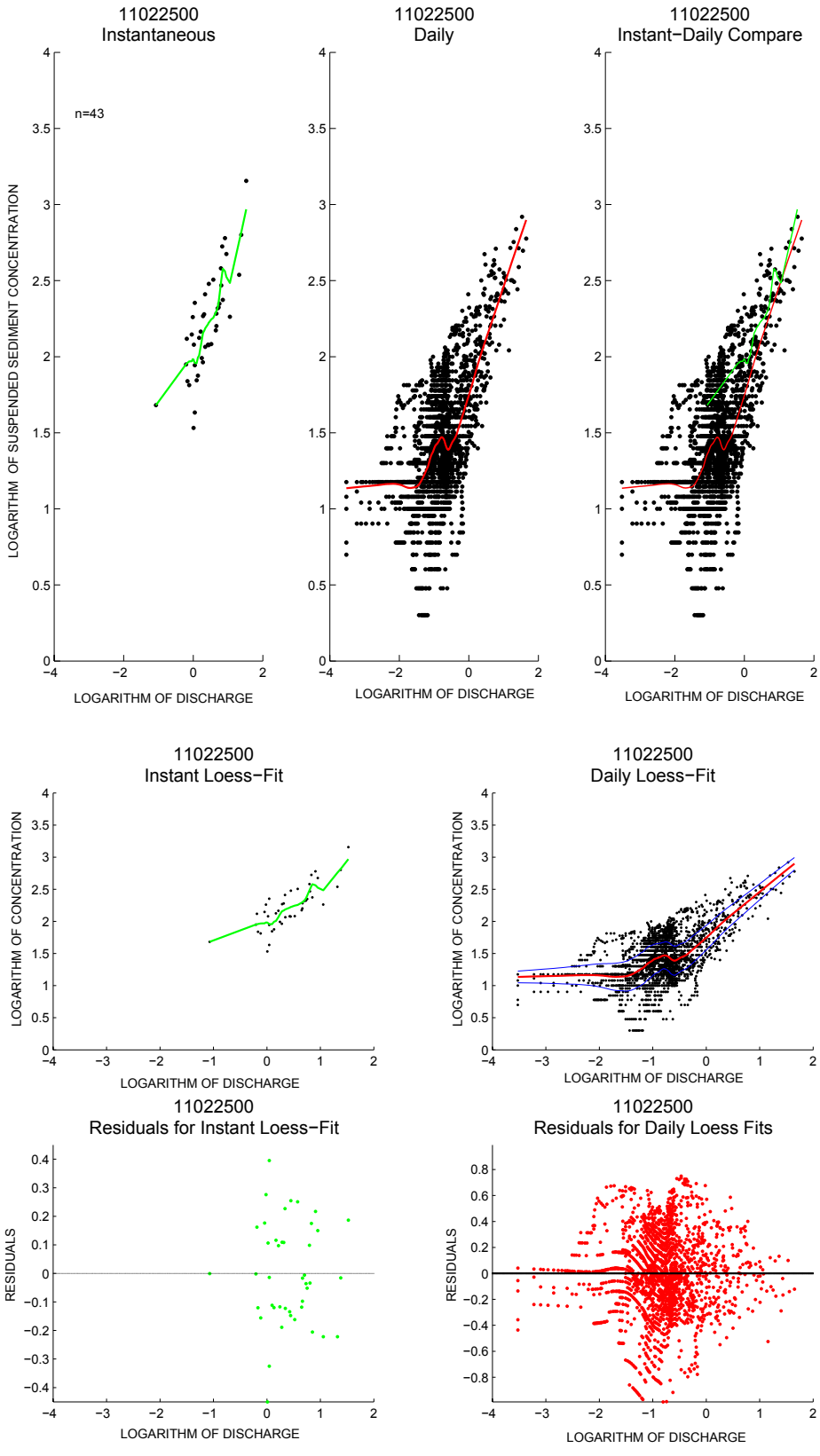

Figure B2 *X*, San Diego River (U.S. Geological Survey gaging sta. 11022500)—Continued.

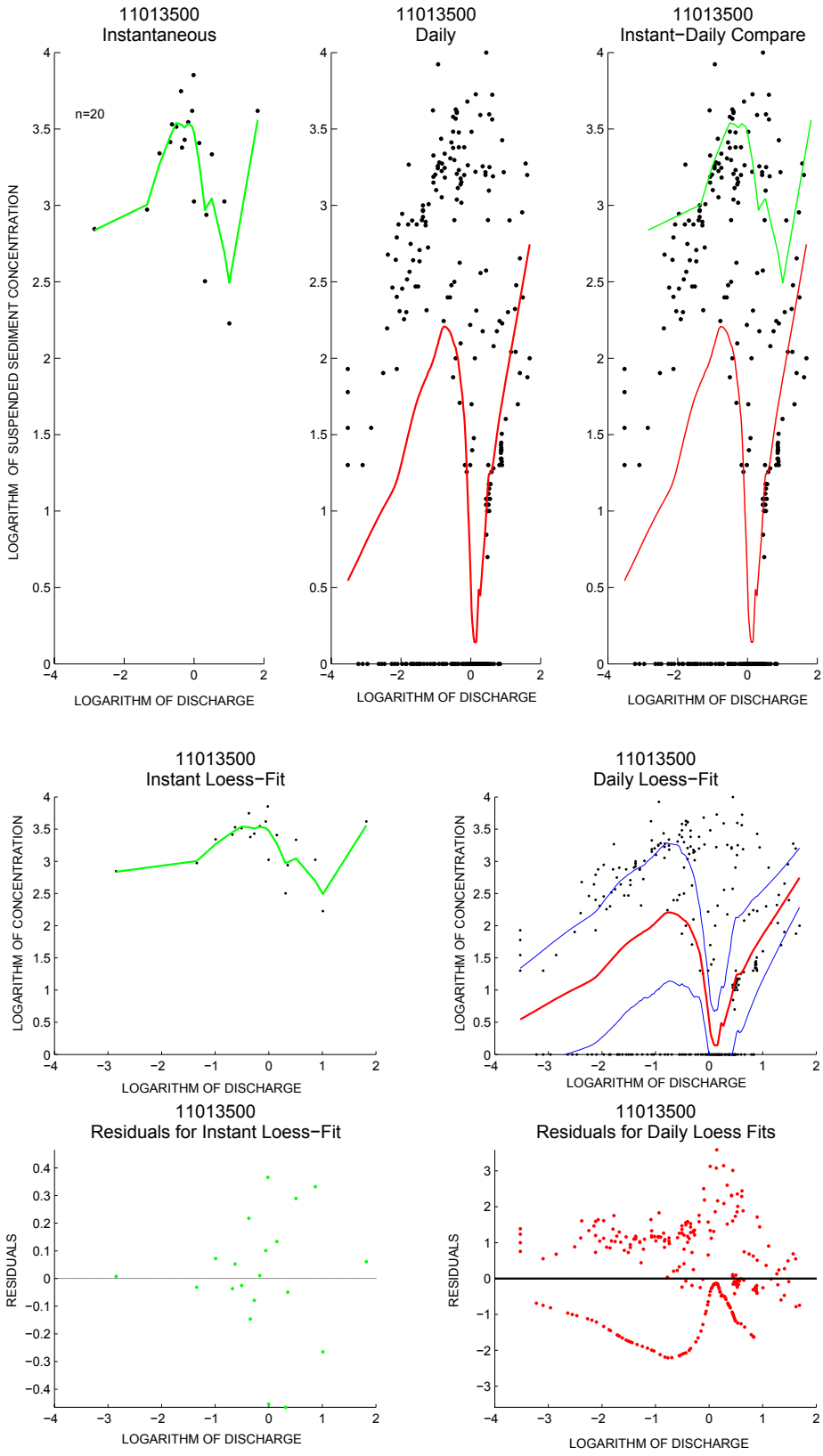

Figure B2 *Y*, Tijuana River (U.S. Geological Survey gaging sta. 11013500)—Continued.

Appendix C. Fine-Sediment-Fraction/Discharge Curves for All Stations

This appendix presents plots of the fine-sediment-fraction/discharge relation for data from all the U.S. Geological Survey gaging stations used in this study (fig. 1). Weighting factors (α values) of the loess rating curves are listed in table C1.

Table C1. Weighting factors (α values) of loess fine-sediment-fraction/discharge rating curves for all the U.S. Geological Survey gaging stations used in this study, listed from north to south.

[USGS, U.S. Geological Survey]

Watershed (fig. 1)	USGS gaging station	α value
Smith River	11532500	0.3
Supply Creek	11530020	0.3
Trinity River	11530000	0.3
Klamath River	11523000	0.3
Redwood Creek	11482500	0.3
Mad River	11481000	0.3
Eel River	11477000	0.3
Russian River	11467000	0.3
Pine Creek	11460170	0.3
Pescadero Creek	11162500	0.3
San Lorenzo River	11160500	0.3
Salinas River	11152500	0.3
Carmel River	11143250	0.3
San Jose Creek	11120510	0.3
Ventura River	11118500	0.3
Santa Clara River	11114000	0.3
Calleguas Creek	11106550	0.3
Santa Ana River	11078000	0.3
San Juan Creek	11046550	0.3
San Mateo River	11046370	0.4
Santa Margarita River	11046000	0.3
San Luis Rey River	11042000	0.3
San Dieguito River	11030500	0.5
San Diego River	11022500	0.3
Tijuana River	11013500	0.4

Figure C1. Loess rating curves (black) of fine-sediment content versus discharge for watersheds used in this study (fig. 1), with $\pm 2\sigma$ deviations (red curves) shown for reference.

A, Smith River (U.S. Geological Survey gaging sta. 11532500).
B, Supply Creek (U.S. Geological Survey gaging sta. 11530020).
C, Trinity River (U.S. Geological Survey gaging sta. 11530000).
D, Klamath River (U.S. Geological Survey gaging sta. 11523000).
E, Redwood Creek (U.S. Geological Survey gaging sta. 11482500).
F, Mad River (U.S. Geological Survey gaging sta. 11481000).
G, Eel River (U.S. Geological Survey gaging sta. 11477000).
H, Russian River (U.S. Geological Survey gaging sta. 11467000).
I, Pine Creek (U.S. Geological Survey gaging sta. 11460170).
J, Pescadero Creek (U.S. Geological Survey gaging sta. 11162500).
K, San Lorenzo River (U.S. Geological Survey gaging sta. 11160500).
L, Salinas River (U.S. Geological Survey gaging sta. 11152500).
M, Carmel River (U.S. Geological Survey gaging sta. 11143250).
N, San Jose Creek (U.S. Geological Survey gaging sta. 11120510).
O, Ventura River (U.S. Geological Survey gaging sta. 11118500).
P, Santa Clara River (U.S. Geological Survey gaging sta. 11114000).
Q, Calleguas Creek (U.S. Geological Survey gaging sta. 11106550).
R, Santa Ana River (U.S. Geological Survey gaging sta. 11078000).
S, San Juan Creek (U.S. Geological Survey gaging sta. 11046550).
T, San Mateo River (U.S. Geological Survey gaging sta. 11046370).
U, Santa Margarita River (U.S. Geological Survey gaging sta. 11046000).
V, San Luis Rey River (U.S. Geological Survey gaging sta. 11042000).
W, San Dieguito River (U.S. Geological Survey gaging sta. 11030500).
X, San Diego River (U.S. Geological Survey gaging sta. 11022500).
Y, Tijuana River (U.S. Geological Survey gaging sta. 11013500).

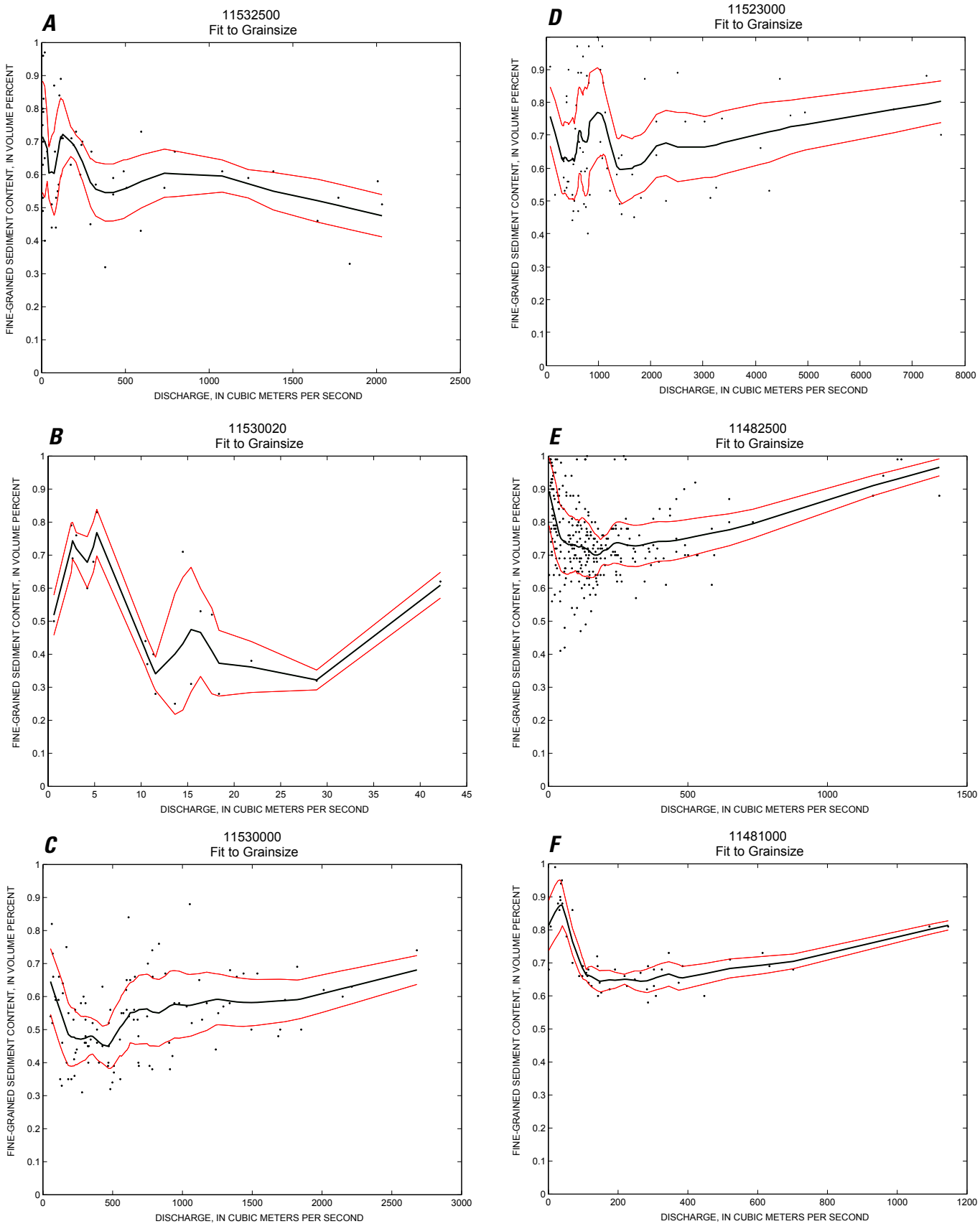
A
11532500
Fit to Grainsize
FINE-GRAINED SEDIMENT CONTENT, IN VOLUME PERCENT
DISCHARGE, IN CUBIC METERS PER SECOND
B
11530020
Fit to Grainsize
FINE-GRAINED SEDIMENT CONTENT, IN VOLUME PERCENT
DISCHARGE, IN CUBIC METERS PER SECOND
C
11530000
Fit to Grainsize
FINE-GRAINED SEDIMENT CONTENT, IN VOLUME PERCENT
DISCHARGE, IN CUBIC METERS PER SECOND
D
11523000
Fit to Grainsize
FINE-GRAINED SEDIMENT CONTENT, IN VOLUME PERCENT
DISCHARGE, IN CUBIC METERS PER SECOND
E
11482500
Fit to Grainsize
FINE-GRAINED SEDIMENT CONTENT, IN VOLUME PERCENT
DISCHARGE, IN CUBIC METERS PER SECOND
F
11481000
Fit to Grainsize
FINE-GRAINED SEDIMENT CONTENT, IN VOLUME PERCENT
DISCHARGE, IN CUBIC METERS PER SECOND

Figure C1.

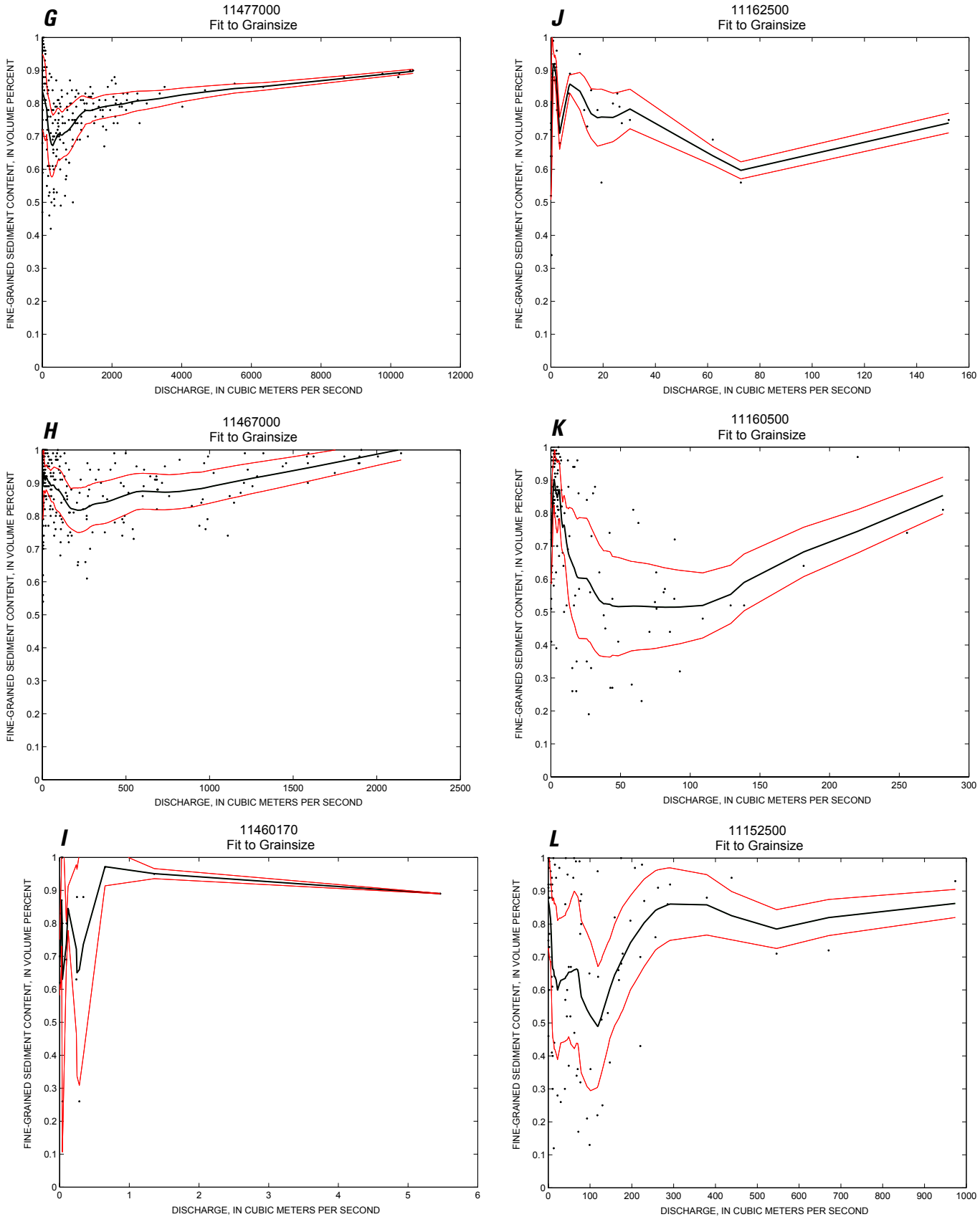

Figure C1—Continued.

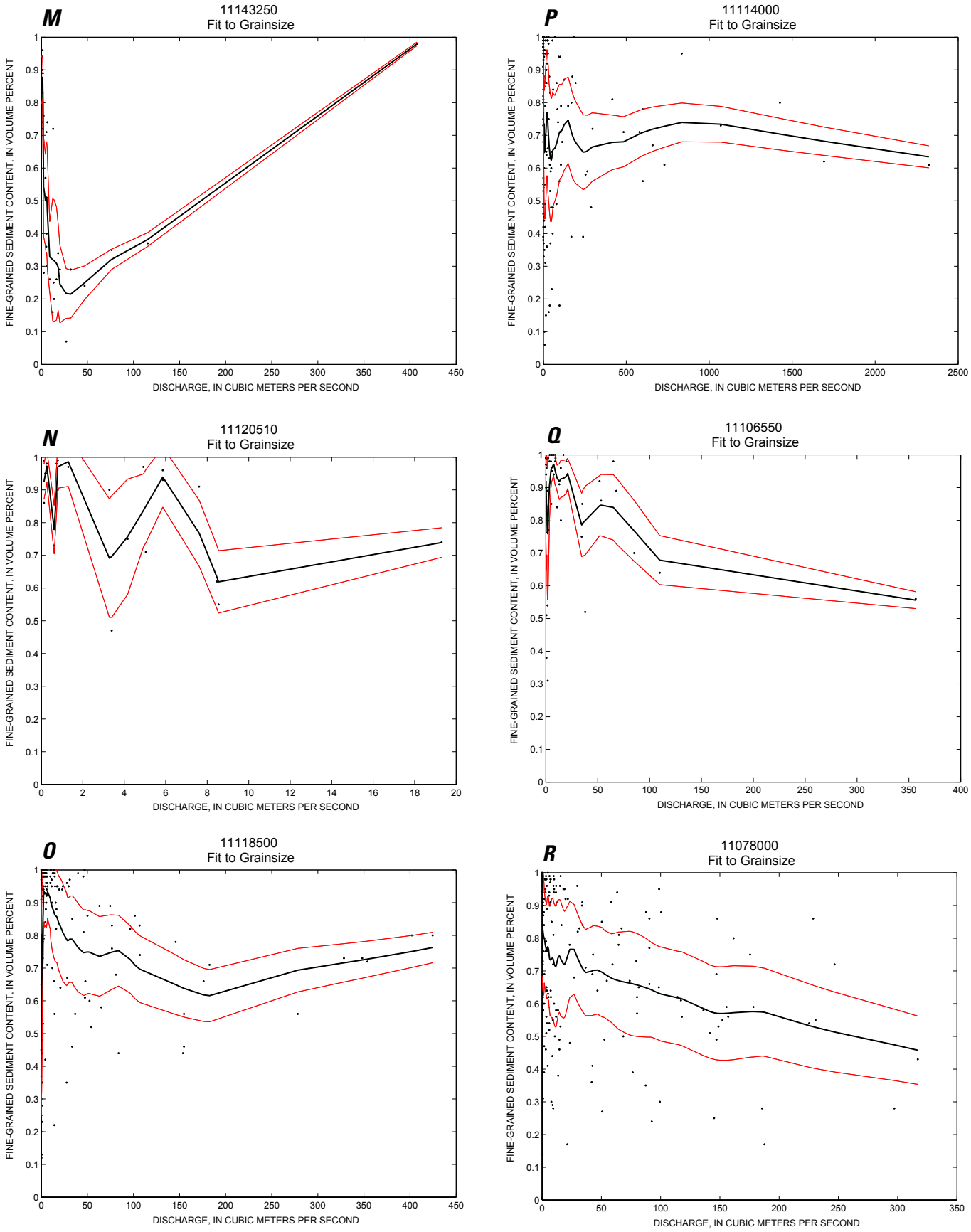

Figure C1—Continued.

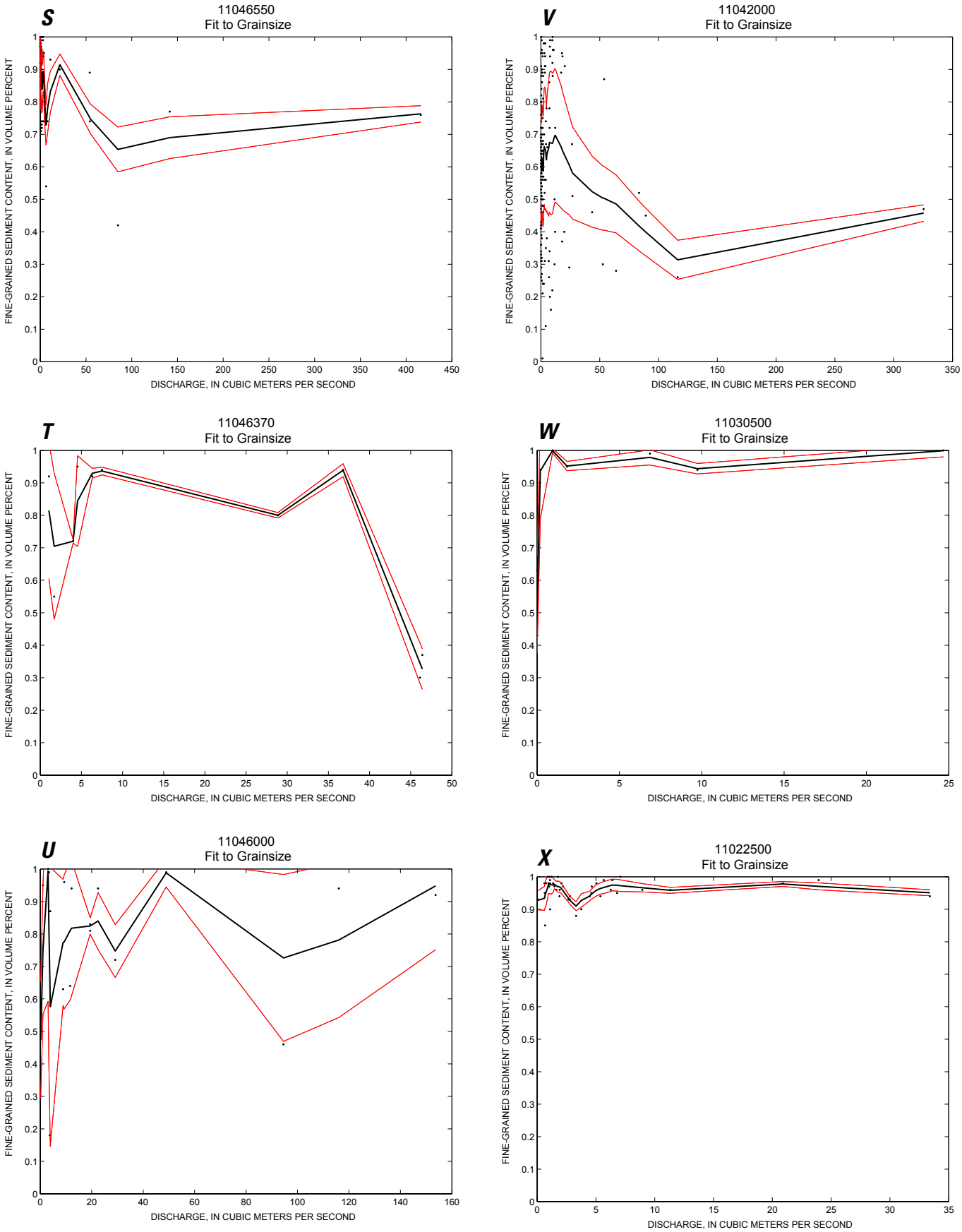

Figure C1—Continued.

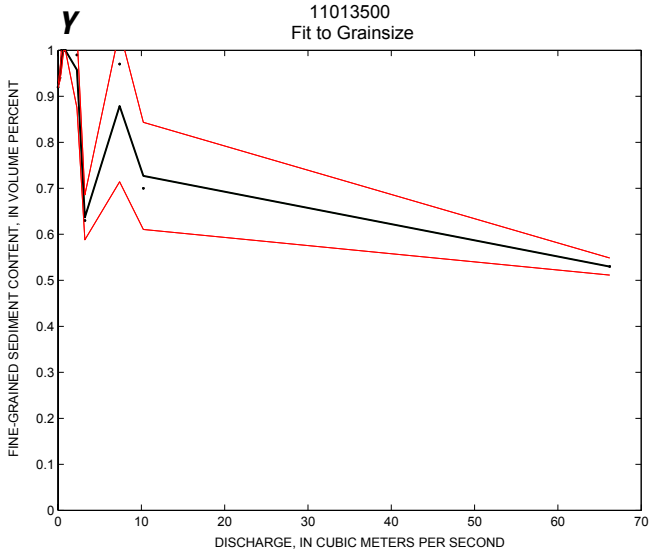

Figure C1—Continued.

Appendix D. Fine-Sediment Contributions to Coastal California from Coastal Cliffs and Bluffs

This appendix presents calculations of the fine-sediment contributions from erosion of coastal cliffs and bluffs in southern California littoral cells (adapted from Patsch and Griggs, 2005).

Table D1. Fine-sediment input from cliffs and bluffs into various sections of the California coast.

[Data on length, height, sand content, and erosion rate for Oceanside and Santa Barbara segments from California Department of Boating and Waterways and California Coastal Conservancy (2002), and for other segments from Patsch and Griggs (2005). Mud content is the left over fraction of sediment, calculated as 100 volume percent minus sand content. Input from bluffs is calculated as (Length of cliff, in meters) × (Height of bedrock, in meters) × (Mud fraction) × (Erosion rate, in meters per year), and from terraces as (Length of cliff, in meters) × (Height of terrace, in meters) × (Mud fraction) × (Erosion rate, in meters per year). Total input is the sum of bluff/cliff and terrace input]

Segment	Length (m)	Bedrock			Terrace			Erosion rate (m/yr)	Input from bedrock (m^3/yr)	Input from terrace (m^3/yr)	Total input (m^3)
		Height (m)	Sand content (vol pct)	Mud content (vol pct)	Height (m)	Sand content (vol pct)	Mud content (vol pct)				
Mission Bay											
Point La Jolla-Calumet Park	5,546	3	39.51	60.49	4	88.12	11.88	0.40	4,025.73	1,054.18	5,080
Calumet Park-Mission Bay	527	9	39.51	60.49	3	88.12	11.88	0.40	1,147.62	75.13	1,223
Ocean Beach Fishing Pier-City Beach	187	4	39.51	60.49	6	88.12	11.88	0.40	180.99	53.32	234
Ocean Beach City Beach-Sunset Cliffs Park	1,747	9	39.51	60.49	3	88.12	11.88	0.40	5,706.51	373.58	6,080
Sunset Cliffs-Point Loma	7,388	30	39.51	60.49	0	88.12	11.88	0.40	80,442.02	0.00	80,442
Total											93,059
Oceanside											
Scripps Pier-Torrey Pines	6,832	28	51.1	48.9	3.4	57.4	42.6	0.15	14,031.56	1,484.32	15,516
Torrey Pines-Del Mar	2,556	7.7	51.1	48.9	3.4	57.4	42.6	0.12	1,154.89	444.25	1,599
Del Mar-Solana Beach	2,858	8	51.1	48.9	3.9	57.4	42.6	0.1	1,118.05	474.83	1,593
Cardiff by the Sea-San Elijo State Park	1,346	4.6	51.1	48.9	6.2	57.4	42.6	0.1	302.77	355.51	658
San Elijo-Encinitas	1,179	14.1	51.1	48.9	2.8	57.4	42.6	0.1	812.91	140.63	954
Moonlight State Beach-Leucadia	3,858	9.9	51.1	48.9	3.7	57.4	42.6	0.2	3,735.39	1,216.20	4,952
Leucadia-Carlsbad Army and Navy	8,047	3.1	51.1	48.9	4.3	57.4	42.6	0.15	1,829.77	2,211.07	4,041
Camp Pendleton-San Onofre	19,680	7.3	51.1	48.9	0.5	57.4	42.6	0.15	10,537.75	628.78	11,167
San Mateo Point-Dana Point	5,767	13.2	51.1	48.9	2.3	57.4	42.6	0.15	5,583.72	847.58	6,431
Total											46,911
Laguna											
Newport Bay-Little Corona Del Mar Beach	1,726	12	33.09	66.91	2	81.63	18.37	0.06	845.03	38.67	884
Little Corona Del Mar-Crystal Cove State Park	74,550	0	0	100	0	0	100	0.06	0.00	0.00	– –
Crystal Cove-Heisler Park	6,926	18	33.09	66.91	3	81.63	18.37	0.06	5,086.33	232.74	5,319
Heisler Park-Southern Laguna Beaches	2,397	8	33.09	66.91	2	81.63	18.37	0.06	782.36	53.70	836
Southern Laguna Beaches-Ruby Street Park	438	11	33.09	66.91	2	81.63	18.37	0.06	196.57	9.81	206
Ruby Street Park-Aliso Beach	2,397	5	33.09	66.91	2	81.63	18.37	0.06	488.98	53.70	543
Aliso Beach-Camel Point	791	8	33.09	66.91	3	81.63	18.37	0.06	258.18	26.58	285
Camel Point-Thousand Steps	1,042	14	33.09	66.91	2	81.63	18.37	0.06	595.18	23.34	619
Thousand Steps-Salt Creek Beech Park	2,144	17	33.09	66.91	5	88.12	11.88	0.40	8,818.96	509.41	9,328
Total											18,020

Table D1. Fine-sediment input from cliffs and bluffs into various sections of the California coast—Continued.

[Data on length, height, sand content, and erosion rate for Oceanside and Santa Barbara segments from California Department of Boating and Waterways and California Coastal Conservancy (2002), and for other segments from Patsch and Griggs (2005). Mud content is the left over fraction of sediment, calculated as 100 volume percent minus sand content. Input from bluffs is calculated as (Length of cliff, in meters) × (Height of bedrock, in meters) × (Mud fraction) × (Erosion rate, in meters per year), and from terraces as (Length of cliff, in meters) × (Height of terrace, in meters) × (Mud fraction) × (Erosion rate, in meters per year). Total input is the sum of bluff/cliff and terrace input]

San Pedro											
Point Vincent-Point Fermin	12,330	30	42.02	57.98	0	– –	– –	0.305	65,412.75	– –	65,413
Anaheim-Bolsa Chica State Park	1,160	30	14.24	85.76	0	– –	– –	0.305	9,102.57	– –	9,103
Total											74,516
Santa Monica											
Point Mugu-Point Dume	9,091	15	23.04	76.96	2	88.84	11.16	0.15	15,997.94	309.32	16,307
Point Dume-Paradise Cove	3,207	12	23.04	76.96	0	88.84	11.16	0.15	4,514.83	0.00	4,515
Paradise Cove-King Harbor	3,652	15	23.04	76.96	2	88.84	11.16	0.15	6,426.63	124.26	6,551
Dockweiler State Beach-Hermosa City Beach	1,487	11	23.04	76.96	2	88.84	11.16	0.15	1,918.96	50.59	1,970
King Harbor-Torrance County Beach	2,451	11	23.04	76.96	2	88.84	11.16	0.15	3,162.99	83.39	3,246
Malaga Cove-Palos Verdes Estates Shoreline Preserve	7,955	91	23.04	76.96	5	88.84	11.16	0.51	283,654.04	2,260.04	285,914
Total											318,503
Santa Barbara											
Rincon Point-Loon Point	5,540	30	0.1	99.9	0.5	60	40	0.305	50,640.31	337.94	50,978
Loon Point-Fernald Point	2,934	21	0.1	99.9	1.7	60	40	0.305	18,773.48	608.51	19,382
Fernald Point-Santa Barbara Cemetery	1,350	29	0.1	99.9	0.1	60	40	0.305	11,928.81	16.47	11,945
Santa Barbara Point-Lighthouse	2,080	14	0.1	99.9	3	60	40	0.152	4,421.81	379.39	4,801
Lighthouse-Arroyo Burro	1,995	14.3	0.1	99.9	4	60	40	0.152	4,332.00	485.18	4,817
Arroyo Burro-Hope Ranch	4,200	13.7	0.1	99.9	0.5	60	40	0.152	8,737.33	127.68	8,865
Goleta Beach-Goleta Point	1,600	6.5	0.1	99.9	3.5	60	40	0.305	3,168.83	683.20	3,852
Goleta Point-Coal Oil Point	1,960	10.2	0.1	99.9	4	60	40	0.152	3,035.75	476.67	3,512
Coal Oil Point-Naples	7,280	10.2	0.1	99.9	1	60	40	0.152	11,275.63	442.62	11,718
Naples-Point Orford	23,640	10.2	0.1	99.9	1	60	40	0.152	36,614.80	1,437.31	38,052
Point Orford-Jalama	28,331	6.5	0.1	99.9	0.1	60	40	0.076	13,981.52	86.13	14,068
Jalama-Spring Canyon	31,596	7.6	0.1	99.9	2	60	40	0.076	18,231.60	1,921.04	20,153
Total											192,143